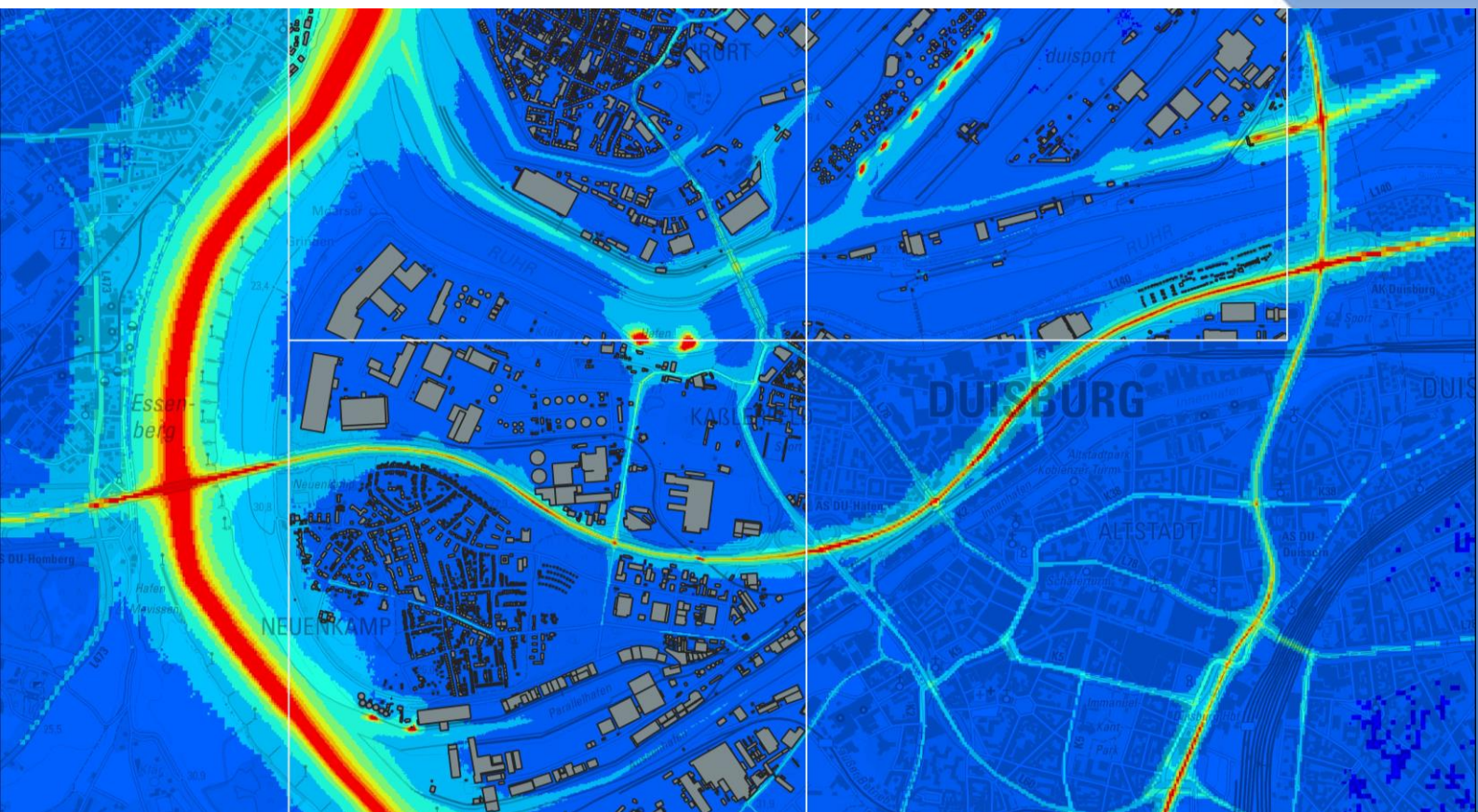


**Action B 4: Modelling, evaluating and scenario building**

**Harbour Monitoring Part F:**

**Root Cause Analysis for Air Quality Measurement Results in the  
Inland Ports of Neuss and Duisburg**



**CLEAN INLAND SHIPPING**

**Project:** CLINSH – Clean Inland Shipping  
**Goal:** The objective of LIFE CLINSH is to improve air quality in urban areas situated close to ports and inland waterways, by accelerating IWT emission reductions.  
**Project reference:** LIFE15 ENV/NL/000217  
**Duration:** 2016 – 2022  
**Project website:** [www.clinsh.eu](http://www.clinsh.eu)



CLINSH is an EU LIFE+ project delivered with the contribution of the LIFE financial instrument of the European Community. Project number LIFE15 ENV/NL/000217

This deliverable is part of B.4 Modelling, evaluating and scenario building.

**Contributors:** Landesamt für Natur, Umwelt und Verbraucherschutz  
Nordrhein-Westfalen (LANUV NRW)

**Version:** 1.2  
**Date:** 2022-07-12

**Authors:** Dr. Dieter Busch (LANUV NRW)  
Anton Bergen, M.Sc. (LANUV NRW)  
Fabian Hüftle, B.Sc. (Ingenieurbüro Rau, Heilbronn)  
Rike Wachsmann, M.Sc. (METCON-UMB, Pinneberg)



**Action B.4: Modelling, evaluating and scenario building**

# **Harbour Monitoring Part F: Root Cause Analysis for Air Quality Measurement Results in the Inland Ports of Neuss and Duisburg**

**Project management:** Dr. Dieter Busch & Anton Bergen  
Fachbereich 77  
Landesamt für Natur,  
Umwelt und Verbraucherschutz (LANUV)  
Nordrhein-Westfalen  
Leibnizstraße 10  
45610 Recklinghausen

**Cover picture:** Background map:  
[https://www.wms.nrw.de/geobasis/wms\\_nw\\_dtk](https://www.wms.nrw.de/geobasis/wms_nw_dtk)  
Data license Germany-  
Zero (<https://www.govdat.de/dl-de/zero-2-0>)

## Table of Contents

List of Figures .....	6
List of Tables.....	9
1. Introduction .....	10
2. Emissions in the investigation area.....	13
3. Setup of the dispersion modeling .....	14
3.1 Model area and spatial resolution .....	14
3.2 Effects of terrain and buildings.....	15
3.3 Emissions .....	17
3.4 Meteorological forcing data .....	20
3.5 Model parameters LASAT.....	26
4. Immissions in the reference year 2018 .....	28
4.1 Preliminary remarks .....	28
4.2 Consideration of a supra-regional background value for NO <sub>x</sub> .....	29
4.3 NO <sub>x</sub> immissions in the Duisburg port area - areal representation .....	29
4.3.1 Total immissions.....	30
4.3.2 Shipping traffic in the port, ships at berth and general port operations .....	30
4.3.3 Ships on the Rhine .....	32
4.3.4 Road Traffic.....	33
4.3.5 Industry.....	33
4.4 NO <sub>x</sub> immissions in the Neuss port area - areal representation.....	35
4.4.1 Total immissions.....	35
4.4.2 Shipping traffic in the port, ships at berth and general port operations .....	36
4.4.3 Ships on the Rhine .....	37
4.4.4 Road traffic .....	38
4.4.5 Industry.....	38
4.5 Measuring sites in the model area.....	40
4.5.1 Calculated source group percentages of NO <sub>x</sub> immissions at the measuring sites . .....	41
4.5.2 Source group shares of NO <sub>x</sub> immissions at selected monitoring stations.....	44
5. Comparison of measured and modeled environmental pollution with nitrogen oxides .....	52
5.1 Quality criteria for modeling results .....	52
5.1.1 Conversion of the NO <sub>2</sub> measured values for comparison with the modeling results .....	52
5.1.2 Comparison of NO <sub>x</sub> values modeled/measured .....	55

5.1.2.1	Duisburg.....	55
5.1.2.2	Neuss .....	58
5.1.3	Classification of the measuring points with regard to source group shares - Tabular representation .....	60
6.	Conclusion and Outlook .....	70
6.1	Conclusion.....	70
6.2	Outlook .....	71
7.	Literature .....	73
8.	Appendix.....	74
8.1	Source group shares at the Duisburg measuring stations (pie charts) .....	75
8.2	Source group shares at the Neuss measuring stations (pie charts).....	90
8.3	Additional source group shares (Port of Duisburg, spatial presentation).....	103
8.4	Additional source group shares (Port of Neuss, spatial presentation) .....	106
9.	CLINSH Partners.....	109

## List of Figures

Fig. 1:	NO <sub>2</sub> air pollution in the Port of Duisburg - Classified annual mean values 2018 ..	11
Fig. 2:	NO <sub>2</sub> air pollution in the Port of Neuss - Classified annual mean values 2018 .....	11
Fig. 3:	Terrain heights (m a.s.l.) in the LASAT total area with the location of the nested model grids for Duisburg and Neuss and anemometer position (red).....	16
Fig. 4:	Synthetic wind roses (SynWSGE) in the port areas of Duisburg (top) and Neuss (bottom) (© 2022 Google, Geobasis-DE/BKG). .....	22
Fig. 5:	Wind roses of the measuring stations potentially suitable as drive data in front of terrain heights (m a.s.l.) in the LASAT total area with mean wind speed (m/s, red). .....	23
Fig. 6:	Data sheet of the measuring station Duisburg-Rheinhafen (DURH) for the measuring period 2018 - 2020.....	25
Fig. 7:	Illustration of the statistical uncertainties for the example of Duisburg. ....	27
Fig. 8:	Total NO <sub>x</sub> immission concentrations in the Duisburg port area - modeled with LASAT. ....	30
Fig. 9:	Proportion of NO <sub>x</sub> immission concentrations caused by port emissions.....	31
Fig. 10:	Proportion of NO <sub>x</sub> immission concentrations caused by shipping traffic on the Rhine River in the Duisburg port area - modeled with LASAT .....	32
Fig. 11:	Proportion of NO <sub>x</sub> immission concentrations caused by road traffic in the Duisburg port area - modeled with LASAT.....	33
Fig. 12:	Proportion of NO <sub>x</sub> immission concentrations caused by industrial sources in the Duisburg port area - modeled with LASAT. ....	34
Fig. 13:	Total NO <sub>x</sub> immission concentrations in the Neuss port area - modeled with LASAT. ....	35
Fig. 14:	Proportion of NO <sub>x</sub> immission concentrations caused by port emissions in the Neuss port area - modeled with LASAT.....	36
Fig. 15:	Proportion of NO <sub>x</sub> immission concentrations caused by shipping traffic on the Rhine River.....	37
Fig. 16:	Proportion of NO <sub>x</sub> immission concentrations caused by road traffic in the Neuss port area - modeled with LASAT.....	38
Fig. 17:	Proportion of NO <sub>x</sub> immission concentrations caused by industrial sources in the Duisburg port area - modeled with LASAT. ....	39
Fig. 18:	Location of the measuring sites in the area of the Duisburg Harbour. ....	40
Fig. 19:	Location of the measuring sites in the area of the Neuss Harbour .....	41
Fig. 20:	NO <sub>x</sub> source group percentages (Duisburg Harbour) - modeled with LASAT. ....	42
Fig. 21:	NO <sub>x</sub> source group percentages (Neuss Harbour) - modeled with LASAT.....	43
Fig. 22:	Polluter analysis for the automatic measuring station Duisburg-Rheinhafen (DURH) .....	44
Fig. 23:	Polluter analysis for the Duisburg CLINSH measuring site DU001. ....	45
Fig. 24:	Polluter analysis for the Duisburg CLINSH measuring site DU011. ....	46
Fig. 25:	Polluter analysis for the traffic measuring site Duisburg Meiderich Bahnhofstraße (DUMB). ....	47

Fig. 26:	Polluter analysis for the automatic measuring station Neuss-Rheinhafen (NERH)...	48
Fig. 27:	Polluter analysis for the Neuss CLINSH measuring site NED018. ....	49
Fig. 28:	Polluter analysis for traffic measuring site Düsseldorf Südring (VDSR).....	50
Fig. 29:	Polluter analysis for traffic measuring site Neuss Batteriestraße (VNEB). ....	51
Fig. 30:	NO <sub>x</sub> ratio between model results and measurements at the measurement sites in the area of the Duisburg Harbour. ....	55
Fig. 31:	NO <sub>x</sub> ratio between model results and measurements at the measurement sites in the area of the Neuss Harbour. ....	58
Fig. 32:	Source group shares at monitoring stations DU001 (left) and DU002 (right). ....	75
Fig. 33:	Source group shares at monitoring stations DU003 (left) and DU004 (right). ....	76
Fig. 34:	Source group shares at monitoring stations DU005 (left) and DU006 (right). ....	77
Fig. 35:	Source group shares at monitoring stations DU007 (left) and DU008 (right). ....	78
Fig. 36:	Source group shares at monitoring stations DU009 (left) and DU010 (right). ....	79
Fig. 37:	Source group shares at monitoring stations DU011 (left) and DU011a (right). ....	80
Fig. 38:	Source group shares at monitoring stations DU012 (left) and DU013 (right). ....	81
Fig. 39:	Source group shares at monitoring stations DU014 (left) and DU015 (right). ....	82
Fig. 40:	Source group shares at monitoring stations DU017 (left) and DU018 (right). ....	83
Fig. 41:	Source group shares at monitoring stations DU019 (left) and DU020 (right). ....	84
Fig. 42:	Source group shares at monitoring stations DU021 (left) and DU021a (right). ....	85
Fig. 43:	Source group shares at monitoring stations DU022 (left) and DU023 (right). ....	86
Fig. 44:	Source group shares at monitoring stations DU024 (left) and DURH (right). ....	87
Fig. 45:	Source group shares at monitoring stations DUMP (left) and DUMB (right). ....	88
Fig. 46:	Source group shares at monitoring station DUFW. ....	89
Fig. 47:	Source group shares at monitoring stations NED001 (left) and NED002 (right) ...	90
Fig. 48:	Source group shares at monitoring stations NED003 (left) and NED004 (right) ...	91
Fig. 49:	Source group shares at monitoring stations NED005 (left) and NED006 (right) ...	92
Fig. 50:	Source group shares at monitoring stations NED006a (left) and NED007 (right). ...	93
Fig. 51:	Source group shares at monitoring stations NED008 (left) and NED009 (right) ...	94
Fig. 52:	Source group shares at monitoring stations NED010 (left) and NED011 (right) ...	95
Fig. 53:	Source group shares at monitoring stations NED012 (left) and NED013 (right) ...	96
Fig. 54:	Source group shares at monitoring stations NED015 (left) and NED016 (right) ...	97
Fig. 55:	Source group shares at monitoring stations NERH (left) and NED018 (right). ....	98
Fig. 56:	Source group shares at monitoring stations NED019 (left) and DDBG (right). ....	99
Fig. 57:	Source group shares at monitoring stations DBIL (left) and VDSR (right). ....	100
Fig. 58:	Source group shares at monitoring stations NEKS (left) and VNEB (right).....	101
Fig. 59:	Source group shares at monitoring station VNEM2. ....	102
Fig. 60:	Proportion of total NO <sub>x</sub> load from rail traffic emissions in the Duisburg port area - modeled with LASAT .....	103
Fig. 61:	Proportion of total NO <sub>x</sub> load from emissions from domestic heating and small combustion plants in the Duisburg port area - .....	104
Fig. 62:	Proportion of total NO <sub>x</sub> load from emissions from aviation and off-road traffic in the Duisburg port area - modeled with LASAT .....	105

Fig. 63:	Proportion of total NO <sub>x</sub> load from rail traffic emissions in the Neuss port area - modeled with LASAT .....	106
Fig. 64:	Proportion of total NO <sub>x</sub> load from emissions from domestic heating and small combustion plants in the Neuss port area - .....	107
Fig. 65:	Proportion of total NO <sub>x</sub> load from emissions from aviation and off-road traffic in Neuss port area - modeled with LASAT .....	108

## List of Tables

Tab. 1:	Annual NO <sub>x</sub> emissions in the study area, analysis year 2018 .....	13
Tab. 2:	Boundaries of the LASAT model areas in UTM coordinates (EPSG 4647) and grid widths (Duisburg).....	14
Tab. 3:	Boundaries of the LASAT model areas in UTM coordinates (EPSG 4647) and grid widths (Neuss). .....	15
Tab. 4:	Overview of the pollution emitter groups and source types of the applied emissions. ....	17
Tab. 5:	Overview of emission sources applied in LASAT calculations. ....	19
Tab. 6:	Overview of meteorological measuring stations in the total model area.....	20
Tab. 7:	Conversion of anemometer heights. ....	26
Tab. 8:	Grading of the model results at the stations in the Duisburg area with respect to source group proportions.....	61
Tab. 9:	Grading of the model results at the stations in the Neuss area with respect to source group proportions.....	66

## 1. Introduction

The "EU Directive on Ambient Air Quality and Cleaner Air for Europe" (2008/50/EC) sets binding limit values for all member states for fine particulate matter (PM<sub>10</sub>: annual mean 40 µg/m<sup>3</sup>) and nitrogen dioxide (NO<sub>2</sub>: annual mean 40 µg/m<sup>3</sup>).

There are eleven major cities in the German state of North Rhine-Westphalia (NRW) with approx. 3.3 million inhabitants directly located near the Rhine. In these densely populated urban areas, the air is polluted by a variety of pollution sources such as industry, domestic heating, road traffic, etc. For a long time in many cities, the limit values of the EU Air Quality Directive for NO<sub>2</sub> could not be complied with due to the high traffic load. Therefore, the responsible authorities established clean air plans, which have been updated several times.

In 2020, for the first time, the EU limit values for NO<sub>2</sub> were complied with at all measuring points of the official state measuring network in NRW. Despite the ongoing improvement in air quality in North Rhine-Westphalia in recent years, compliance with the binding limit values of the EU Air Quality Directive still remains a challenge, especially in urban agglomerations. This requires the development of clean air plans that stipulate effective measures to improve air quality in the short term. In addition to road traffic, which is usually the decisive factor in inner cities, emissions from inland waterway vessels are also a significant source of air pollution for municipalities along waterways. However, there was still room for improvement in the description of inland waterway vessel emissions at the beginning of the CLINSH project.

In order to improve the data situation concerning the pollution caused by inland waterway vessel emissions, the CLINSH project therefore investigated NO<sub>2</sub> pollution in the air on the Rhine, in Europe's largest inland port of Duisburg and in the port of Neuss/Düsseldorf at more than 50 measuring sites.

This port monitoring has made it possible to create a so far unique database on the pollution of the air with nitrogen oxides caused by ship emissions and port operations. Exceedances of the EU limit value for nitrogen dioxide (NO<sub>2</sub>, 40 µg/m<sup>3</sup> annual mean) applicable to residential areas and other publicly accessible areas were only detectable at three CLINSH monitoring sites in the Port of Duisburg in 2018 (**Fig. 1**). Two of these measuring sites (DU003 and DU004) were located directly at the lock basin of the Meiderich lock (operating area). The annual mean NO<sub>2</sub> concentrations of around 47 µg/m<sup>3</sup> measured here were clearly attributable to lock operations (**LANUV Fachbericht 115/CLINSH Report Harbour Monitoring Part A**). The third measuring site with an annual NO<sub>2</sub> mean value of about 43 µg/m<sup>3</sup> was located in the area of a large construction site at the entrance of harbour basin A into the harbour channel, which leads to the assumption that this contributed to the high pollution values. However, this could not be resolved with certainty, since the emission quantities caused by the trucks and construction machinery driving on the construction site could not be recorded precisely.

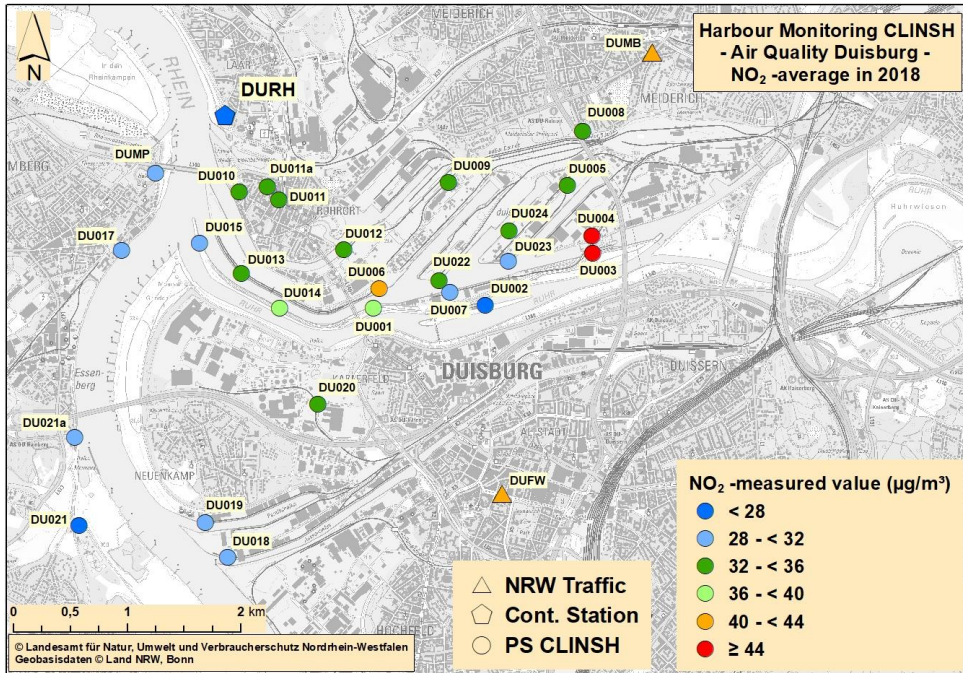


Fig. 1: NO<sub>2</sub> air pollution in the Port of Duisburg - Classified annual mean values 2018

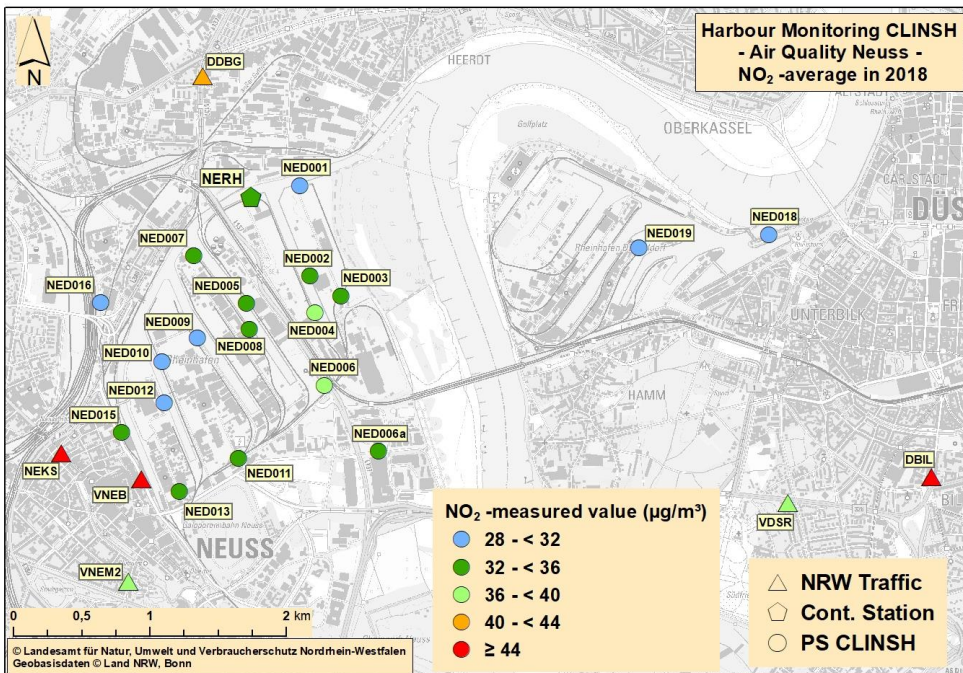


Fig. 2: NO<sub>2</sub> air pollution in the Port of Neuss - Classified annual mean values 2018

Overall, it was found that the annual mean NO<sub>2</sub> concentrations measured at the CLINSH monitoring sites were significantly lower than expected in the run-up to the measurement program. This was particularly true for the measuring points on the Rhine, which were directly influenced by the emissions from approx. 80,000 ships per year. In the Neuss harbour area, the annual mean values for the NO<sub>2</sub> pollution were below 40 µg/m<sup>3</sup> at all CLINSH special monitoring sites, while several traffic monitoring sites (triangles) in the study area still showed exceedances in 2018 (**Fig. 2**). Detailed presentations of the investigation results can be found in the **LANUV Fachbericht 115/CLINSH Report: Harbour Monitoring Part A**.

In order to identify the contribution of shipping traffic and port operations to air pollution in detail, the respective causes of pollution at the measuring points were clarified using very elaborate LASAT modeling. To achieve this, a modeling grid of 5 x 5 m was selected in the harbour areas and the building cubatures were included in the modeling. The emission inventories of the state of NRW for the individual source groups served as emission data basis for the dispersion modeling. This includes not only the emissions from shipping, but also emissions from road and rail traffic, aviation, industry, small combustion plants and off-road traffic. Some port-specific emission sources were additionally surveyed for the CLINSH project (see **LANUV-Fachbericht 123/CLINSH Report Harbour monitoring Part C**).

Depending on the emitter group, the emissions are included in the modelling as point, line or area sources.

This report describes the basic principles and results used to determine the polluter shares of immissions with the LASAT dispersion model.

## 2. Emissions in the investigation area

In the following, the emissions determined in the **LANUV Fachbericht 123/CLINSH Report Harbour Monitoring Part C** for all emitter groups are listed in summary for the overall study area. A detailed summary of emissions for the two harbour areas can be found in the CLINSH report.

The NO<sub>x</sub> emissions of all emitter groups in the considered study area are summarised in the following table (**Tab. 1**). The largest share of NO<sub>x</sub> emissions (64 %) is caused by industrial installations requiring a permit. They are predominantly released via chimneys at higher altitudes and therefore have almost no effect at ground level.

The share of road traffic (ground level emission release) in the total load is 16 % and that of shipping 11 %. In contrast, all other emitter groups (air traffic, off-road and small combustion plants) only contribute a maximum of 4 % to the total NO<sub>x</sub> emissions.

Tab. 1: Annual NO<sub>x</sub> emissions in the study area, analysis year 2018

Pollution emitter group	Investigation area	
	NO <sub>x</sub> Emissions [t/yr]	Share
Shipping traffic	3,251.914	11%
Road traffic	4,971.364	16%
Industry	19,510.646	64%
Rail transport incl. port railway	330.377	1%
Air traffic	912.948	3%
Off-road traffic	407.651	1%
Small combustion plants	1,151.264	4%
Total	30,536.164	100%

## 3. Setup of the dispersion modeling

### 3.1 Model area and spatial resolution

The dispersion modelling is carried out on six nested grid levels. The grid parameters are summarised in **Tab. 2** and **Tab. 3**. The largest model area has an extension of about 25 km x 41 km with a spatial resolution of 160 m. This covers the two port areas of Duisburg and Neuss as well as a radius of at least 5 km in the vicinity of each port area in an overall area.

Five further grid levels are nested in this model area, whereby the model areas decrease with each level, always having half the grid width, of the grid level they are nested in. The model calculations for Neuss and Duisburg were split up due to more efficient utilisation of the computing capacities.

The first grid level represents the entire area and is identical for both computations. The further model levels are each nested down to the port areas of Duisburg and Neuss.

At level 6 (5 m resolution), three model areas are located next to each other in the port area of Duisburg and two independent model areas are located next to each other in the port area of Neuss in order to cover the port areas with a sufficiently high resolution as extensively as possible (**Fig. 3**).

The vertical grid resolution is kept constant at 3 m up to an altitude of 150 m. The grid resolution increases to 300 m up to the top of the model at 1,500 m.

Tab. 2: Boundaries of the LASAT model areas in UTM coordinates (EPSG 4647) and grid widths (Duisburg).

Grid (name)	Grid width	Western boundary	Grid (name)	Grid width	Western boundary
1 („160m“)	160 m	32 331 000	32 356 120	5 668 000	5 709 120
2 („Dui_80m“)	80 m	32 336 920	32 349 720	5 695 200	5 708 000
3 („Dui_40m“)	40 m	32 338 200	32 348 440	5 696 480	5 706 720
4 („Dui_20m“)	20 m	32 339 480	32 347 040	5 698 040	5 705 160
5 („Dui_10m“)	10 m	32 340 760	32 345 760	5 699 320	5 703 880
6-1 („Dui_5m-1“)	5 m	32 341 450	32 343 550	5 699 500	5 701 500
6-2 („Dui_5m-2“)	5 m	32 341 450	32 343 550	5 701 500	5 703 300
6-3 („Dui_5m-3“)	5 m	32 343 550	32 345 500	5 701 500	5 703 300

Tab. 3: Boundaries of the LASAT model areas in UTM coordinates (EPSG 4647) and grid widths (Neuss).

Grid (name)	Grid width	Western boundary	Grid (name)	Grid width	Western boundary
1 („160m“)	160 m	32 331 000	32 356 120	5 668 000	5 709 120
2 („Neu_80m“)	80 m	32 334 680	32 347 480	5 669 120	5 681 920
3 („Neu_40m“)	40 m	32 335 960	32 346 200	5 670 400	5 680 640
4 („Neu_20m“)	20 m	32 337 260	32 344 820	5 672 920	5 679 080
5 („Neu_10m“)	10 m	32 338 540	32 343 540	5 674 200	5 677 800
6-1 („Neu_5m-1“)	5 m	32 338 640	32 341 140	5 674 500	5 677 000
6-2 („Neu_5m-2“)	5 m	32 341 140	32 343 500	5 675 500	5 677 000

### 3.2 Effects of terrain and buildings

Fig. 3 shows the terrain relief in the model area as well as the nested model grids in the vicinity of the Duisburg and Neuss port areas and the anemometer position (cf. section 3.4). The terrain elevations vary between 20 m and 50 m throughout most of the total area. The highest elevation is about 175 m at the eastern border of the model area south of the Ruhr River.

Since in particular the smaller-scale terrain structures within the port areas can also be relevant for the dispersion of emissions in the port area, the model calculations are carried out with diagnostic wind field modeling taking into account the terrain influences.

In the dispersion calculations, all buildings with a black background in Fig. 3 are also taken into account in the model grids of the finest level in the port areas of Duisburg and Neuss. These are mainly large port buildings, which can significantly influence the dispersion of emissions.

The large buildings, as well as the smaller ones, can be resolved with sufficient accuracy due to the small grid widths of the innermost grids of 5 m. The modeled building heights are up to 51 m in the port area of Duisburg, the highest building in the port area of Neuss has a height of 75 m. Small-scale flow obstacles that change due to container operations (storage, stacking) and material handling (piles, stockpiles) at transshipment sites were not considered in the modeling.

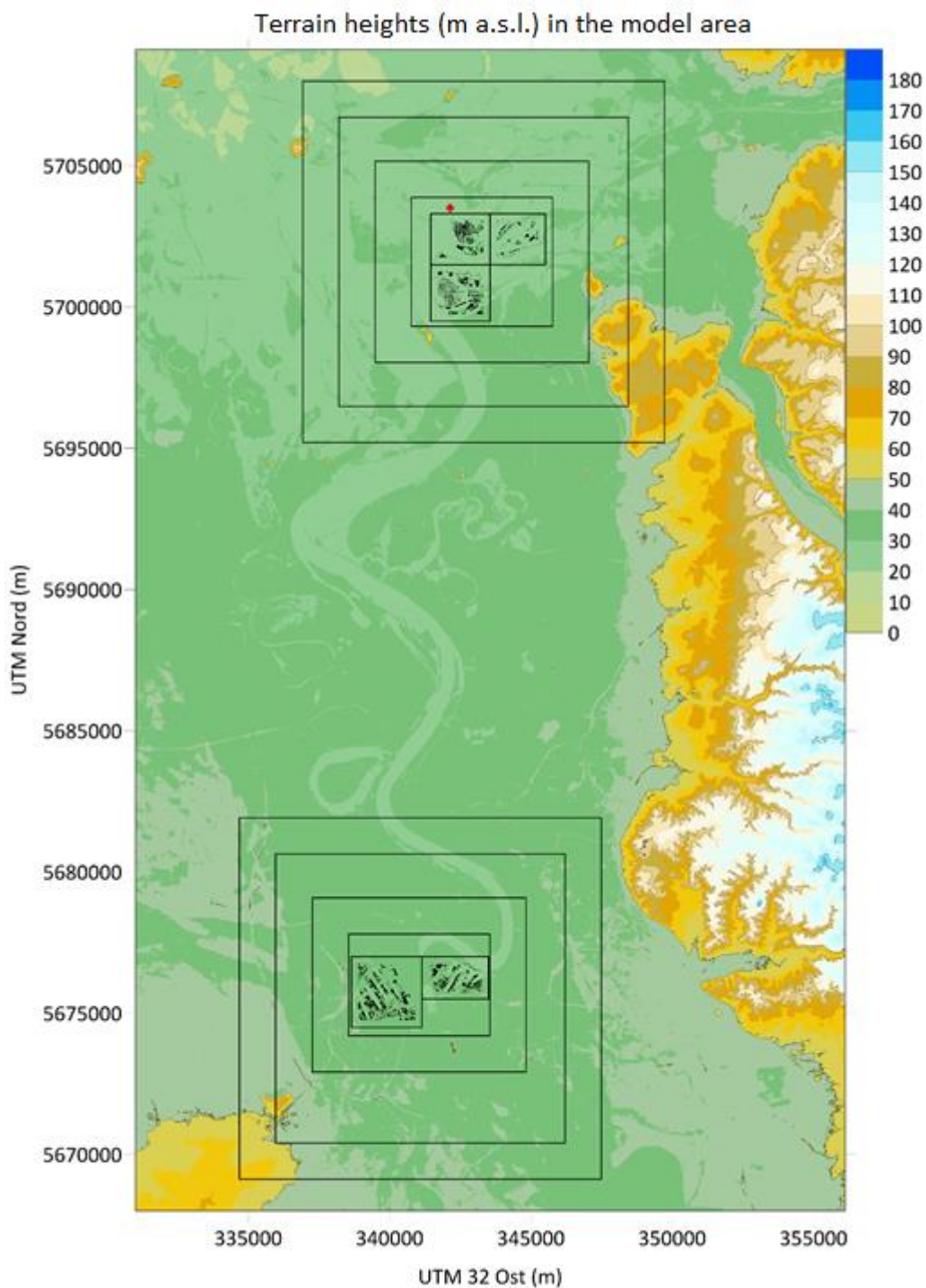


Fig. 3: Terrain heights (m a.s.l.) in the LASAT total area with the location of the nested model grids for Duisburg and Neuss and anemometer position (red).

### 3.3 Emissions

In the LASAT model calculations, NO<sub>x</sub> emissions were determined separately from six polluter groups, where each polluter group can be composed of multiple polluters and source types. The emissions were provided as annual averaged emission rates (see **Tab. 4**).

Tab. 4: Overview of the pollution emitter groups and source types of the applied emissions.

Pollution emitter group	NO <sub>x</sub> Identifier	Pollution emitter	LASAT- Source type	Emission height [m]
Ship emissions harbour	nox_ship_ha	Tanker (at berth)	Point source	0.1
		All other ships (at berth)	Line source	4
		Car loading Neuss	Line source	0.5
		Ships (travelling)	Line source	4
		Locks	Line source	4
		Ships traveling to the locks	Line source	4
		Industrial trucks	Area source	2
Rail transport	nox_rail	Port railway	Line source	4
		DB railway	Line source	4
		Shunting Operations	Area source	4
Road traffic	nox_road	Road traffic	Line source	0.5
Plants requiring a permit	nox_gena	Plants requiring a permit	Point sources	Variable: 2 -250
Ship emission on the Rhine	nox_ship_rh	Ships travelling on the Rhine River	Line sources	4
Other traffic	nox_traff	Air traffic	Area sources (1 km <sup>2</sup> raster)	Variable: 0 -900
		Off-road traffic	Area sources (1 km <sup>2</sup> raster)	5
Small combustion plants	nox_huk	Small combustion plants	Area sources (1 km <sup>2</sup> raster)	Variable: 5 -15

Emissions are emitted from line and point sources as well as area and grid sources throughout the model area. At the finest model level, the buildings in the port areas of Duisburg and Neuss are taken into account. However, this means that the grid and area sources in the finest grids would lie partially within the cells of the buildings. In order to still be able to consider the emission via grid and area sources, two dispersion calculations are carried out for each area (**Tab. 5**).

In the first calculation, no buildings are considered and emissions are released via grid and area sources throughout the model area. In addition, the release of emissions occurs through those point and line sources that are outside the finest grid layers.

This approach is due to the fact that no buildings can be considered by the model in the areas outside the finest model areas. Nevertheless, since only one roughness length can be applied for the entire model area (**section 3.4**), the roughness in the vicinity of the sources would be underestimated in the model calculations with buildings for those regions lying outside the finest model areas. To address this issue, all line and point sources that lie outside the finest model regions are included in the calculations without explicitly modeled buildings and a correspondingly higher roughness length (**section 3.4**).

In the second calculation, emissions are released via the line and point sources within the finest model levels, taking into account the modeled buildings.

For this purpose, the line sources were separated at the grid boundaries, if necessary, and the emission sources were assigned to the respective model areas via different identifiers. Lastly, the results of the model calculations with buildings and without buildings within the finest grids are summed up to evaluate the respective port areas.

The overview in **Tab. 5** shows the release of emissions in four different dispersion calculations. The term "surrounding area" includes all areas of the total area, which lie outside the finest grid levels of the port areas of Duisburg and Neuss.

Tab. 5: Overview of emission sources applied in LASAT calculations.

Sources taken into account	Dispersion modeling			
	Duisburg		Neuss	
	Without buildings $z_0 = 0.5 \text{ m}$	With buildings $z_0 = 0.2 \text{ m}$	Without buildings $z_0 = 0.5 \text{ m}$	With buildings $z_0 = 0.2 \text{ m}$
Point and Line sources - Surrounding area	X		X	
Point and Line sources – inner area Neuss	X			x
Point and Line sources – inner area Duisburg		x	X	
Area and Raster sources – entire area	x		x	

### 3.4 Meteorological forcing data

The dispersion calculations are performed involving modeling of the terrain. Therefore, a suitable meteorological forcing data set has to be found.

Within the entire model area of the dispersion calculations (**Fig. 3**) there are one measuring station of the DWD (Düsseldorf) and eight measuring stations of the LANUV, where meteorological data are also collected. Two measuring stations (Duisburg-Rheinhafen (DURH) and Neuss-Rheinhafen (NERH)) were operated specifically for the CLINSH project to record nitrogen oxides, particulate matter and meteorology.

The following **Tab. 6** shows an overview of the available measuring stations within the model area.

Tab. 6: Overview of meteorological measuring stations in the total model area

Name	Abbreviation	Position (UTM E/N in m)	Measuring height over ground [m]	Measuring period
Düsseldorf (DWD)	1078	32 344 430/ 5 685 107	10	2011 - 2020
Duisburg-Bruckhausen (LANUV)	DUB2	32 342 769/ 5 706 247	10	2014 - 2020
Duisburg-Rheinhafen (LANUV/ CLINSH)	DURH	32 342 132/ 5 703 510	10	2018 - 2020
Mülheim-Styrum (LANUV)	STYR	32 351 664/ 5 702 415	21	2011 - 2020
Duisburg-Buchholz (LANUV)	BUCH	32 3443 41/ 5 695 043	21	2011 - 2020
Krefeld Hafen (LANUV)	KRHA	32 337 735/ 5 690 498	10	2011 - 2020
Ratingen-Tiefenbroich (LANUV)	RAT2	32 348 032/ 5 685 882	10	2011 - 2020
Düsseldorf-Reisholz (LANUV)	REIS	32 350 398/ 5 673 001	22	2011 - 2020
Neuss Rheinhafen (LANUV/CLINSH)	NERH	32 339666/ 5676747	10	2018 - 2019

Although the DWD station Düsseldorf is located relatively undisturbed on the airport site, the wind rose shows an implausible narrow main maximum of 10° latitude from the south-southeast, which cannot be satisfactorily explained either by local (buildings) or regional

effects (terrain relief). Therefore, this monitoring station is not used as a meteorological drive dataset.

The wind roses of the LANUV stations Duisburg-Bruckhausen and Krefeld (port) show local influences by surrounding buildings/trees. These measuring stations are therefore also not used as a meteorological drive dataset.

The measuring station Duisburg-Rheinhafen has a measuring height of only 10 m with a distance of only about 30 m to neighboring buildings to the east. The wind rose shows low frequencies in the 90°-120° sector, which indicates influence by the neighboring buildings. In all other directions, the station is exposed and is therefore considered further for the time being.

The Ratingen-Tiefenbroich station (LANUV) is no longer tested for suitability due to 94% data gaps in the 2011-2020 measurement period.

The station Neuss Rheinhafen shows prominent channelized wind directions, which could be influenced by high buildings in the harbour area and/or by the channelizations through the harbour basins. Here, as well, a use as a drive dataset is therefore not an option.

After this first review of the station locations and check for local influences, only the data from the Duisburg-Rheinhafen (DURH, 2018-2020), Mülheim-Styrum (STYR, 2011 - 2020), Duisburg-Buchholz (BUCH, 2011-2020) and Düsseldorf-Reisholz (REIS, 2011 - 2020) monitoring stations can be considered as suitable meteorological forcing datasets.

The measuring station to be selected should provide a good representation of the wind conditions, taking into account the influence of the terrain, especially in the port areas. Modeled data in the port areas are also used to further compare the monitoring stations and test their suitability for the LASAT model calculations (**Fig. 4**). The synthetic wind roses (SynWSGE) show a southwest maximum in the port area of Duisburg with a secondary maximum from the northeast. In the port area of Neuss, the main maximum is slightly turned to west-southwest and a secondary maximum from southeast direction occurs.

In **Fig. 5**, the wind roses at the potentially suitable LANUV measuring stations are shown in front of the terrain relief in the model area and supplemented by the wind speed averaged over the observed measuring period.

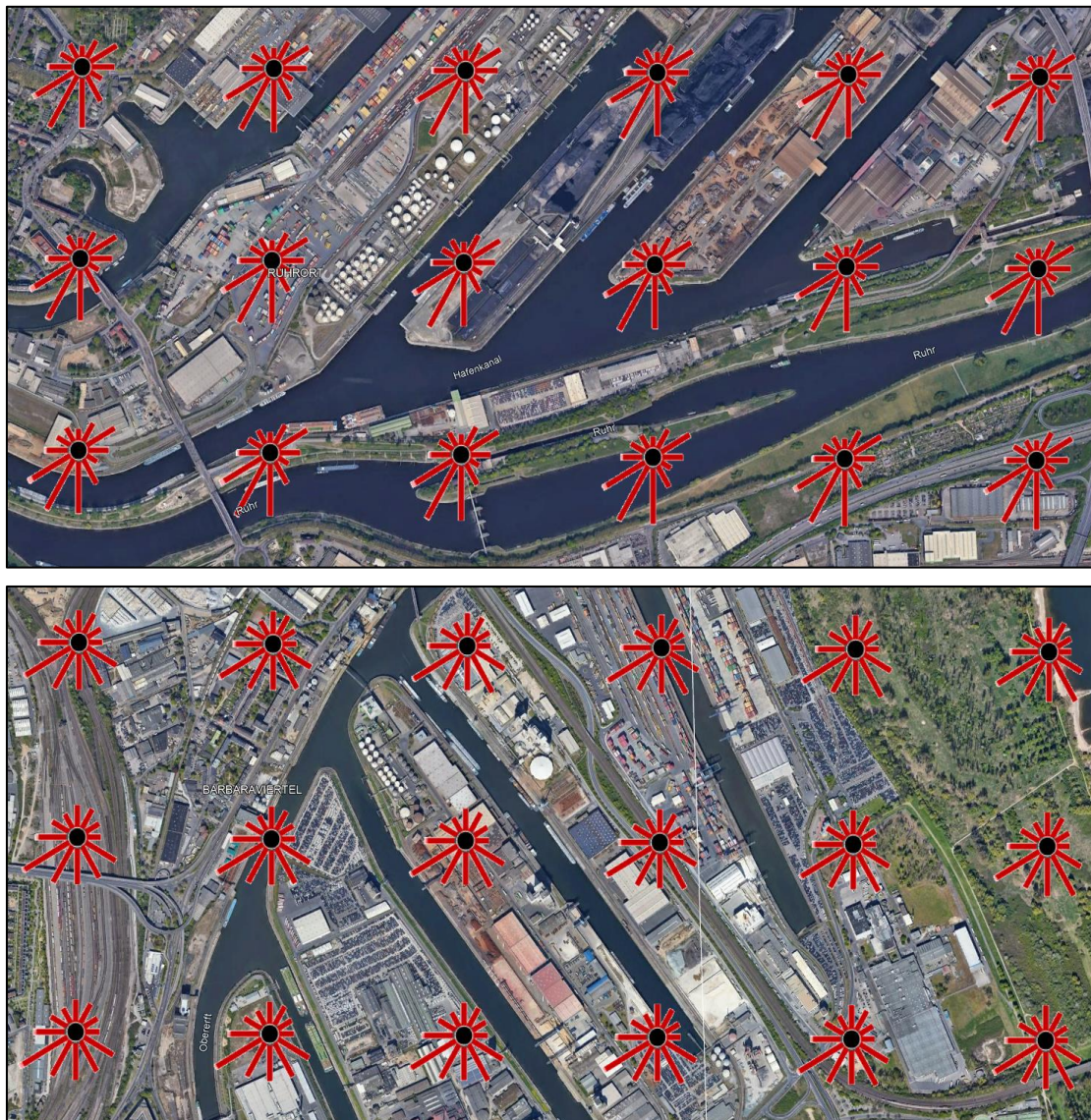


Fig. 4: Synthetic wind roses (SynWSGE) in the port areas of Duisburg (top) and Neuss (bottom) (© 2022 Google, Geobasis-DE/BKG).

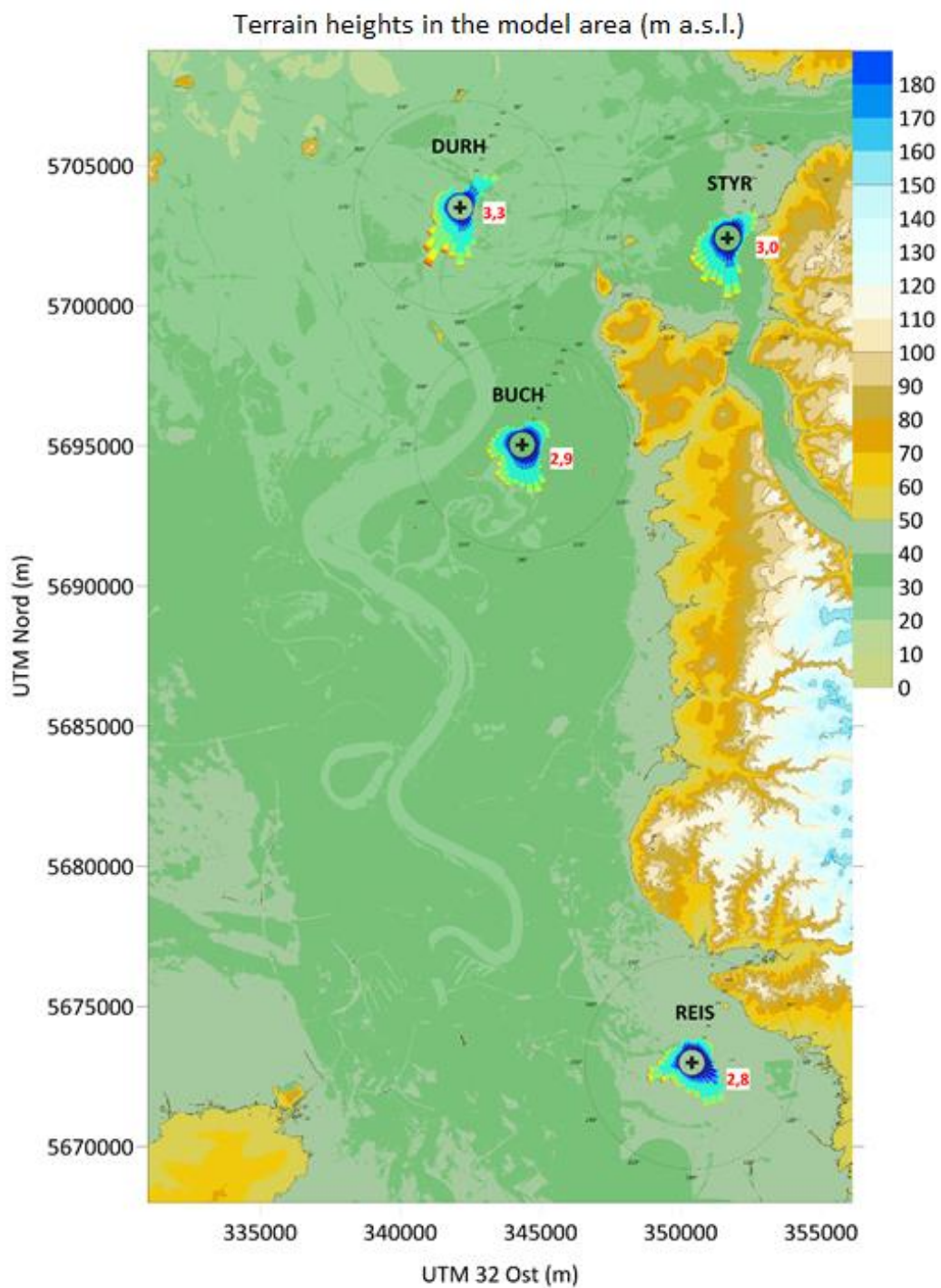


Fig. 5: Wind roses of the measuring stations potentially suitable as drive data in front of terrain heights (m a.s.l.) in the LASAT total area with mean wind speed (m/s, red).

Synoptically, a maximum from southwesterly wind directions with a secondary maximum around eastern wind directions can be expected over western Germany in topographically less disturbed locations.

The STYR station (2011-2020) has a pronounced southern component, which can be explained by frequent outflow from the Ruhr valley. The measurement station is thus influenced by the smaller-scale topography, which is already taken into account in the model calculations. It is therefore not suitable as a driving dataset for the entire model area.

The station BUCH (2011-2020) shows a very broad distribution, but its maximum is located at south-southeast. This maximum is obviously related to a channelization along the marginal heights of the Rhine valley. This can also be seen in the synthetic wind roses in the port area of Neuss (**Fig. 4**; lower figure). In principle, the station data would be suitable as a driver for the model calculations despite the obvious topographic influences, since with the selected model area, the Rhine valley is only partially covered and thus the wind field modeling cannot fully represent its influences. The terrain influences, not computed by the model, would thus be given by the meteorological forcing data. However, this drive data set would underestimate the synoptically induced southwesterly winds in the Duisburg port area.

The station REIS (2011-2020) shows an even stronger maximum from the southeast, which would also approximately fit the port area of Neuss. However, the secondary maximum at the REIS station occurs from a westerly direction, while maxima from the southwest are present in the port areas of Duisburg and Neuss. These could not be well mapped with the drive data set of the station REIS and the considered terrain influence up to the Neuss and especially the Duisburg port area.

The DURH station (2018-2020) shows a southwest maximum with a secondary maximum from the northeast. Both correspond at least approximately to the synoptic conditions in the region and coincide with the synthetic data in the Duisburg area. The also increased frequencies around southerly wind directions may still be due to the course of the Rhine upstream. Using the data from this station, the diagnostic wind field modeling in the Duisburg port area would calculate very similar characteristic wind conditions. In addition, it is expected that the eastern boundary heights in the area of the port of Neuss will provide for a slight redirection of south-southwesterly to southerly wind directions to south to southeast in the model as well. Thus, the characteristic wind conditions there would also be met in a good approximation.

It should be noted, however, that the wind rose of the DURH station shows missing easterly components, since the station is influenced from the east by surrounding buildings and has a measuring height of only 10 m. Actually, the station should be excluded for this reason. However, the other mapped measuring stations without local influences and with higher measuring heights also show this "absence" of the easterly components. Overall, the local influence of the station DURH in this direction plays only a minor role.

**Conclusion:**

After considering all the facts, a LASAT calculation with terrain using the AKS Duisburg-Rheinhafen (DURH, 2018-2020), shown in **Fig. 6**, appears to be the most suitable. The coverage data from the DWD station in Düsseldorf were used to calculate the dispersion categories.

The roughness length of the station environment can be estimated from aerial photography to be  $\sim 0.46$  m ( $\sim 60$  % urban green space/road ( $z_0 = 0.1$  m) /  $\sim 40$  % urban area ( $z_0 = 1$  m)).

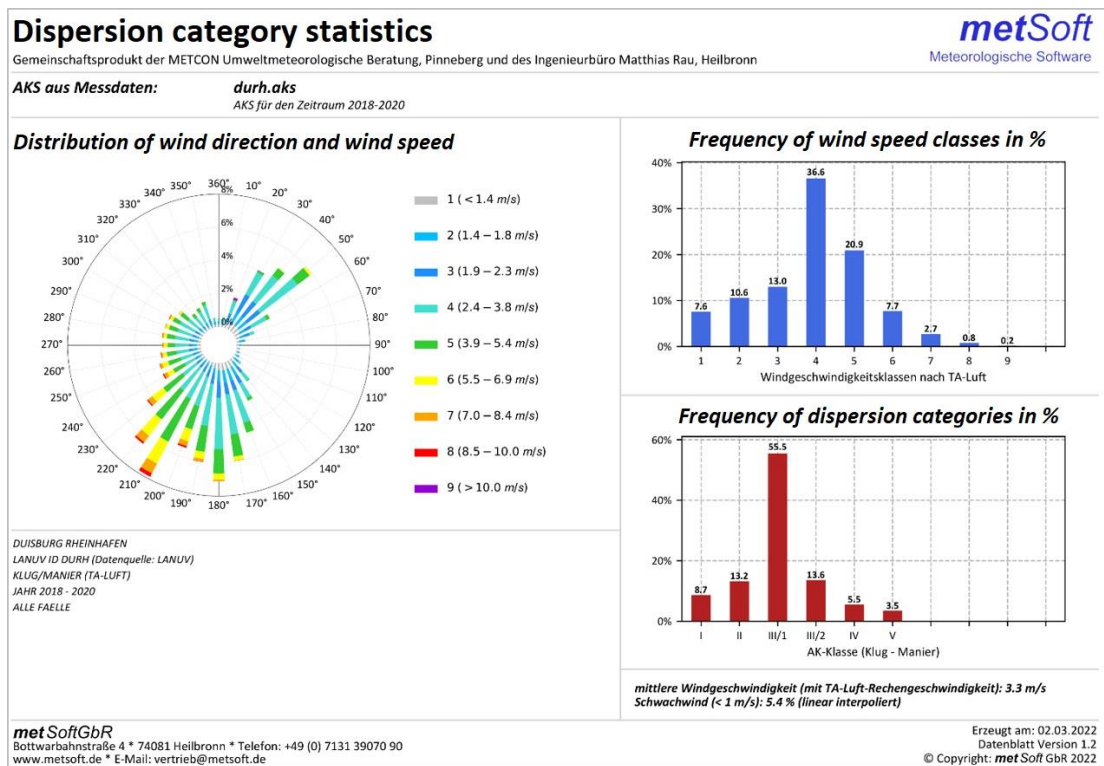


Fig. 6: Data sheet of the measuring station Duisburg-Rheinhafen (DURH) for the measuring period 2018 - 2020.

The measuring station DURH lies within the model area, so that the LASAT anemometer position can also be set to the site coordinates. As already explained in section 3.3, two LASAT calculations are carried out for each area.

In the calculations where the development is not modelled even within the finest areas, the roughness length is set to  $z_0 = 0.5$  m according to the LBM classes for the model area. In cases where buildings in the port areas of Duisburg and Neuss are explicitly modelled, a different roughness length must be applied to the model area. Otherwise, the influence of the buildings

would be taken into account via the roughness length as well as via the explicitly modelled buildings and would thus be imposed "twice". For the model calculations with buildings, a roughness length corresponding to the LBM classes of  $z_0 = 0.2$  m is applied.

The anemometer heights must be converted to other roughness lengths for both model calculations (see **Tab. 7**).

Tab. 7: Conversion of anemometer heights.

Values at location of dispersion calculation									
roughness length (m)	0.01	0.02	0.05	0.1	0.2	0.5	1	1.5	2
displacement height (m)	0.06	0.12	0.3	0.6	1.2	3	6	9	12
anemometer height (m)	4.0	4.0	4.2	5.8	8.2	13.2	19.5	24.7	29.4
anemometer height (0.1m)	040	040	042	058	082	132	195	247	294

### 3.5 Model parameters LASAT

All settings in LASAT were configured in order for the modeling to comply with the standard of the new TA Luft 2021. In particular, this includes the use of the new boundary layer model V5.3 and the PLURIS model integrated in LASAT to calculate the plume rise from hot and impulsive sources. However, dry and wet deposition of  $\text{NO}_x$  were not calculated, which is a conservative approach with regard to concentrations.

In Lagrangian particle models, as realized in LASAT 3.4, the path of virtual particles is traced. The quality of the computations therefore depends, among other things, on the number of released particles (particle rate). The released quantity is determined by the parameter rate. The modeling was performed with  $\text{rate} = 4000$ , which corresponds to the quality level 3 in a calculation with dispersion category statistics instead of a time series in the standard model AUSTAL2000. This is significantly better than the generally recommended quality level.

With  $\text{rate} = 4000$ , statistical uncertainties of 3 % are almost universally achieved for all computation runs in which a simultaneous release of all emissions is applied. This is shown in the example in **Fig. 7** for shipping traffic on the Rhine (left figure) in the overall area (Duisburg - without buildings) and shipping traffic in the port (right figure) in the port area of Duisburg (Duisburg - with buildings). The statistical uncertainty increases to over 3 % only at large source distances because of low immissions.

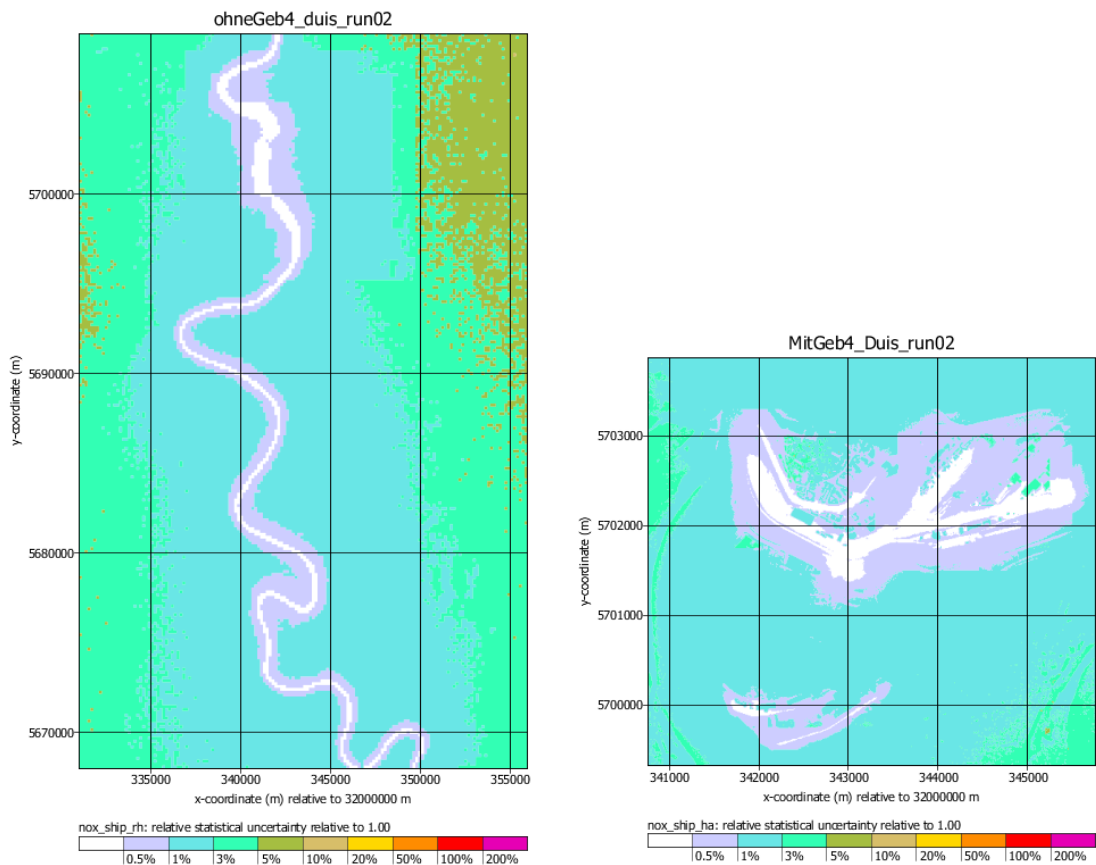


Fig. 7: Illustration of the statistical uncertainties for the example of Duisburg.

## 4. Immissions in the reference year 2018

### 4.1 Preliminary remarks

This chapter presents the results of the immission modellings carried out with LASAT. As described in the previous chapters, the NO<sub>x</sub> immission concentrations were computed separately for individual source groups in order to be able to identify the spatially distributed share of the respective source group in the total immission load. The main focus for the CLINSH project is the determination of the immission share caused by shipping traffic. In this context, a distinction was made between the NO<sub>x</sub> immission concentrations caused by shipping traffic on the Rhine and those caused by shipping traffic and port operations in the port areas.

In the course of the CLINSH project, measurement data were recorded at 28 measuring sites (27 passive samplers (incl. DUMP) and one continuous measuring station (DURH)) in the Duisburg port area. In addition, the measurement data for two traffic measurement stations ("NRW traffic" - DUFW and DUMB) in the Duisburg area were also observed as part of the project. Overall, 30 measurement sites were located in the Duisburg area.

In the Neuss harbour area, NO<sub>2</sub> immission concentrations were determined at 20 measuring locations in total (19 passive samplers and one continuous measuring point). In addition, in the area of Neuss, measurement data are available from the state measurement network (LANUV) for six traffic measuring stations from "NRW traffic", as well as data from a further passive sampler with road influence (DBIL), which could also be considered within the framework of the project. Overall, 26 measurement sites were located in the Neuss area.

In this chapter, the NO<sub>x</sub> percentage shares of the individual source groups for the monitoring sites are determined and presented (polluter analysis). The comparison of spatially modeled ambient air concentrations with locally measured concentrations often causes problems. Therefore, it was decided not to limit the evaluation to a presentation of the polluter shares at the measuring sites and a comparison of the total NO<sub>x</sub> emissions modeled or measured at the measuring points, but also to present the NO<sub>x</sub> shares of the individual source groups in the area. In the following **chapters 4.3** and **4.4**, the spatially modeled NO<sub>x</sub> immission concentrations, the share of shipping traffic in the total NO<sub>x</sub> load on the Rhine and the ports, and the shares of road traffic in the total NO<sub>x</sub> immission load are presented. The shares of the other source groups in the spatially computed total NO<sub>x</sub> immission concentration are compiled in the appendix. The comparison of the modeled and measured NO<sub>x</sub> immission concentrations at the selected measuring sites is given in **chapter 5**.

## **4.2 Consideration of a supra-regional background value for NO<sub>x</sub>**

The dispersion computations were performed with the LASAT model for each source group individually and provide the source group-specific, year-averaged additional load as NO<sub>x</sub> values in the result.

The air pollution at any given point is usually composed of both an existing background pollution in the large-scale advected air (regional background), and the emission sources acting locally on this air (local additional pollution). The latter add up onto the background pollution and subsequently lead to the locally measurable air pollution.

Without the influence of local or regional emission sources, there is usually already a baseline load in all regions of the EU, originating from both long-distance transport of emissions from other regions and from supra-regional sources. In order to be able to determine the total immission concentration properly, this so-called background load must be determined appropriately.

In the scope of the clean air planning, the LANUV has recommended a consistent approach to determine a resilient background pollution for the Rhineland. For the routine modeling of the LANUV, the background pollution "Rhineland" is defined as the mean value of six so-called "background measuring stations" that are not directly dominated by road traffic.

However, since in this study the emissions of the different source groups are determined on a large scale within the entire study area, the estimate based on these background stations, all still containing large-scale immission components, appears to be too conservative. As part of the measurement program in Bimmen-Lobith, the so-called rural background pollution was determined based on measurements, which can largely be classified as unpolluted by other sources. In 2018, this value was approximately 14 µg/m<sup>3</sup> (NO<sub>2</sub>), which, taking into account a stoichiometric conversion corresponds to an annual mean value of 20 µg/m<sup>3</sup> NO<sub>x</sub>. This value was used in the modelings for the CLINSH-Project as the NO<sub>x</sub> background load.

## **4.3 NO<sub>x</sub> immissions in the Duisburg port area - areal representation**

In this chapter, the spatially computed NO<sub>x</sub> total immission concentrations as well as the shares of port immissions (ships in port traffic, ships at berth and general port operations) and immissions from ships sailing on the Rhine are presented, because of the lowest model level. The lowest model level roughly corresponds to an average height of 1.5 m above ground.

### 4.3.1 Total immissions

Fig. 8 shows the modeled total NO<sub>x</sub> emissions for the port area of Duisburg. Clearly recognizable are the high local pollution strands along the Rhine, along the harbour basins and along the busy road axes, for example the BAB 40 (west-east) and the BAB 59 (north-south). Some strongly predominantly ground-level emitting sources also stand out clearly. However, the high NO<sub>x</sub> immission level along the Rhine is dominant in the depicted study area.

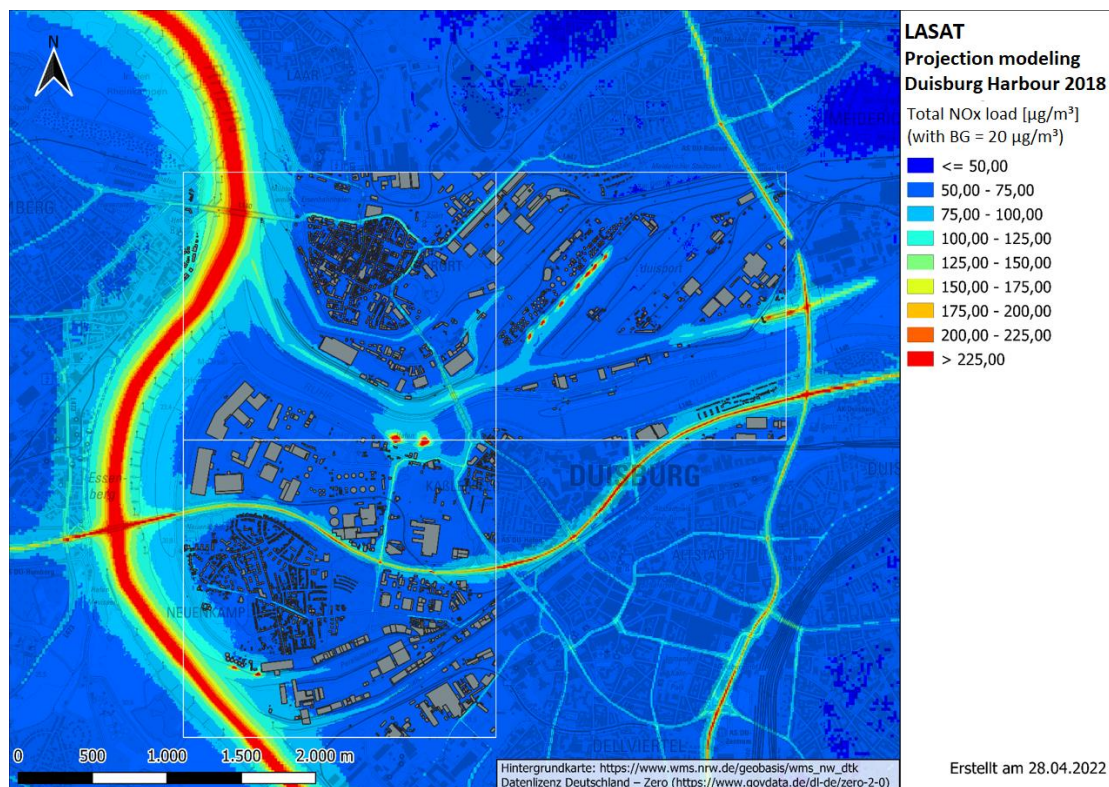


Fig. 8: Total NO<sub>x</sub> immission concentrations in the Duisburg port area - modeled with LASAT.

#### 4.3.2 Shipping traffic in the port, ships at berth and general port operations

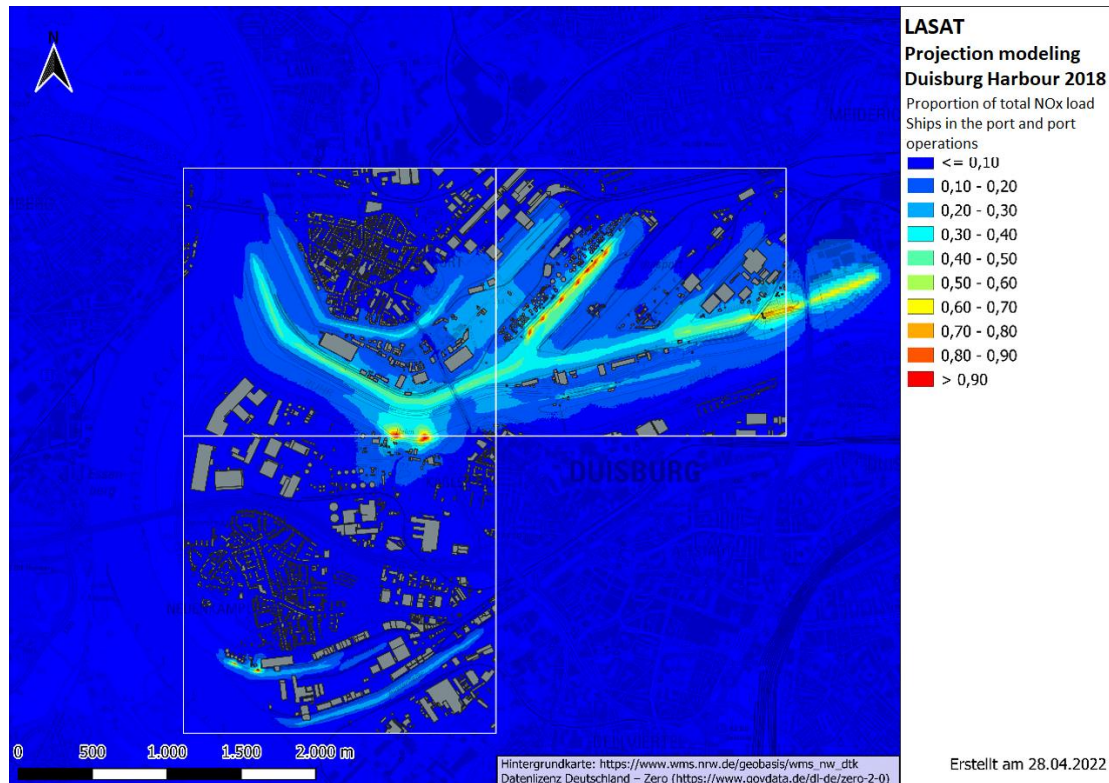


Fig. 9 shows the share of NO<sub>x</sub> immissions caused by port operations in the total NO<sub>x</sub> load for the extended port area of Duisburg. A high NO<sub>x</sub> immission share of almost 40 % to 50 % can be observed along the fairways in the access to the port or in the port itself, which, however, decreases quite quickly with increasing distance from the respective fairway. In addition, locally very high NO<sub>x</sub> immission concentrations can be observed in the immediate vicinity of the tank depots in the area of the south bank of the Ruhr, in the area of the tank depots on the northern bank of the basin between the coal island and the oil island, and further east in the lock area. These high NO<sub>x</sub> concentrations are mainly caused by the unloading operations of the tankers, which are carried out with the onboard pumps. However, the NO<sub>x</sub> immission concentrations also subside quite quickly. In the area of the harbour basins, the share of port immissions mainly ranges between 10 % and 20 %. However, at the periphery of the finely resolved harbour areas in the model, the share of NO<sub>x</sub> immission concentrations due to the port operations is well below 10%. On the northwestern boundary of the Duisburg urban area, the proportion of NO<sub>x</sub> immissions lies at 5 % and below.

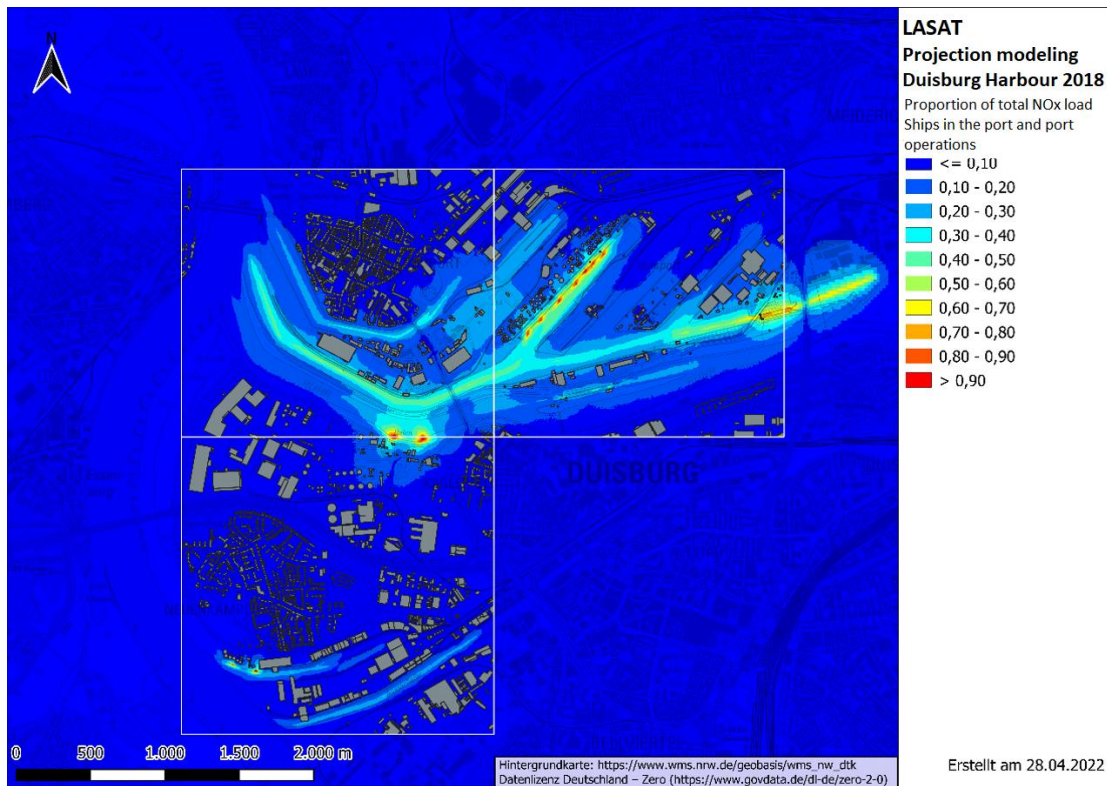
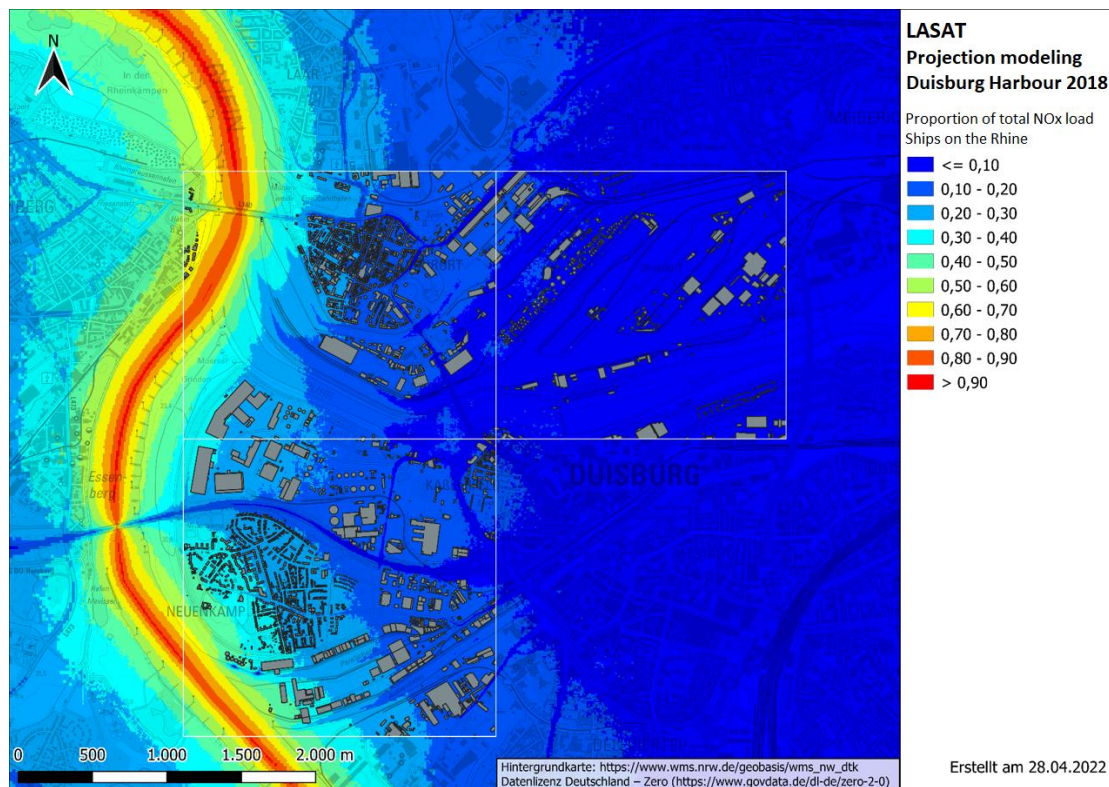


Fig. 9: Proportion of NO<sub>x</sub> immission concentrations caused by port emissions in the Duisburg port area - modeled with LASAT (a value of 1.0 corresponds to a share of 100 %).

### 4.3.3 Ships on the Rhine

**Fig. 10** shows the proportion of total NO<sub>x</sub> emissions caused by shipping traffic on the Rhine for the extended port area of Duisburg. As expected, the highest NO<sub>x</sub> immission concentrations are found along the shipping channel. They account for 80-90 % of the total NO<sub>x</sub> immissions. The proportion decreases to 70-80 % towards the shore area. With increasing distance to the Rhine, a further continuous decrease is to be expected. On the right bank of the Rhine, the proportion in the area of the nearest settlement Laar ranges from 30 - 40 % in the western part, while on the eastern border it is still 20-30 %. Up to the Duisburg city area, the share of immissions from ships on the Rhine in the total immissions decreases to about 10 %. On the left bank of the Rhine, the share attributable to Rhine shipping ranges between 30 and 40 % in Homberg and between 20 and 30 % in the Hochemmerich area, according to model calculations.



**Fig. 10:** Proportion of NO<sub>x</sub> immission concentrations caused by shipping traffic on the Rhine River in the Duisburg port area - modeled with LASAT (a value of 1.0 corresponds to a share of 100%).

#### 4.3.4 Road Traffic

**Fig. 11** shows the share of NO<sub>x</sub> immissions caused by road traffic in the total NO<sub>x</sub> load for the extended port area of Duisburg. Very high shares can be seen along the roads, as is to be expected. In particular, the two highways BAB 40 and BAB 59 stand out strikingly. The shares decrease continuously with increasing distance from the roadways. In the port area, they range generally between 20 % and 30 %. In the area of the Altstadt (southeast of the harbour), with shares of 30 % and 40 %, it is evident that road traffic is the dominant source of NO<sub>x</sub> pollution here.

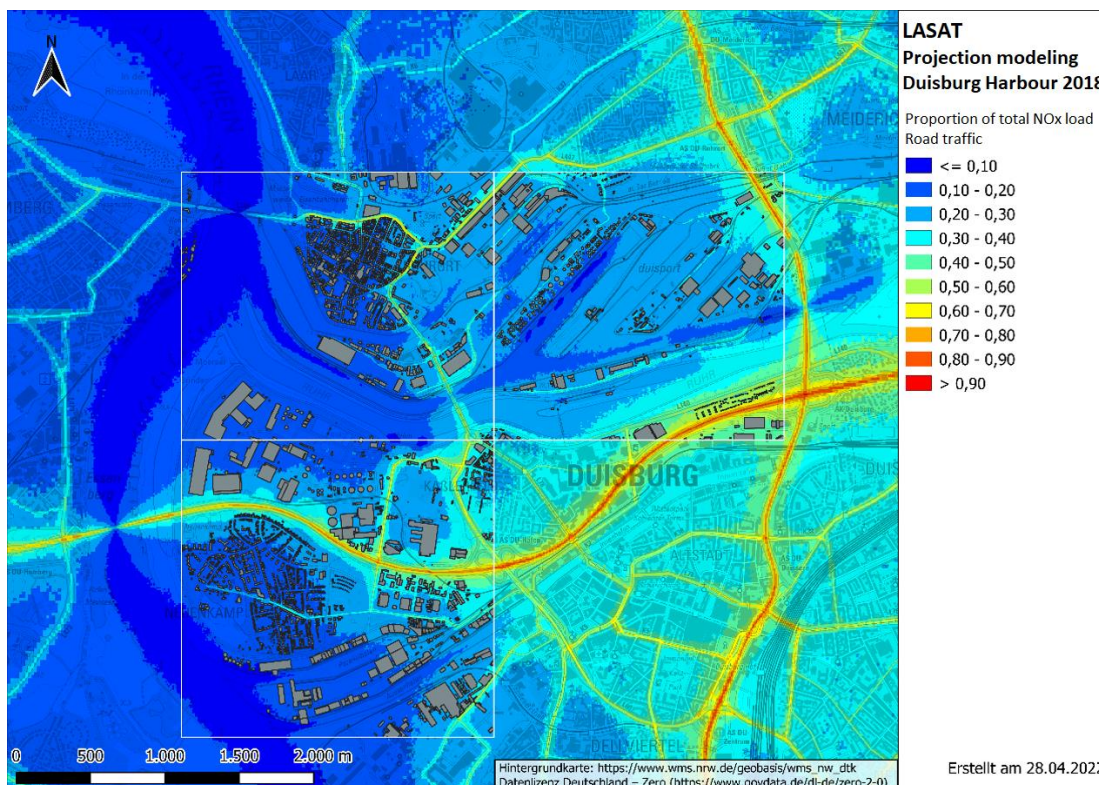


*Fig. 11: Proportion of NO<sub>x</sub> immission concentrations caused by road traffic in the Duisburg port area - modeled with LASAT (a value of 1.0 corresponds to a share of 100 %).*

#### 4.3.5 Industry

In the 25\*41 km overarching study area, about 19,500 t of NO<sub>x</sub> were emitted from industrial facilities requiring permits in 2018. However, since these quantities are usually emitted via stacks at a higher altitude, their ground-level local effect on air quality in the study area remains rather low. **Fig. 12** shows the ground-level effect of industrial emissions in the Duisburg port area. In 2018, 1,277 t NO<sub>x</sub> were emitted by industrial sources in this area.

When looking at the chart, it must be noted that the scaling here differs from those of the other charts. In most settlement areas, the industrial polluter share is in the order of about

6 % - 12 %. In a few places in the study area, there are locally limited higher impact shares of over 18 % (shown in red).

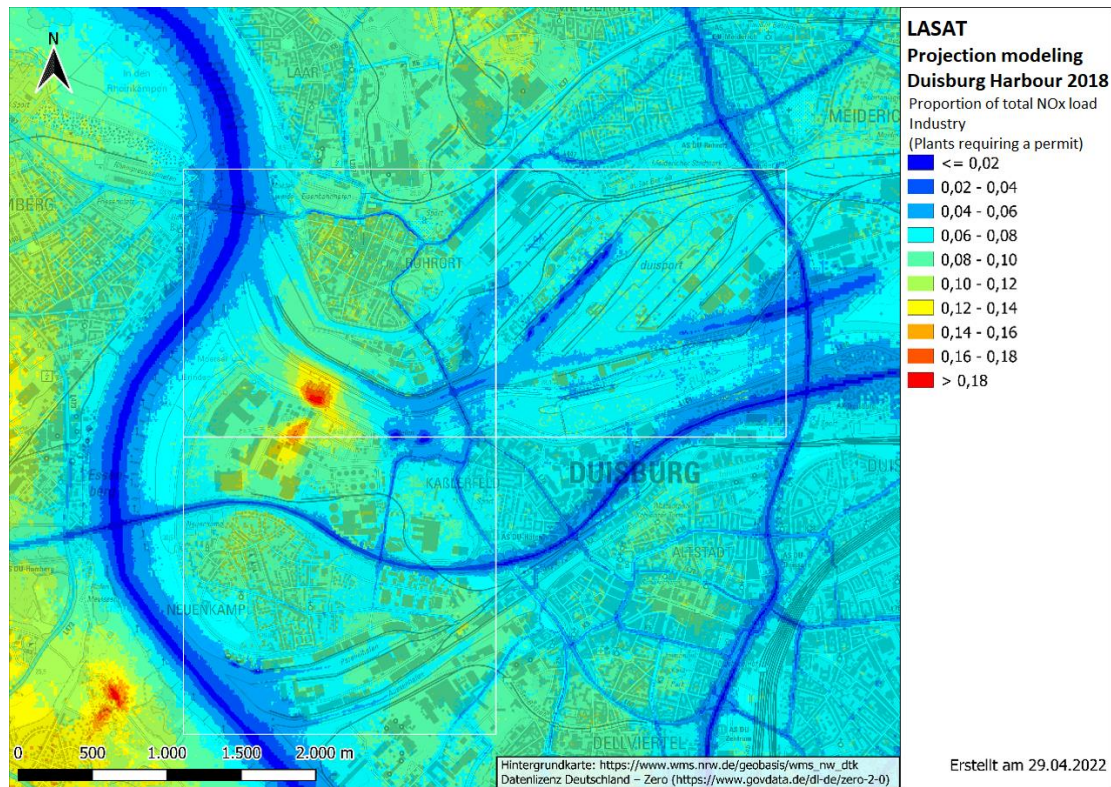


Fig. 12: Proportion of NO<sub>x</sub> immission concentrations caused by industrial sources in the Duisburg port area - modeled with LASAT (a value of 0.1 corresponds to a share of 10 %).

#### 4.4 NO<sub>x</sub> immissions in the Neuss port area - areal representation

In this chapter, the spatially modeled immission shares of the Rhine ship immissions as well as the port immissions and the NO<sub>x</sub> total load concentrations resulting from the lowest model level are presented. The lowest model level roughly corresponds to a mean height of 1.5 m above ground level.

##### 4.4.1 Total immissions

Fig. 13 shows the spatially modeled total NO<sub>x</sub> immissions for the port area of Neuss. Here, again, the high local load strands along the Rhine, along the harbour basins and along the busy road axes, for example the Willy Brandt Ring, the Düsseldorfer Straße, the BAB 52 and the B7, are evident. A few strong, predominantly ground-level emitting sources also stand out clearly. However, the high NO<sub>x</sub> immission level along the Rhine is dominant in the study area shown.

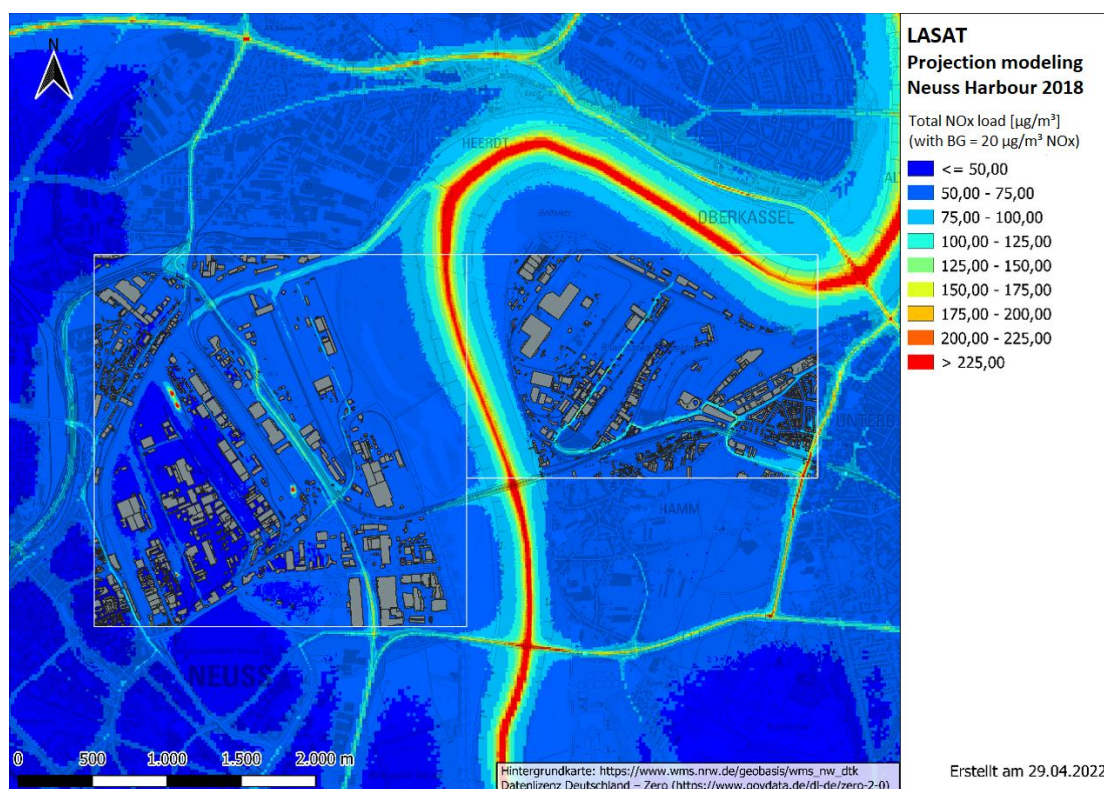


Fig. 13: Total NO<sub>x</sub> immission concentrations in the Neuss port area - modeled with LASAT.

#### 4.4.2 Shipping traffic in the port, ships at berth and general port operations

Fig. 14 shows the proportion of NO<sub>x</sub> immissions caused by port operations in the total NO<sub>x</sub> immission for the extended port area of Neuss. Along the fairways in the approach to the port or in the port itself, a high NO<sub>x</sub> immission share of almost 40 to 50 % can be observed, which, however, also in Neuss decreases quite quickly with increasing distance from the respective fairway. In addition, locally very high NO<sub>x</sub> immission concentrations can be seen in the immediate vicinity of the tank farms and other industrial sources in Basin III, however, these also subside quite quickly. At the periphery of the port areas, which are finely resolved in the model, the share of NO<sub>x</sub> immission concentrations due to the port operations is well below 10 %.

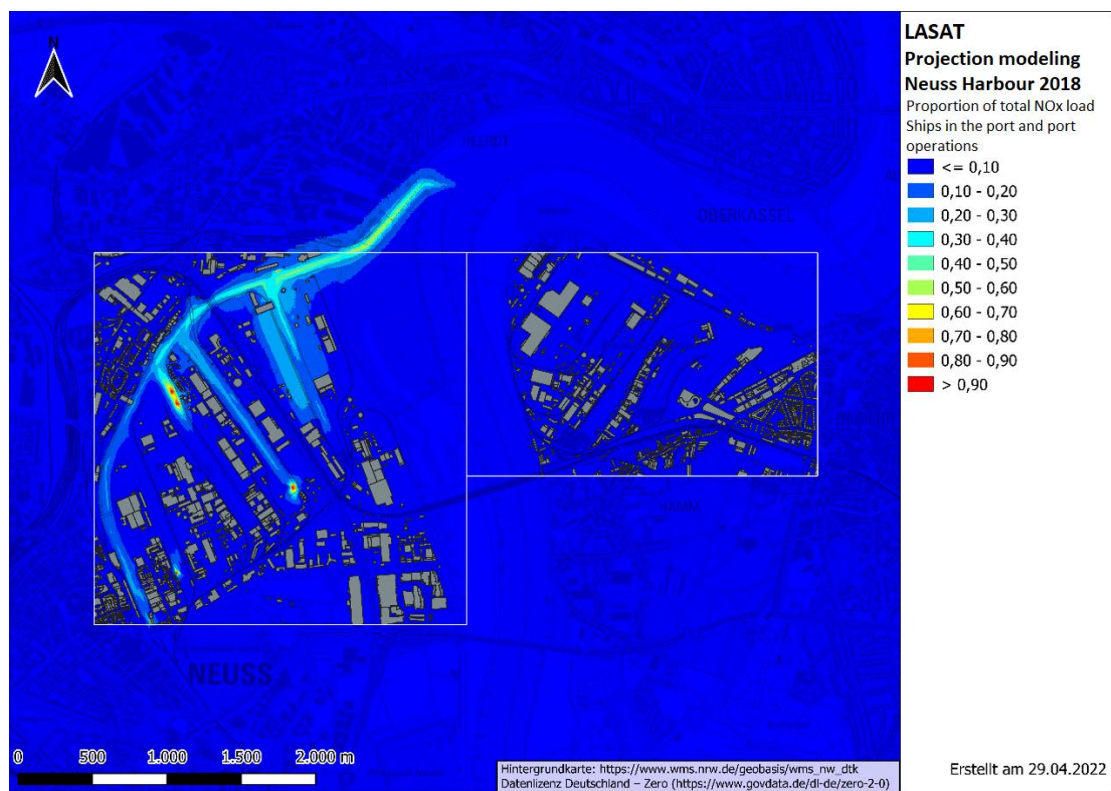


Fig. 14: Proportion of NO<sub>x</sub> immission concentrations caused by port emissions in the Neuss port area - modeled with LASAT (a value of 1.0 corresponds to a share of 100 %).

#### 4.4.3 Ships on the Rhine

Fig. 15 shows the proportion of total NO<sub>x</sub> immissions caused by shipping traffic on the Rhine for the extended port area of Neuss. As expected, like in the Duisburg area, the highest NO<sub>x</sub> immission concentrations are found along the shipping channel. They range from 80-90 % of the total NO<sub>x</sub> immissions and decrease to 60-70 % by the time they reach the shoreline. With increasing distance to the Rhine, a further continuous decrease is to be expected. On the right bank of the Rhine, the proportion in the area of the Düsseldorf port lies at 20-30 %. In the area of the "Am Handelshafen" housing, the share is still over 20 %. On the left bank of the Rhine, the share due to emissions from Rhine shipping ranges from 10 to 20 % according to model calculations in Neuss, and up to 10 % in the area of the housing in Weissenberg, which lies to the west of the port area and the railroad facilities, at up to 10 %.

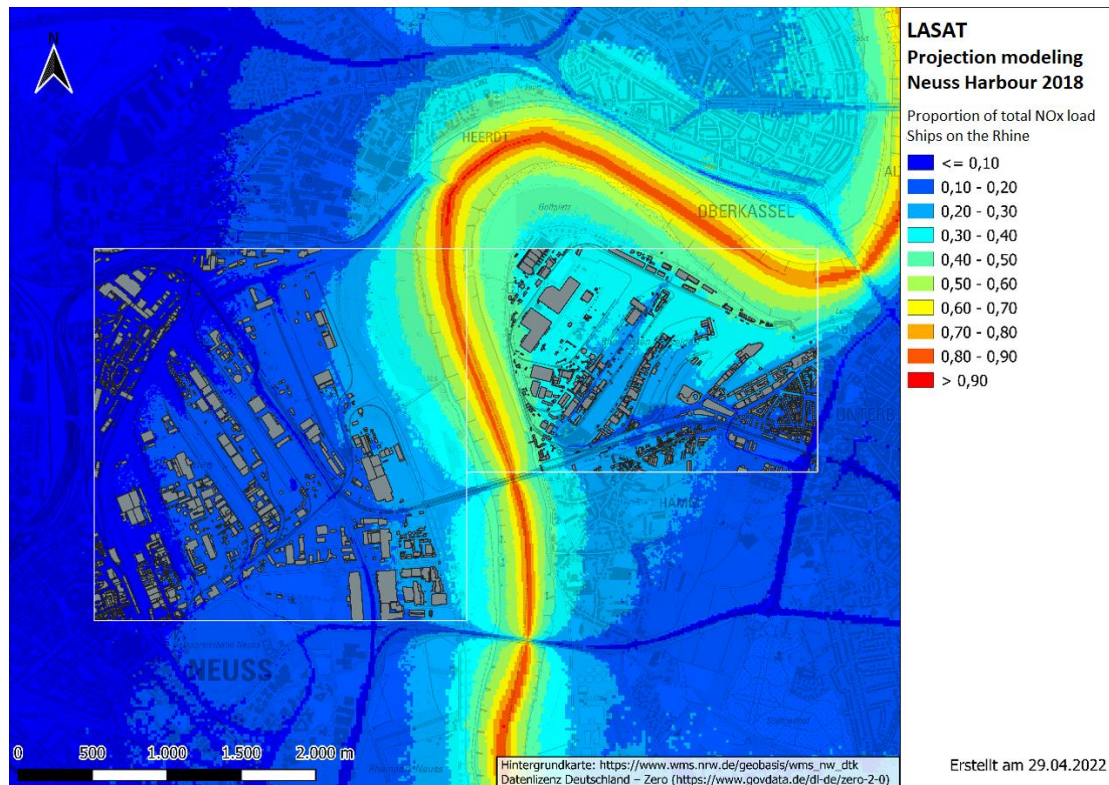


Fig. 15: Proportion of NO<sub>x</sub> immission concentrations caused by shipping traffic on the Rhine River in the Neuss port area - modeled with LASAT (a value of 1.0 corresponds to a share of 100%).

#### 4.4.4 Road traffic

Fig. 16 shows the shares of NO<sub>x</sub> immission concentrations in the total NO<sub>x</sub> load in the extended port area of Neuss that are attributable to road traffic emissions. Similar to Duisburg, the heavily trafficked roads with very high shares of road traffic immissions are also clearly visible in Neuss. The B1 and the B7/BAB52 are prominent in this respect. In the port area itself, the share of road traffic is predominantly 10 % to a maximum of 20 %, with occasional shares of 30 %. In the area of the city center (southwest of the port), but also on the right side of the Rhine south of the port of Düsseldorf, NO<sub>x</sub> immission shares of between 20 % and 40 % can also be seen in the area. As in Duisburg, it is clear that road traffic in the inner city area is the dominant source of nitrogen oxide pollution in residential areas.

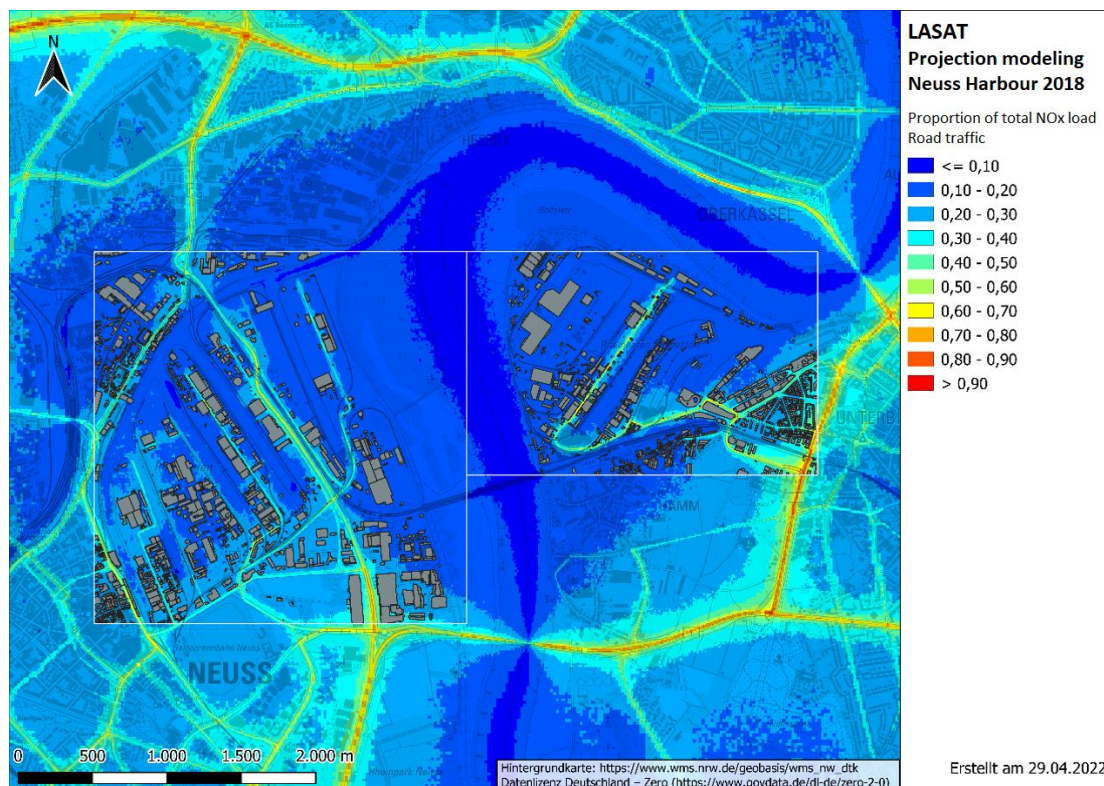


Fig. 16: Proportion of NO<sub>x</sub> immission concentrations caused by road traffic in the Neuss port area - modeled with LASAT (a value of 1.0 corresponds to a share of 100 %).

#### 4.4.5 Industry

In the study area shown in Fig. 17, 404 t NO<sub>x</sub> were emitted in 2018 by installations requiring a permit. As in Duisburg, their ground-level local impact on air quality remains rather low in the Neuss/Düsseldorf port area.

When looking at the chart, it must be noted that the scaling here differs from that of the other charts. The cause shares of industrial emissions in the settlement areas are in the range of 4 % - 8 %. At three locations in the study area, locally higher ground-level impact shares of industrial emissions of up to 18 % (shown in red) can also be seen in Neuss/Düsseldorf.

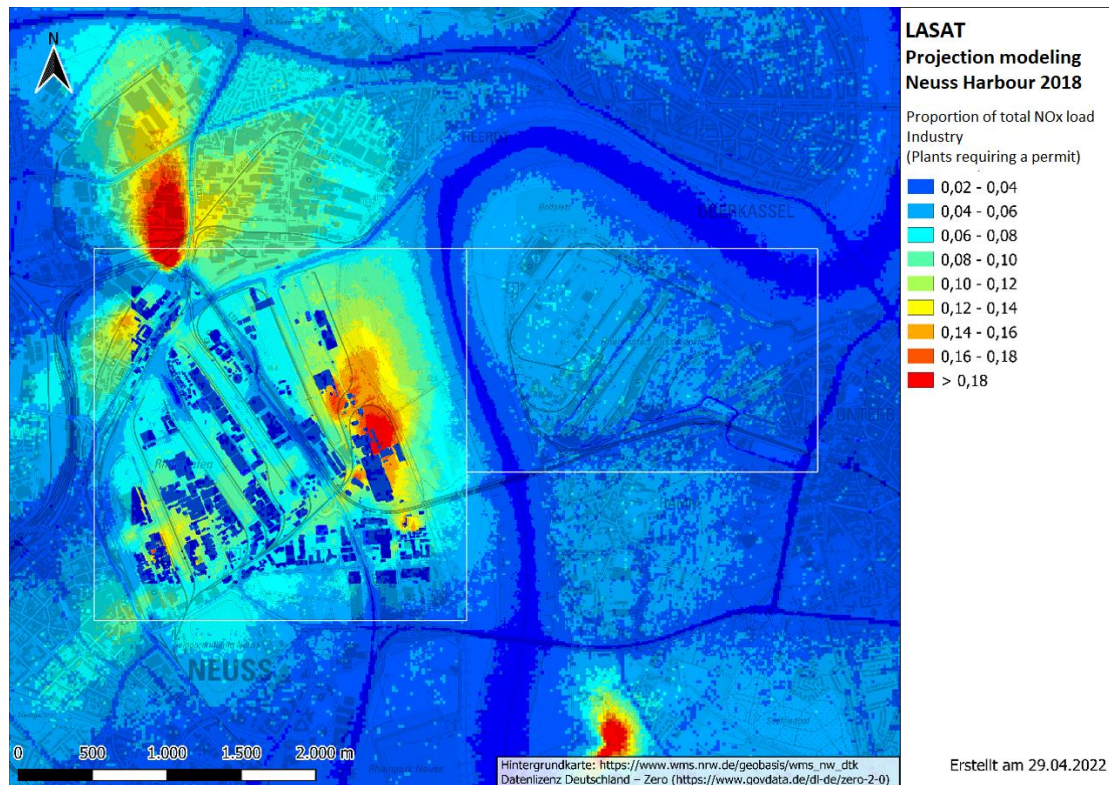
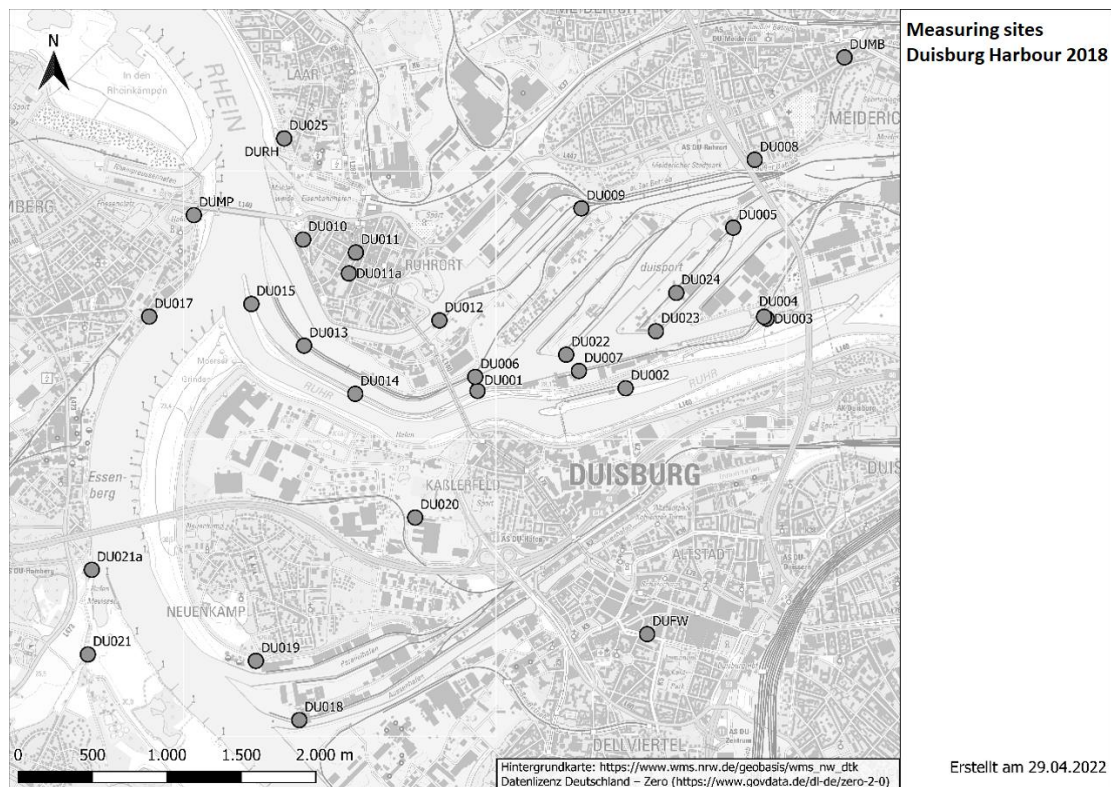


Fig. 17: Proportion of NO<sub>x</sub> immission concentrations caused by industrial sources in the Duisburg port area - modeled with LASAT (a value of 0.1 corresponds to a share of 10 %).

#### 4.5 Measuring sites in the model area

As mentioned in **chapter 4.1**, a polluter analysis was derived from the immission modeling for 57 measurement locations. The results of the polluter analysis are documented below in various forms of presentation. This is followed by a comparison of the measurement results from 2018 with the immission concentrations modeled at the respective measurement site. The modeled and measured NO<sub>x</sub> annual mean values are compared. Subsequently, an analysis of the observed deviations between modeling and measurement is carried out (see **chapter 5.1.2**).

**Fig. 18** and **Fig. 19** provide a cartographic overview of all measurement locations with their respective codes for the two port areas.



**Fig. 18:** Location of the measuring sites in the area of the Duisburg Harbour.

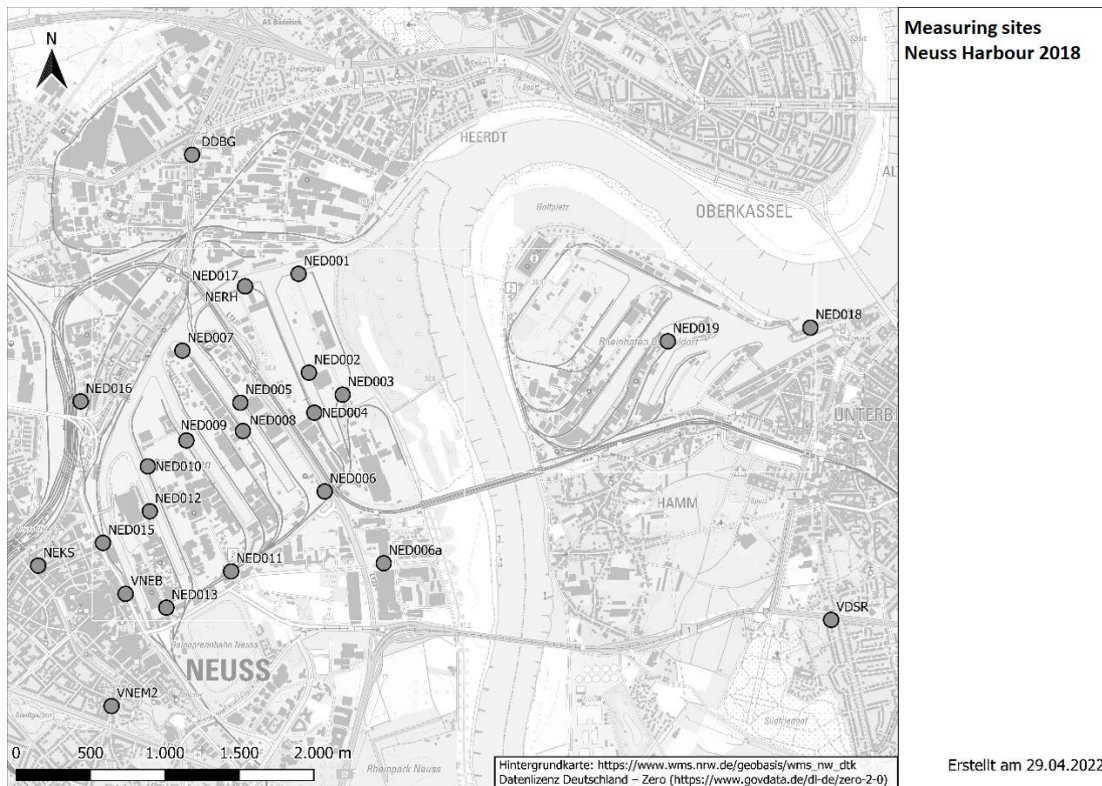


Fig. 19: Location of the measuring sites in the area of the Neuss Harbour

#### 4.5.1 Calculated source group percentages of NO<sub>x</sub> immissions at the measuring sites

The NO<sub>x</sub> shares in the total NO<sub>x</sub> immission for the respective differentiated source groups were computed for each of the measuring sites. They are shown for the two port areas in the following two bar charts. It is noticeable in the Duisburg port area (Fig. 20) that the immissions due to the industrial/commercial sources are in a range below 10 % of the total NO<sub>x</sub> immissions at all measuring point locations. The NO<sub>x</sub> emissions caused by small combustion plants and domestic heating range from about 3 % to 6 % at almost all measuring points, the share caused by rail traffic amounts to a maximum of 3 %. The source group "other traffic" (off-road traffic and aviation) also has only small shares with a maximum of 4 %.

Large differences occur in the immission shares at the individual measuring point locations for the source groups ships on the Rhine, road traffic and ships in the port. Since these source groups are sources with low emission release heights, the proportions thus roughly reflect the location of the measuring point. For example, the measuring sites DU015, DU018 and DU019 and DURH all show a high immission share due to shipping traffic on the Rhine. They are located on the right bank of the Rhine at a maximum distance of 200 m from the shore.

The stations DU017, DU021, DU021a and DUMP, which are all located on the left bank of the Rhine and partly even closer to the river bank, show even higher shares due to shipping traffic.

The stations DU008 as well as DUMB and DUFW show relatively high contributions from road traffic. These are measuring stations in the immediate vicinity of roads with high levels of traffic. A very high proportion due to shipping traffic in the harbour area can be seen at measuring stations DU003, DU004 and, to a somewhat lesser extent, DU006 and DU013. These are all located close to harbour basins and/or landing stages or in the lock area. The percentage of regional background also varies accordingly; since the background concentration was considered constant for the whole study area, it also reflects the level of the measured total NO<sub>x</sub> immission: The higher the percentage of the background NO<sub>x</sub> concentration, the lower the total NO<sub>x</sub> immission.

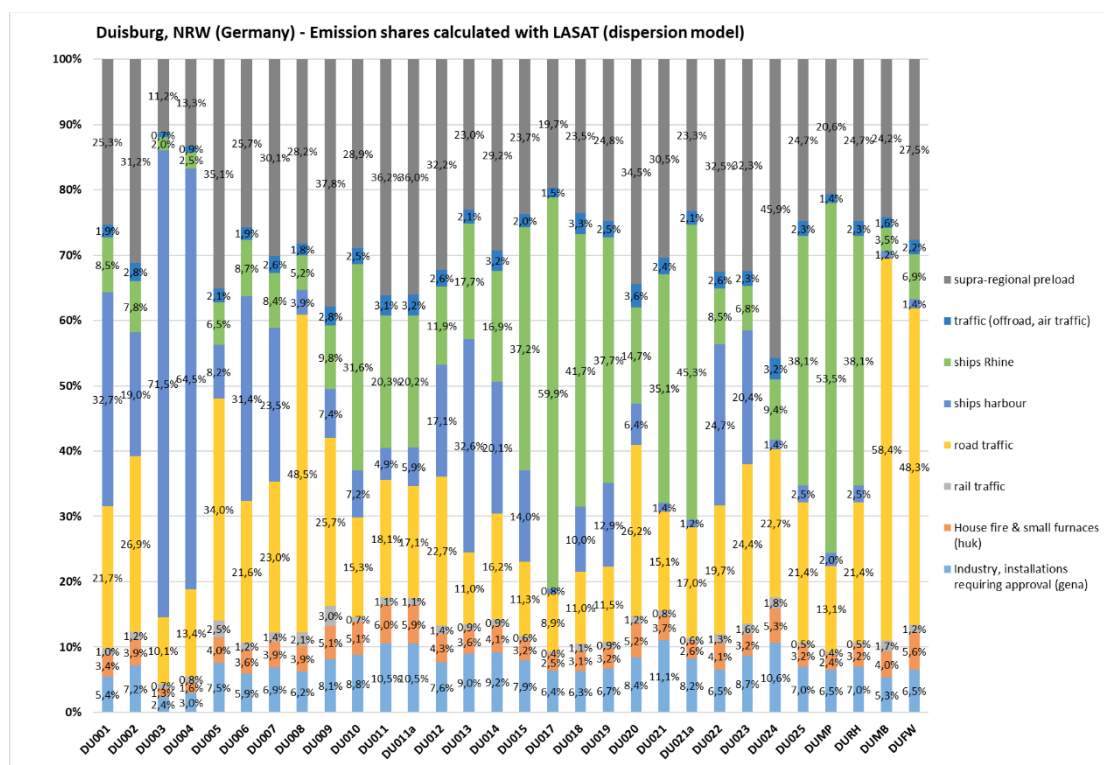


Fig. 20: NO<sub>x</sub> source group percentages (Duisburg Harbour) - modeled with LASAT.

Fig. 21 shows the polluter shares at the measuring point locations in the Neuss port area. Compared to the port area in Duisburg, the calculated share caused by industry/commerce is significantly higher at some measuring sites, e.g. at stations NED003 and NED004. The proportion of small combustion plants/domestic heating is at a similarly low level as in the Duisburg port area. At most of the measurement sites, the share of rail traffic is somewhat higher than in the Port of Duisburg. At the maximum, the proportion caused by rail traffic is 19.6 % (NED016), located directly on the tracks to the north of the Neuss train station. Except for this measurement location, the three source groups considered in advance have a maximum share of approx. 20 %.

A high share due to shipping traffic on the Rhine with a share clearly above 20 % can be seen at the measurement sites NED006a, NED018 and NED019, which also have the smallest distance to the shore area. Quite high shares by road traffic show the stations NED006, NED012, NED013, NED015 and VNEB within the port area and of course, the traffic stations DBIL, VDSR, DDBG VNEM2 and NEKS, which are all located outside the actual port area. The highest percentages due to shipping traffic in the port area with significantly more than 20 % are found at the stations NED017 and NERH, which are also quite close to port basins and/or docks. The regional background percentage varies similarly to the port area of Duisburg.

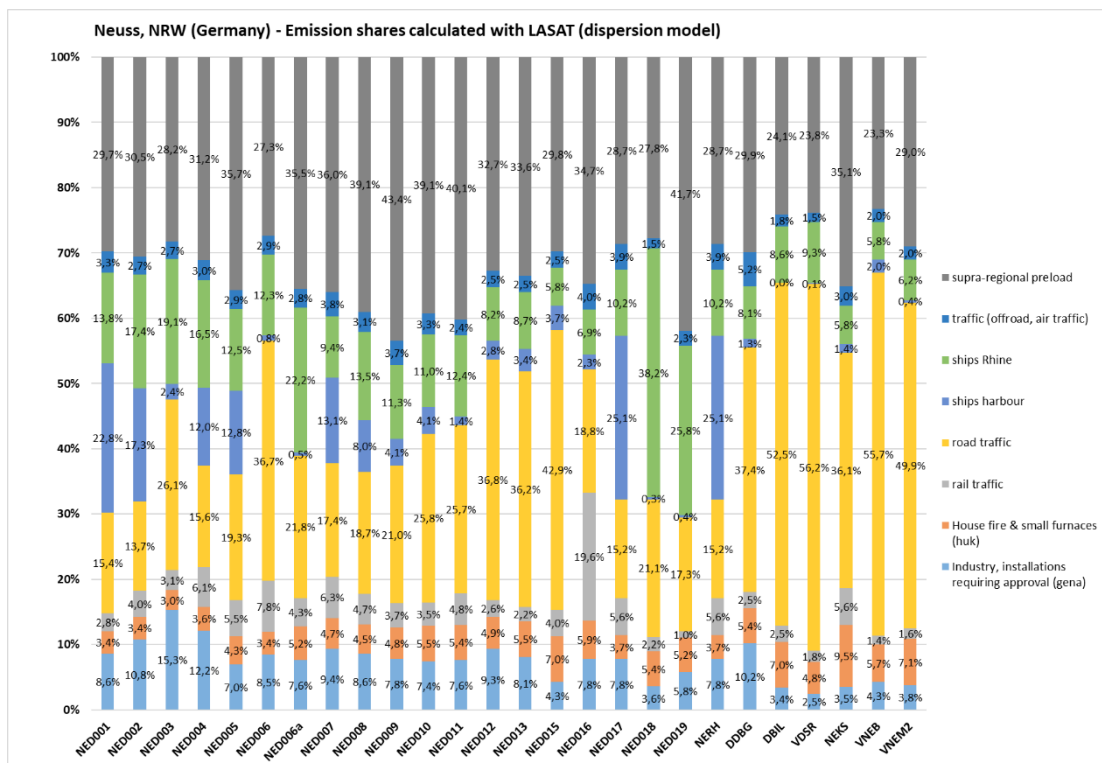


Fig. 21: NO<sub>x</sub> source group percentages (Neuss Harbour) - modeled with LASAT.

#### 4.5.2 Source group shares of NO<sub>x</sub> immissions at selected monitoring stations

In the following, the source group shares at individual selected measuring points are examined in more detail:

**Fig. 22** shows the modeled pollution shares of the emitters at the CLINSH measuring station Duisburg-Rheinhafen (DURH, NO<sub>2</sub> annual mean 2018: 27 µg/m<sup>3</sup>). The emission shares of ships sailing on the Rhine in the NO<sub>x</sub> pollution lie here at about 38 %. General "background pollution" (about 25 %) and road traffic in Duisburg (about 21 %) also contribute significant pollution shares. Emissions from ships in the port and from port operations play only a minor role at this station, accounting for about 2.5 % of pollution. The ground-level effects of the industrial emissions present in the study area also play a rather subordinate role with about 7 % load share of the NO<sub>x</sub> immissions.

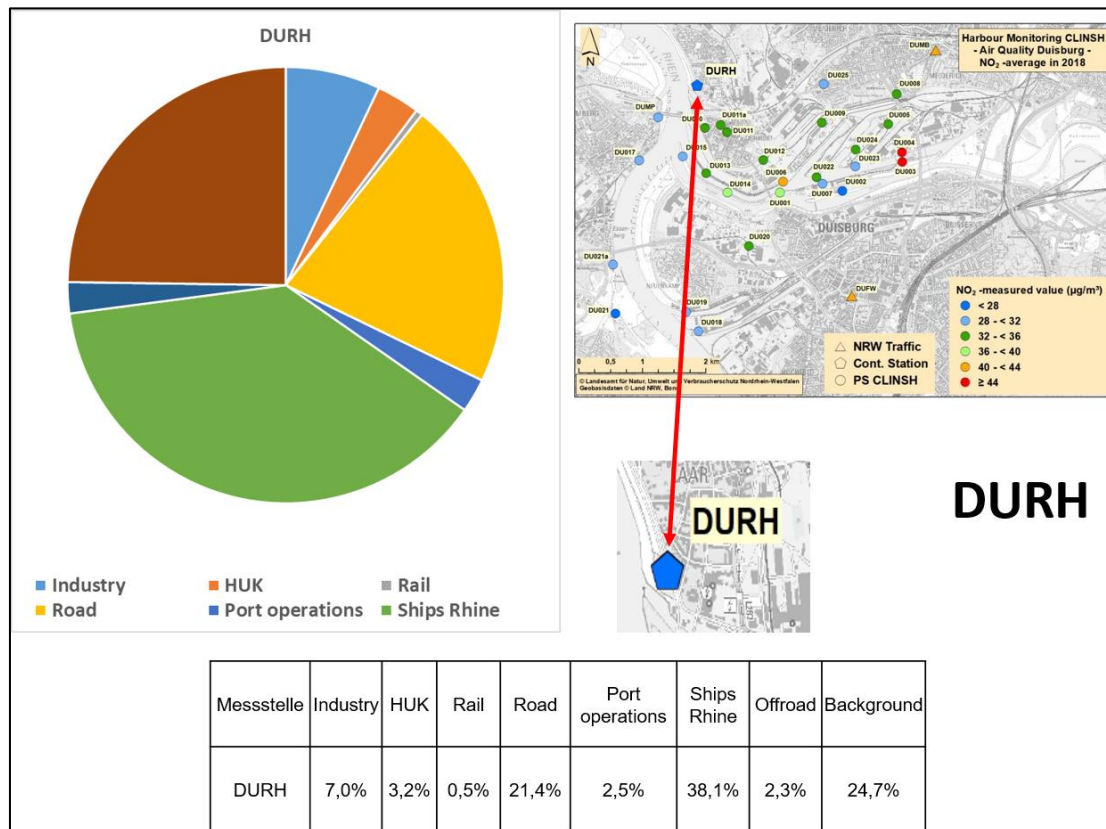


Fig. 22: Polluter analysis for the automatic measuring station Duisburg-Rheinhafen (DURH)

As expected, the measuring points located directly in the port have a high proportion of pollution caused by ships sailing and docking in the port area (port operations), including other emitters from general port operations. **Fig. 23** shows the respective load shares using the example of measuring site DU001. The port operations achieve a share of pollution (NO<sub>x</sub>) of about 33 %, closely followed by the background pollution (25 %) and the Duisburg road traffic. The share of ships sailing on the Rhine still reaches 8.5 % at this measuring site.

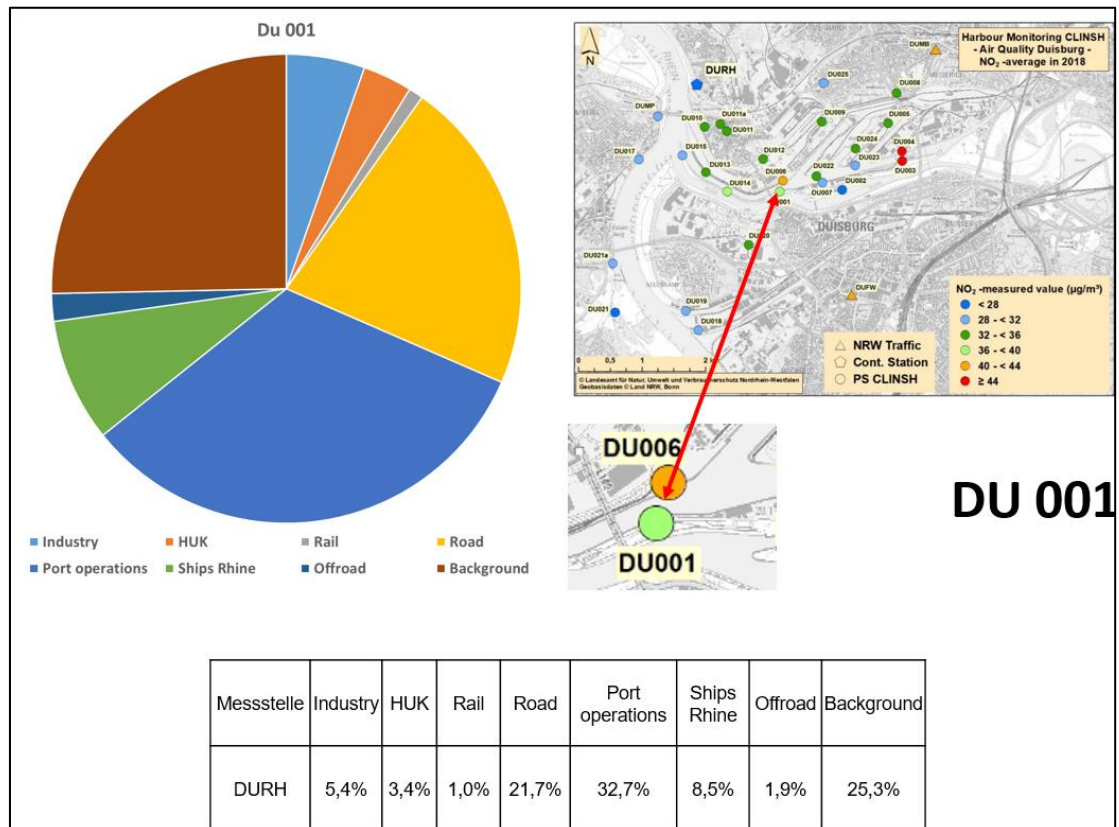


Fig. 23: Polluter analysis for the Duisburg CLINSH measuring site DU001.

Measuring station DU011 is located in a quiet residential area with small residential streets between the Rhine and the harbour (Fig. 24). The EU limit value for NO<sub>2</sub> applicable here was safely complied with in 2018 with an annual mean of 35 µg/m<sup>3</sup>. The cause analysis for NO<sub>x</sub> pollution shows the highest pollution share for the background pollution with about 36 %. Ships on the Rhine reach a share of about 20 %, followed by road traffic (18 %), the ground-level effect of industrial emissions (about 1 %) and port operations (about 5 %).

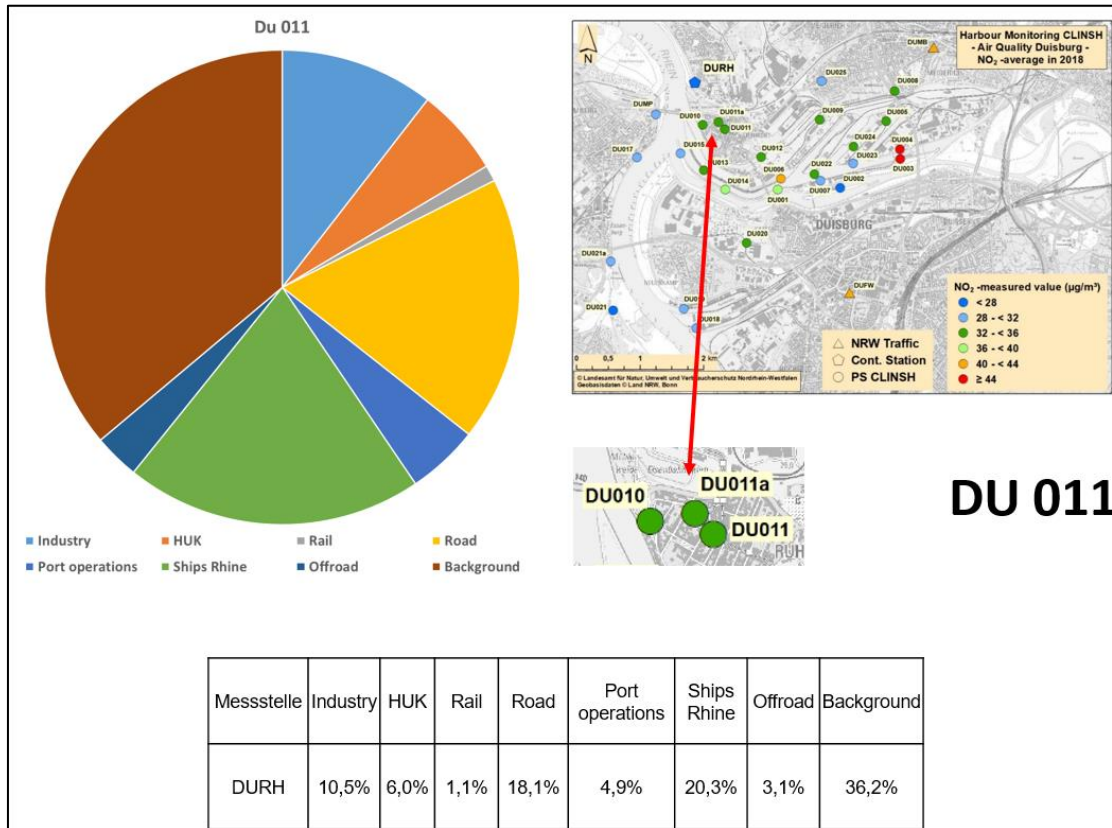


Fig. 24: Polluter analysis for the Duisburg CLINSH measuring site DU011.

The traffic measuring station DUMB ( $\text{NO}_2$  annual mean in 2018:  $42 \mu\text{g}/\text{m}^3$ ) set up at a traffic hotspot in Duisburg-Meiderich, shows a clearly different polluter profile for the  $\text{NO}_x$  pollution (Fig. 25). Here, as expected, road traffic has a dominant polluter share of the  $\text{NO}_x$  pollution with more than 58 %. The second highest contribution to the present air pollution is made by background pollution with about 24 %. Emissions from shipping traffic on the Rhine (approx. 3.5 %) and port operations (1.2 %) play only a minor role.

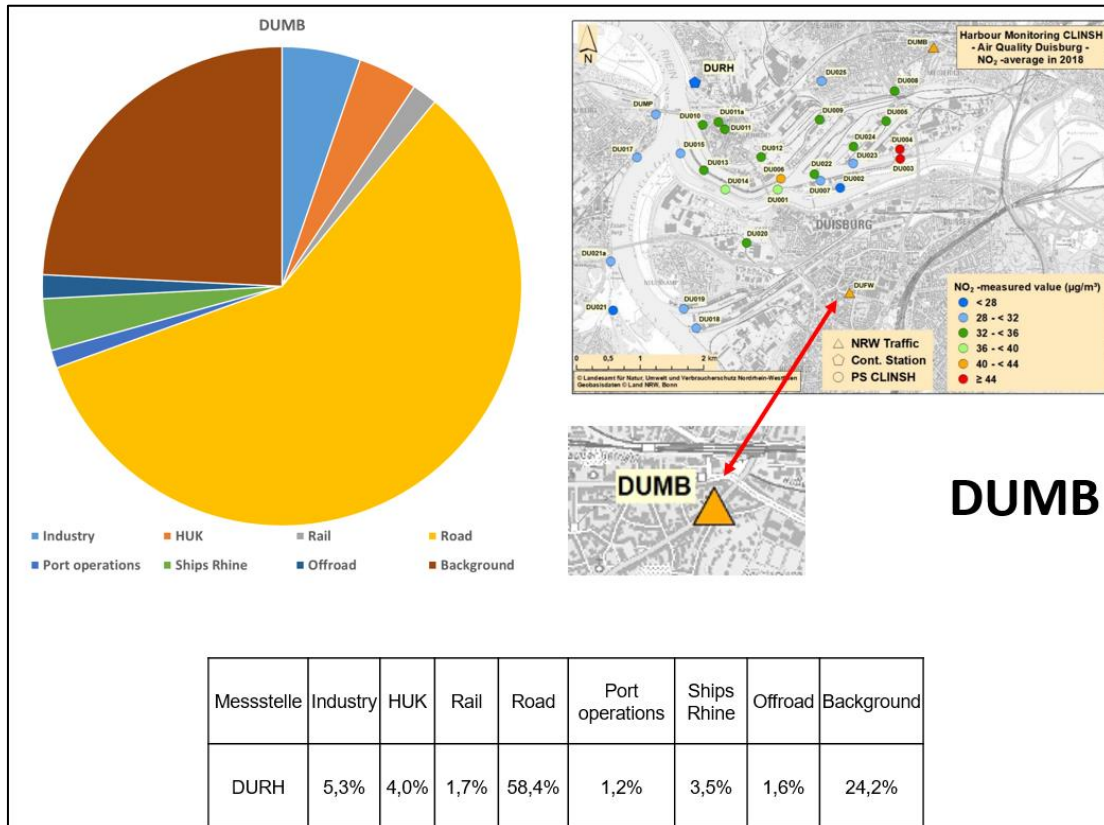


Fig. 25: Polluter analysis for the traffic measuring site Duisburg Meiderich Bahnhofstraße (DUMB).

Similar polluter profiles can also be seen in the Neuss/Düsseldorf study area. The analysis of the modeling for the pollution situation at the automatic measuring station Neuss Rheinhafen (NERH, NO<sub>2</sub> annual mean value in 2018: 33 µg/m<sup>3</sup>), located directly in the port area (Fig. 26), resulted in the following pollution profile for NO<sub>x</sub>: The background pollution represents the largest pollution share for NO<sub>x</sub> with about 28 %. As expected, port operations follow in second place with about 25 %. Here in the port, the road traffic also has a significant NO<sub>x</sub> load share with 15 %. Ship emissions on the Rhine (lee side) east of the measuring point cause about 10 %, followed by the ground level effect of industrial emissions with about 8 %.

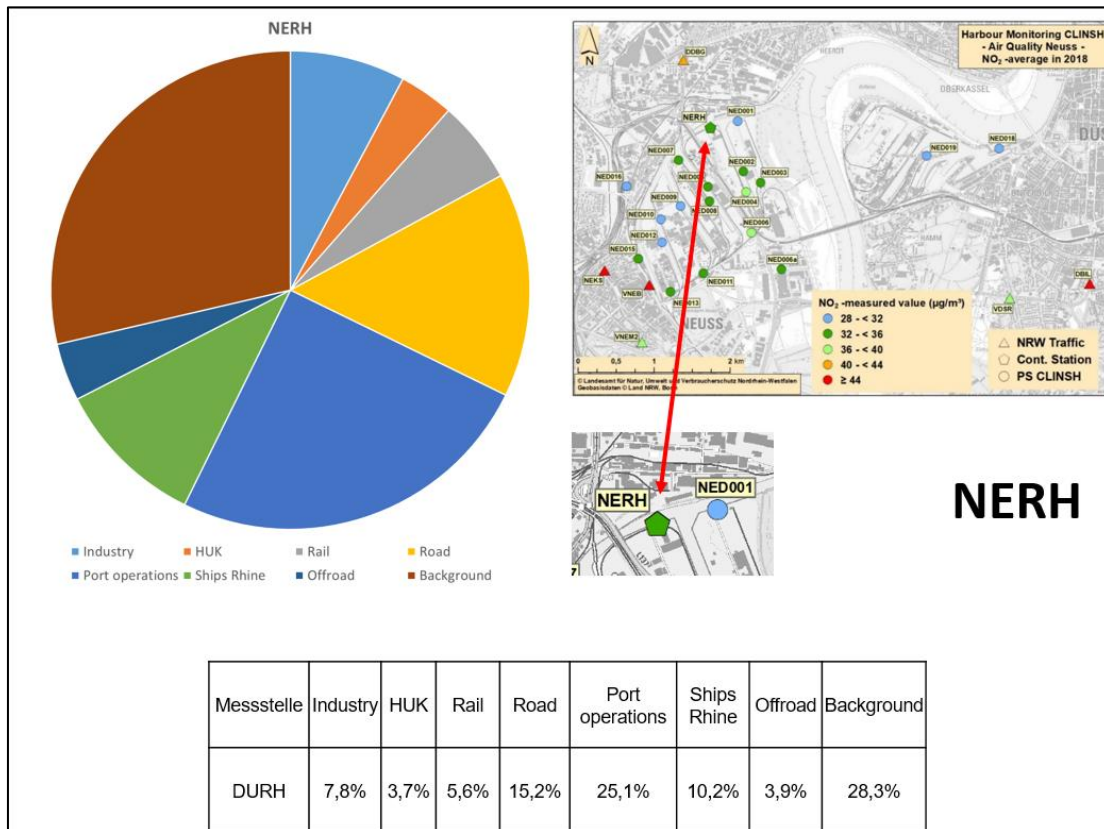


Fig. 26: Polluter analysis for the automatic measuring station Neuss-Rheinhafen (NERH)

At the measuring point NED018 near the Rhine (annual mean value NO<sub>2</sub> in 2018: 31 µg/m<sup>3</sup>) on the eastern bank of the Rhine, the shipping traffic on the Rhine results in high pollution shares of about 38 % for NO<sub>x</sub>, as expected (Fig. 27). This is followed by the background pollution with about 28 %. Emissions from road traffic in Neuss/Düsseldorf contribute about 21 % to the NO<sub>x</sub> load, followed by domestic heating and small combustion plants with about 5 %. Emissions from port operations play virtually no role here, with a pollution share of about 0.3 %.

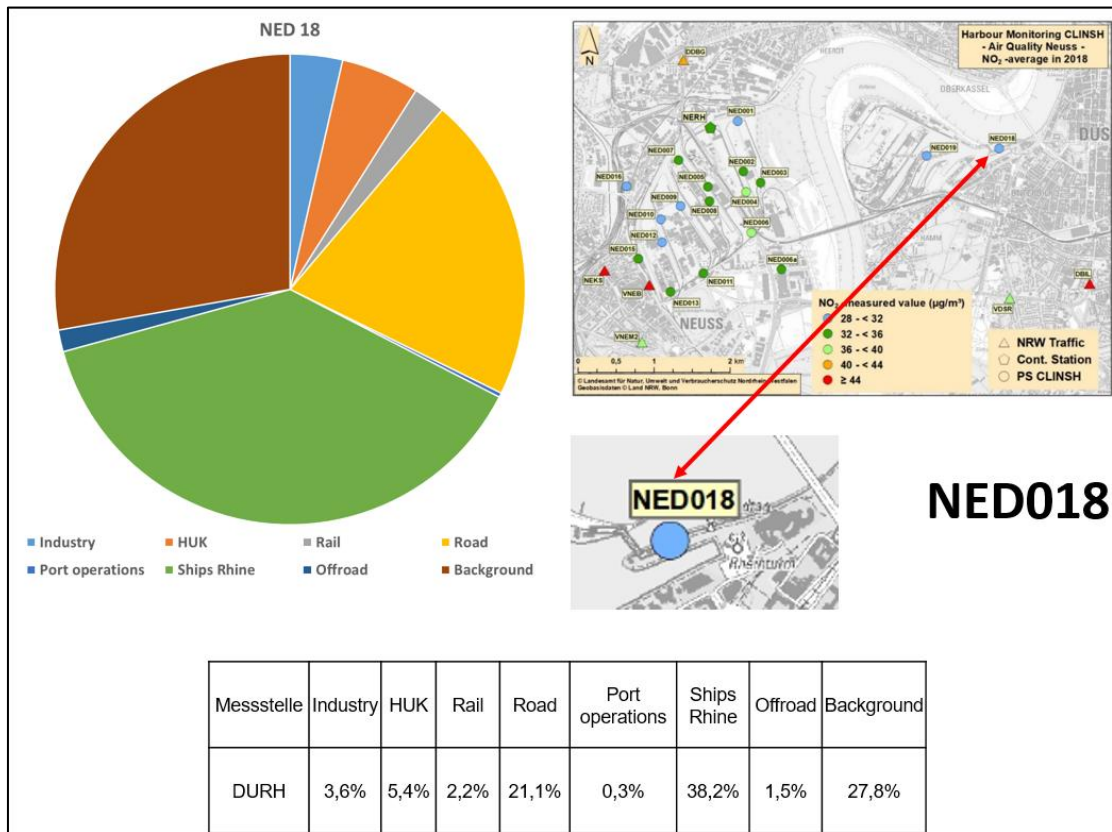


Fig. 27: Polluter analysis for the Neuss CLINSH measuring site NED018.

The traffic measuring station Düsseldorf-Südring (VDSR, NO<sub>2</sub> annual mean value in 2018: 39 µg/m<sup>3</sup>) of the state measuring network, located in the Düsseldorf settlement area, shows the NO<sub>x</sub> pollution patterns typical for traffic measuring stations (Fig. 28). Road traffic plays a dominant role here with a pollution share of 56 %, followed by background pollution with a share of about 24 %. NO<sub>x</sub> emissions from shipping traffic on the Rhine (about 9 %) and from domestic heating and small combustion plants (about 5 %) play only a minor role. The share of port operations of only about 0.1 % is negligible.

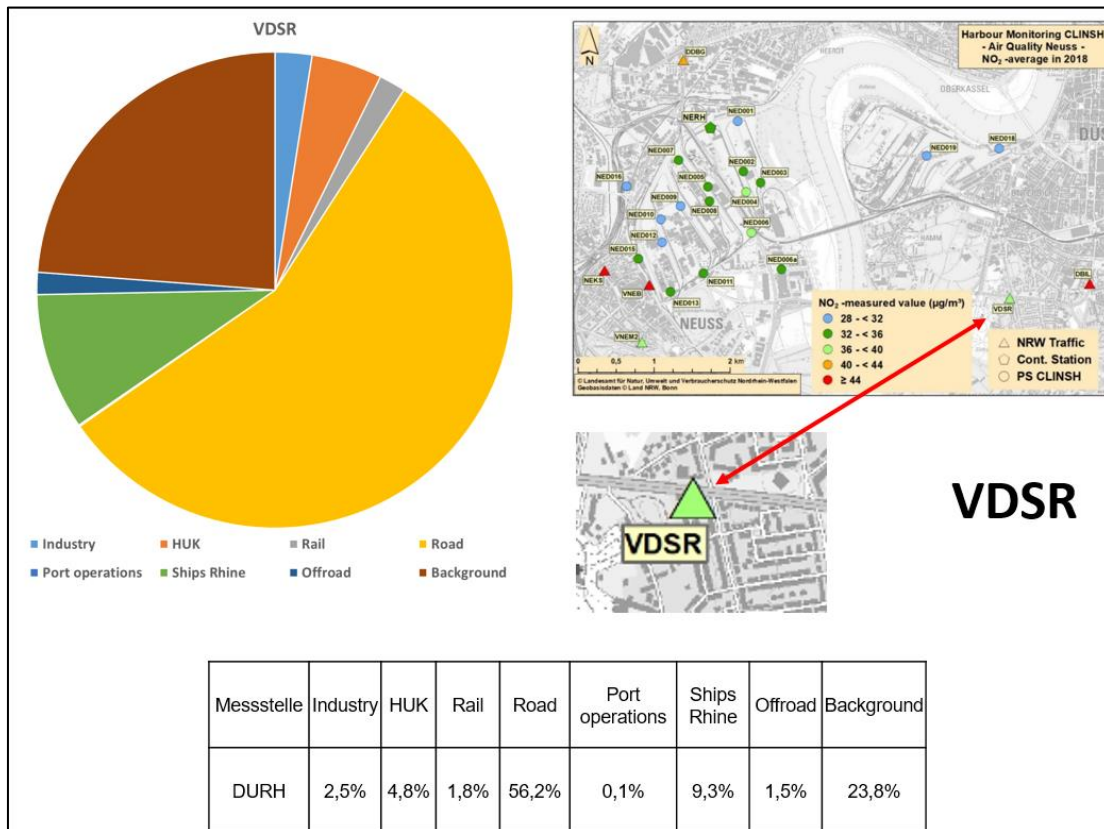


Fig. 28: Polluter analysis for traffic measuring site Düsseldorf Südring (VDSR).

The modeling result for the traffic monitoring station Neuss Batteriestraße (VNEB, annual mean NO<sub>2</sub> value in 2018: 45 µg/m<sup>3</sup>), which is located directly at the port, also shows a similar polluter profile for NO<sub>x</sub> pollution (Fig. 29).

Here, as well, road traffic plays a dominant role for NO<sub>x</sub> with a pollution share of 56 %, followed by background pollution with a share of about 23 %. Emissions from shipping traffic on the Rhine (about 6 %) and from domestic heating and small combustion plants (about 6 %) also play only a minor role. The share of port operations is somewhat higher in the immediate vicinity of the port, at about 2 %, than in the measuring points of the state measuring network further away from the port.

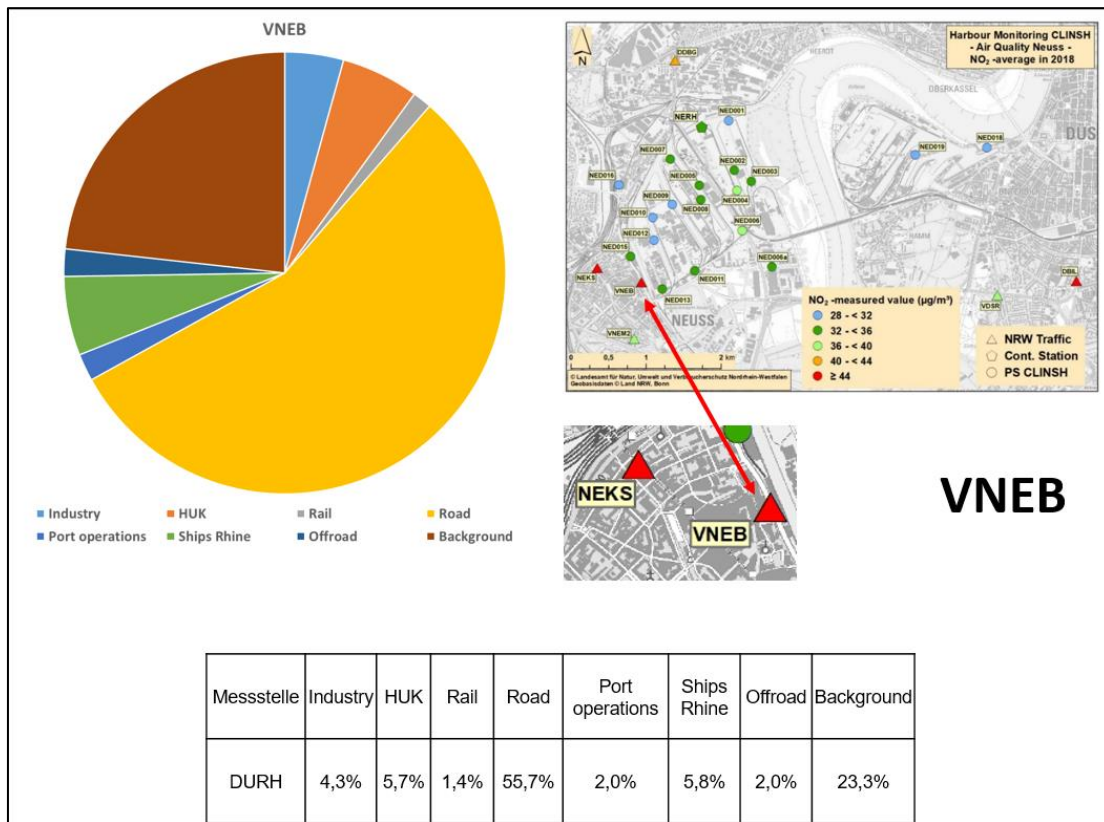


Fig. 29: Polluter analysis for traffic measuring site Neuss Batteriestraße (VNEB).

## 5. Comparison of measured and modeled environmental pollution with nitrogen oxides

### 5.1 Quality criteria for modeling results

Modeling of air pollution scenarios based on emission inventories is an important tool for investigating the causes of pollution, future pollution trends and for forecasting the effects of measures. For such investigations, several different modeling methods are available, which are specifically adapted to the respective problems (large-scale background pollution, small-scale urban pollution, local pollution in special pollution situations such as street canyons).

Therefore, it is particularly important to carefully select the appropriate modeling procedure for the respective load situations and also to carefully check the emission-side input parameters for their respective suitability.

Since it is almost impossible to represent all local load and environmental factors in real terms in a modeling process, modeling results may deviate from the real measured load values. The choice of an inappropriate modeling approach or an incomplete representation of all relevant emission sources in the modeling can therefore lead to significant deviations between modeled and measured values.

Therefore, it is important to compare modeled pollution scenarios with the results of real measured air pollution and thus to validate the results of the modeling. Modeling results that reflect the real (measured) pollution situation within a range of +/- 20 % can already be classified as "very good". It can be assumed that such results are then also suitable for the prognosis of different future load scenarios.

For the CLINSH project, very ambitious procedures were chosen, both for the special measurement programs and for the modeling, which led to a very good validity of the results.

#### 5.1.1 Conversion of the NO<sub>2</sub> measured values for comparison with the modeling results

The EU has set binding annual average limits for nitrogen dioxide (NO<sub>2</sub>). Other nitrogen oxides have not been regulated. The nitrogen oxide compounds in the exhaust gases of internal combustion engines essentially consist of a mixture of nitrogen monoxide (NO) and nitrogen dioxide. Directly at the exhaust pipe, NO predominates in diesel engines.

However, this mixing ratio at the exhaust gas outlet into the atmosphere does not remain constant, but changes continuously in spatial and temporal terms. Shortly after the emission into the ambient air, a part of the NO load is converted to NO<sub>2</sub> due to air-chemical processes, whereby an interplay of different influencing factors (temperature, solar radiation, ozone concentrations, etc.) occurs. This interplay is individually dependent on the situation at the different measurement locations.

In practice, the two components NO and NO<sub>2</sub> are therefore combined to form NO<sub>x</sub> for comparison with real measured values. If only NO<sub>2</sub> values are available, the NO components are determined using mathematical methods.

The polluter analysis, carried out as part of the CLINSH project, are also based on computations of this form and relate to nitrogen oxides (NO<sub>x</sub>). In contrast, the passive samplers, the majority of the monitoring stations were equipped with, measured only nitrogen dioxide (NO<sub>2</sub>). In order to compare the measured values with the modeling results, the NO<sub>2</sub>/NO<sub>x</sub> conversion has to be taken into account. Therefore, NO<sub>2</sub> measurements were converted to NO<sub>x</sub> for the polluter analysis.

The chemical conversion of NO<sub>x</sub> to NO<sub>2</sub> is extremely complex and dependent on a number of parameters such as UV radiation, ozone value, temperature. In this study, the simplified Romberg approach with parameters according to Schlamberger (**Schlamberger 2020**) was used, which is based on current measurement data and thus implicitly integrates the ozone chemistry. It was chosen the parameter set that was derived for all source categories for the period 2008 to 2019 with the following parameter values: A: 28.17 B: 31.28 C: 0.21.

In the study area, the continuous measuring stations DURH and NERH were operated in Duisburg and Neuss. Here, both NO<sub>2</sub> and NO<sub>x</sub> were recorded at five-second intervals. In addition, a passive sampler was installed at each of the two continuous measuring sites.

At the measuring point DURH in Duisburg, a NO<sub>2</sub> value of 27 µg/m<sup>3</sup> (official measured value NRW) and a NO<sub>x</sub> value of 49.2 µg/m<sup>3</sup> were measured in 2018. The passive sampler DU025 at the same location showed a NO<sub>2</sub> value of 30 µg/m<sup>3</sup> in the same period. According to the NO<sub>2</sub>/NO<sub>x</sub> conversion according to Schlamberger, this leads to NO<sub>x</sub> values of 47.6 µg/m<sup>3</sup> (DURH) and 57.4 µg/m<sup>3</sup> (DU025). It becomes clear that the conversion from NO<sub>2</sub> to NO<sub>x</sub> alone can almost double the error bandwidth of the different NO<sub>2</sub> measured values from 12 % (NO<sub>2</sub> side) to 21 % (NO<sub>x</sub> side calculated according to Schlamberger).

Since both NO and NO<sub>2</sub> measurements are available at the DURH automatic monitoring station, it is possible to compare actual and modeled NO<sub>x</sub> levels. In comparison to the calculation based on the measurement results, the LASAT modeling (based on the emissions) resulted in a NO<sub>x</sub> load of 81.0 µg/m<sup>3</sup>, which means an overestimation of approx. 70 % to the determined NO<sub>x</sub> measured values according to Schlamberger. However, at the passive sampler DU025, which has the same location, the overestimation is only approx. 41%. The deviation of the values between DURH and DU025 results only from the different measured value for NO<sub>2</sub>.

The situation in Neuss is similar at the same measuring sites NERH and NED017. At the measuring point NERH, a NO<sub>2</sub> value of 33 µg/m<sup>3</sup> and a NO<sub>x</sub> value of 63.4 µg/m<sup>3</sup> were measured in 2018. The passive sampler NED017 at the same location showed a NO<sub>2</sub> value of 34 µg/m<sup>3</sup> in the same period. This leads according to the NO<sub>2</sub>/NO<sub>x</sub> conversion of Schlamberger to NO<sub>x</sub> values of 66.1 µg/m<sup>3</sup> (NERH) and 70.1 µg/m<sup>3</sup> (NED017). By converting

NO<sub>2</sub> to NO<sub>x</sub>, it becomes here clear as well that the error bandwidth of the different NO<sub>2</sub> measured values can almost double from 3.6 % (NO<sub>2</sub> side) to 6 % (NO<sub>x</sub> side calculated according to Schlamberger). In comparison, a NO<sub>x</sub> value of 69.6 µg/m<sup>3</sup> was computed at the automatic measuring site NERH with the LASAT-model, which means an overestimation of approx. 5 % to the determined NO<sub>x</sub> measured values according to Schlamberger. Passive sampler NED017, at the same location, shows only a slight underestimation of just under 1%. The deviation of the values between NERH and NED017 results again only from the different measured value for NO<sub>2</sub>.

These comparisons for the automatic measuring sites in Duisburg and Neuss show that deviations in the total NO<sub>x</sub> load of at least 10 % - 20 % can occur due to the conversion from NO<sub>2</sub> to NO<sub>x</sub> or due to different measuring methods. In Neuss (NERH), the modeling reproduces the measured immission situation very well. The measured values of both measuring methods are very close to each other. In Duisburg (DURH), the immission situation is clearly overestimated by the model computation. Again, both methods provide measured values that are close to each other, but compared to Neuss (NERH), the deviation between the two measurement methods is nevertheless more than twice as high.

For air quality monitoring, the chemiluminescence method (DIN EN 14211) (automatic measuring method) as well as the measuring method with passive samplers are used. The former is the reference measurement method for determining NO<sub>2</sub> pollution in ambient air. However, the measurement method using passive samplers meets the criteria for equivalence of the two measurement methods (see **LANUV Fachbericht 108**). If measured values are available for a measurement location from both methods, the value obtained via the chemiluminescence method is the official measured value.

This representation of sensitivity with respect to NO<sub>2</sub>/NO<sub>x</sub> conversion suggests that NO<sub>x</sub>-side deviations of +/-20 % between modeled value and measured value represent good agreement.

### 5.1.2 Comparison of NO<sub>x</sub> values modeled/measured

The following chapters 5.1.2.1 and 5.1.2.2 present and discuss the ratios of the modeled total NO<sub>x</sub> loads to the NO<sub>x</sub> immission values derived from the NO<sub>2</sub> measurement results according to chapter 5.1.1 for the port areas of Duisburg and Neuss.

#### 5.1.2.1 Duisburg

Fig. 30 shows the NO<sub>x</sub> ratios between model results and measurements at the measurement sites in the Duisburg area.

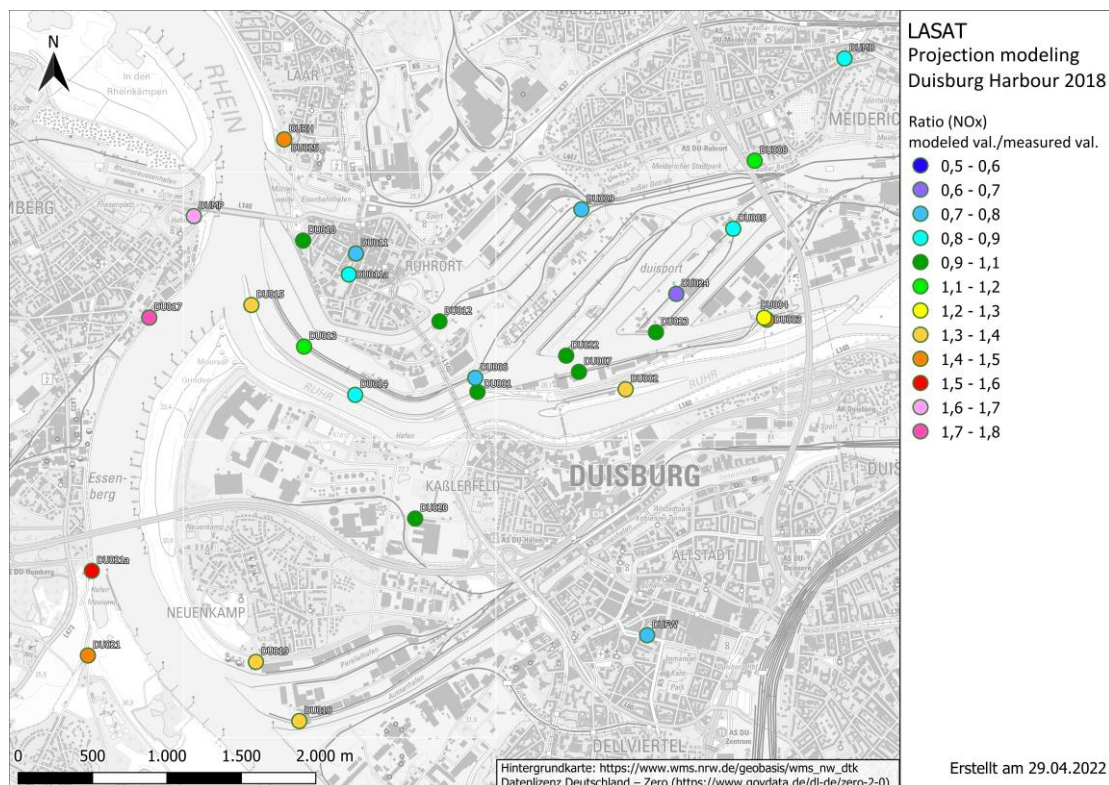


Fig. 30: NO<sub>x</sub> ratio between model results and measurements at the measurement sites in the area of the Duisburg Harbour.

The circles colored light blue to light green indicate the measurement locations where the model underestimates the measurement by a maximum of 20 % (light blue) or overestimates by a maximum of 20 % (light green). Deviations within this range are considered a good match. These include the measurement locations DU001, DU005, DU007, DU008, DU010, DU011a, DU012, DU013, DU014, DU020, DU022 and DU023. It is noticeable at these measurement sites that they are often surrounded by several source groups, but obviously have a sufficiently large distance in particular to the source groups with near-ground

emissions. Thus, it can be assumed that, on the one hand, the measurement is probably not too locally influenced and, on the other hand, the measurement location is outside the strong immission gradients that form in the immediate vicinity of a ground level line or point source during the computation. At stations DU003 and DU004, which are quite close to each other at the lock chamber, higher total NO<sub>x</sub> immissions are modeled compared to the measurement. At station DU003 the model result is about 50 % higher and at station DU004 about 26 % higher than the measurement. The contribution of emissions from the source "harbour" is also by far the highest at these stations, at over 60 %.

Looking at the two measuring sites, it becomes clear that the immission concentration is very strongly determined by the emission source "ship". The aim of these measuring points was to describe the actual impact of the presumed "emission hotspot lock" more precisely also in its maximum impact. For the modeling approach used, the location of these measuring points is somewhat problematic.

The emissions of the berthing ships or the ships in the lock are strongly determined by the position of the exhaust gas discharge relative to the measuring point. The exhaust system is usually located at the stern of the vessels, so emissions from the larger vessels are more likely to be emitted at either end of the lock basin. However, these emissions are included in the modeling as a line source, since they cannot be specified in a more differentiated way. This difference may be because the real emission site of a ship is often located at a considerable distance from the measurement site and therefore the dispersion in the immediate vicinity is different from the dispersion caused by a line source in the model.

If the passive sampler were located at a somewhat greater distance from the dominant ship source in this case, better agreement would most likely be expected. In such cases, where in the near field of a source a strong influence by the source release itself is to be expected, it is more advantageous for a comparison between measurement and modeling if a measurement profile is recorded.

At the measuring station DU002, the measurement is also clearly overestimated by the model. Here, the immission caused by the ships in the harbour still shows a share of almost 20%. It is noticeable that the measuring site is still in an area where the model computations show a strong immission gradient. This could indicate that the measuring site does not adequately represent the load spatially.

Measuring site DU006 is located vis-à-vis to measuring site DU001 on the northern side of the harbour basin. While the total NO<sub>x</sub> immission measured at measuring site DU001 agrees well with the calculation, the model underestimates the measured value at measuring site DU006 by about 24 %. Upon closer examination, it is noticeable that the flow obstacles due to significant industrial plants (silo plants) in the direct vicinity of DU006 were not represented in the model. On the emission side, the truck transshipment directly passing the station was not recorded separately. Therefore, a slight underestimation on the model side seems quite plausible.

At measurement site DU009, the measured value is also underestimated in the model results by approx. 30%. A closer look at the location reveals that a large container terminal located directly next to the measuring point with constantly changing container stacks could not be captured by the building cubatures in the model. This, however, significantly influences the wind field and thus the dispersion. Furthermore, no emission data were available for the shunting area east of the measuring site.

The two measuring sites DU011 and DU011a are both located within a residential neighborhood. While the measured value is underestimated only slightly (16 %) at measuring site DU011a, the calculation at measuring site DU011 underestimates more clearly, by about 24 %. Basically, a similar situation exists in terms of construction. However, the residential streets in the vicinity of the two measurement sites are not recorded separately in terms of emissions. It is therefore reasonable to assume that these have a somewhat greater influence on measuring site DU011.

The closer the measuring sites are to the shipping channel of the Rhine, the larger the share of the NO<sub>x</sub> immissions caused by this shipping. It is noticeable that at all measurement sites located close to the Rhine (< 500m), the modeling overestimate the NO<sub>x</sub> values derived from the NO<sub>2</sub> measurements, in some cases significantly.

For the measurement sites on the right bank of the Rhine (DU015, DU018 DU019) the overestimation ranges between 36% and 39%, further north at the permanent measurement site DURH (70 %).

On the left bank of the Rhine, the modeled NO<sub>x</sub> total immission concentrations exceed the measured values by about 50 % to a maximum of 70 % (DU017, DU021, DU021a, and DUMP). Due to the good agreement at many measurement sites between measurement and calculation, which are rather dominated by other source groups, as well as the justifiable deviations at some sites where the agreement is not quite as good (see discussion above), it cannot be excluded that ship emissions on the Rhine were overestimated. Therefore, at the stations close to the Rhine, where the share of the source "Rhine ships" predominates, the effect is correspondingly strong.

At the traffic monitoring stations, the modeling underestimates the NO<sub>x</sub> levels converted from the NO<sub>2</sub> measurements (18% at DUMB and 24% at DUFW). At both sites, there are buildings in the vicinity of the measuring site, which were not explicitly taken into account in the model because they lie outside the port area. The housing construction creates a street canyon character in real terms, which leads to a reduction in dilution and is thus not represented in the model.

### 5.1.2.2 Neuss

**Fig. 31** shows the NO<sub>x</sub> ratios between model results and measurements at the measurement sites in the Neuss area. The legend is identical to that in **Fig. 30** (Port of Duisburg). The circles colored light blue to light green represent the measurement locations at which the model underestimates the measurement by a maximum of 20 % (light blue) or overestimates it by a maximum of 20 % (light green). These deviations are considered as good compliance. The measurement sites falling into this category are NED001 to NED003, NED006, NED07 to NED010, NED012, NED013, and NED15 to NED017 and NERH. At these measurement sites, the flow obstacles and emissions in the immediate vicinity of the respective measurement site are obviously well represented in the model. It can also be assumed that the measurements at these locations are not too strongly influenced locally.

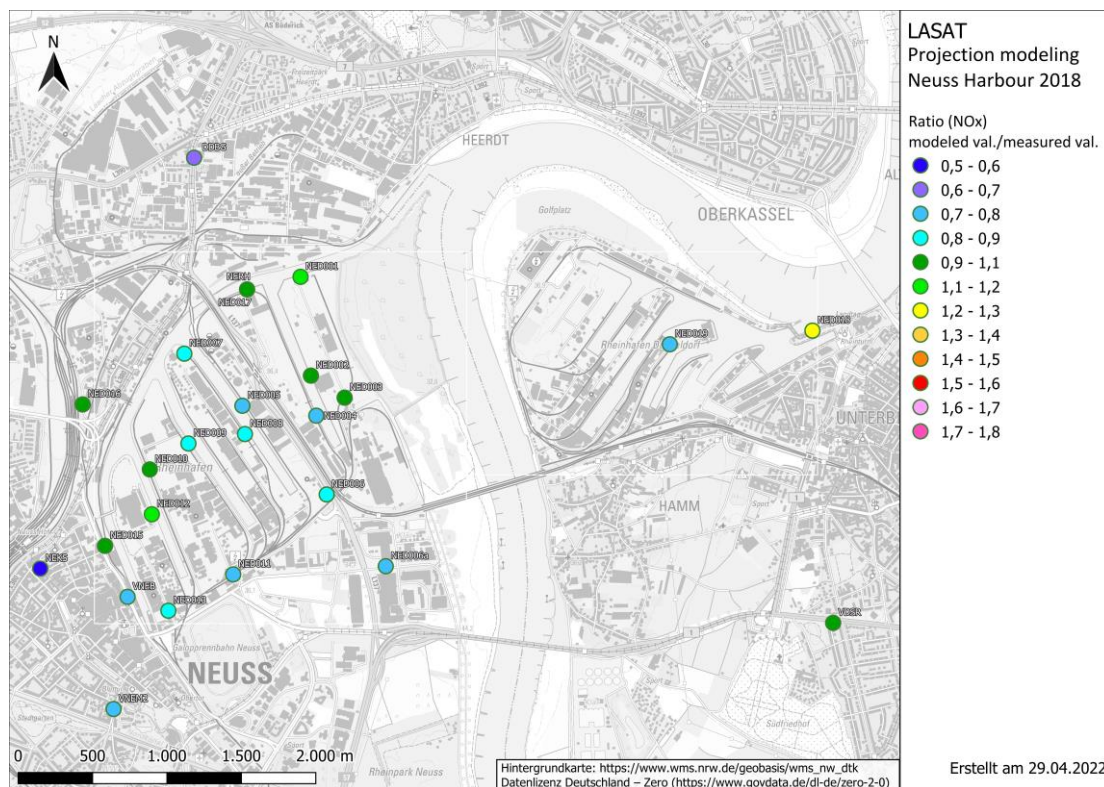


**Fig. 31:** NO<sub>x</sub> ratio between model results and measurements at the measurement sites in the area of the Neuss Harbour.

At the above-mentioned measuring sites, a good compliance can be seen. Nevertheless, the model results overestimate or underestimate the NO<sub>x</sub> values converted from the NO<sub>2</sub> measurements by a maximum of 20 %. However, there is usually a valid explanation for this. For example, at site NED006 the model calculates 83 % of the measured value, at site NED008 80 %, and at site NED013 88 % of the respective NO<sub>x</sub> load determined from the measured NO<sub>2</sub>

value. However, it is noticeable at these locations that there are some flow obstacles in the surrounding area that are not captured by the model. Some of these are stacked containers, bulk material stockpiles or temporarily erected halls or roofs that were not represented in the model input data (3D building model LOD1). Nevertheless, they can locally influence the flow and dispersion field and thus be responsible for the fact that the calculated value is somewhat underestimated.

At the measurement site NED009, the model also underestimates the NO<sub>x</sub> load determined from the measured NO<sub>2</sub> value by 81 %. A large motor vehicle transshipment center can be identified in the immediate vicinity of the site, for which no emissions are given in the emission register, but which certainly releases additional emissions that are hence not included in the model.

At the measurement sites NED004 and NED005, the model underestimates the NO<sub>x</sub> values converted from the NO<sub>2</sub> measurements by 23 % and 25 %, respectively. In both cases, the actual significant emission seems to be well represented in the model. However, some flow obstacles (e.g. variable container storage, etc.) are not included in the model near the site.

At sites NED006a and NED011, the model also underestimates the NO<sub>x</sub> levels determined from the NO<sub>2</sub> measurements by about 25 % and 24 %, respectively. At site NED006a, significant road emissions are obviously missing from the emission inventory, at NED011, a local vehicle transshipment with its emissions is not included in the emission inventory.

At site NED018 at the eastern edge of the model area with fine building resolution, the modeling overestimates the NO<sub>x</sub> load determined from the measured NO<sub>2</sub> value by 22 %. The share due to the Rhine ships is shown at this location with 38 %. As in the case of Duisburg, it is to be expected that the Rhine emissions are overestimated, which is reflected accordingly in the modeling results at the stations near the Rhine. The fact that the modeled value is "only" 22 % above the NO<sub>x</sub> load converted from the measured NO<sub>2</sub> value and not significantly higher compared to the locations near the Rhine in the area of the port of Duisburg is presumably because the nearby ship emissions in the Rhine port of Düsseldorf were not reflected in the emission register.

The stations DBIL, DDBG, NEKS, VNEB and VNEM2 are predominantly traffic stations where vehicle emissions are dominant (see also source group shares in **Fig. 21**). At these stations, the modeling significantly underestimates the NO<sub>x</sub> loads converted from the NO<sub>2</sub> measurements in some cases. At all of these locations, there is a pronounced housing construction in the vicinity of the measuring point, which was not explicitly resolved in the model, since it is located outside the port area. Due to the development a street canyon-like situation prevails, which in real terms leads to a reduction in dilution and thus causes this underestimation in the model.

At the traffic measurement station VDSR, the agreement between modeling and measurement is very good, although in the vicinity of the measuring site the buildings were

also not dissolved. However, there is only little development in the vicinity of the measurement site and thus only a weak influence is to be expected.

### **5.1.3 Classification of the measuring points with regard to source group shares - Tabular representation**

In the following tables (**Tab. 8** and **Tab. 9**), all measurement sites evaluated for the port areas of Duisburg and Neuss are listed and color-coded with regard to their suitability in relation to the source group shares determined based on the model calculations. In our opinion, the determined percentages of green highlighted measurement sites are well suited for further evaluations. In contrast, measurement sites highlighted in red are less suitable. These are almost without exception measurement sites which, due to their proximity to the Rhine, are strongly influenced by emissions from Rhine shipping and which may have been overestimated.

Stations not highlighted in color show differences in measurement and modelling, referable either to structural or emission-related conditions that were not included in the available input data for the modeling and thus could not be sufficiently taken into account.

Tab. 8: Grading of the model results at the stations in the Duisburg area with respect to source group proportions.

Measuring station	Masurement 2018 NO <sub>2</sub> (NO <sub>x</sub> ) [µg/m <sup>3</sup> ]	Measurement 2018 NO <sub>x</sub> (converted from NO <sub>2</sub> ) [µg/m <sup>3</sup> ]	LASAT 2018 NO <sub>x</sub> [µg/m <sup>3</sup> ]	NO <sub>x</sub> -ratio LASAT to Measurement	Rating
DU001	36.4	77.7	78.9	102%	Model fits well (102%) Flow obstacles and emissions in the immediate vicinity well represented in the model.
DU002	27.1	47.9	64.2	134%	Model overestimates significantly (134%) Immission share of lock appears to be too high. Location of real emissions horizontally probably deviates strongly from model implementation. Possibly, the activity of the lock, which is represented in the model as a line source, does not reflect the actual emission pattern.
DU003	47.4	119.4	178.7	150%	Model overestimates significantly (150%) Immission share of lock appears to be too high. Location of real emissions horizontally and vertically probably strongly deviating from model implementation. (corresponding location of DU004 and DU003)
DU004	47.3	119.0	150.0	126%	Model slightly overestimates (126%) Immission share of lock appears to be too high. Location of real emissions horizontally and vertically probably strongly deviating from model implementation. (corresponding location of DU004 and DU003, therefore similar to be expected, but somewhat farther from the source and therefore lower error).
DU005	32.9	65.8	57.0	87%	Model fits well (87%) Flow obstacles in the immediate vicinity only partially well represented in the model. Emissions well captured. Slight underestimation to be expected.
DU006	43.2	102.9	77.8	76%	Model slightly underestimates (76%) Flow obstacles in the immediate vicinity only partially well represented in the model, significant industrial facilities not represented. Emissions partially well mapped, truck handling on nearby open area not mapped. Slight underestimation to be expected.
DU007	31.3	60.6	66.4	110%	Model fits well (110%) Flow obstacles and emissions in the immediate vicinity well represented in the model..

Measuring station	Masurement 2018 NO <sub>2</sub> (NO <sub>x</sub> ) [µg/m <sup>3</sup> ]	Masurement 2018 NO <sub>x</sub> (converted from NO <sub>2</sub> ) [µg/m <sup>3</sup> ]	LASAT 2018 NO <sub>x</sub> [µg/m <sup>3</sup> ]	NO <sub>x</sub> -ratio LASAT to Measurement	Rating
DU008	32.0	62.8	70.9	113%	Model fits well (113%) Flow obstacles and emission not well represented in the model. The proportion of road is slightly increased because the road actually runs over the bridge and the measuring point is offset below it, but the model does not capture the turnover of the parking space in the surrounding area.
DU009	35.2	73.5	52.9	72%	Model slightly underestimates (72%) Flow obstacles in the direct vicinity only partially well represented in the model, significant logistics facilities not represented. Emissions partially well captured, some access roads not captured in terms of emissions.
DU010	35.7	75.3	69.3	92%	Model fits well(92%) Flow obstacles in the immediate vicinity well represented in the model. Local side roads not included in emissions. Underestimation to be expected, but due to the proximity to the Rhine probably somewhat compensated by high share of Rhine shipping (32%).
DU011	35.1	73.2	55.3	76%	Model slightly underestimates (76%) Flow obstacles in the immediate vicinity well represented in the model. Analogous to measuring point DU011, however, neighborhood streets not recorded in the emission register, therefore underestimation to be expected.
DU011a	32.9	65.8	55.5	84%	Model fits well (84%) Flow obstacles in the immediate vicinity well represented in the model. Analogous to measuring point DU011, however, neighborhood streets not recorded in the emission register, therefore underestimation to be expected.
DU012	33.5	67.8	62.1	92%	Model fits well (92%) Flow obstacles and emissions in the immediate vicinity well represented in the model.
DU013	34.9	72.5	87.0	120%	Model fits well (120%) Flow obstacles and emissions in the immediate vicinity well represented in the model.

Measuring station	Masurement 2018 NO <sub>2</sub> (NO <sub>x</sub> ) [µg/m <sup>3</sup> ]	Measurement 2018 NO <sub>x</sub> (converted from NO <sub>2</sub> ) [µg/m <sup>3</sup> ]	LASAT 2018 NO <sub>x</sub> [µg/m <sup>3</sup> ]	NO <sub>x</sub> -ratio LASAT to Measurement	Rating
DU014	36.6	78.4	68.5	87%	Model fits well (87%) Flow obstacles well represented in the model except for relevant vegetation in the direct vicinity. Emissions well recorded, only ship emissions from the ships south of the Ruhr not recorded in the emission register.
DU015	31.6	61.5	84.3	137%	Model overestimates significantly (137%) (right bank of the Rhine) Immission share of Rhine shipping is high (37%), not conclusively explainable overestimation of ship emissions on the Rhine, Flow obstacles and remaining emissions (ship shares port of Duisburg) well represented in the model.
DU017	30.4	57.8	101.7	176%	Model overestimates significantly (176%) (left bank of the Rhine) Immission share of Rhine shipping is very high (60%), not conclusively explainable overestimation of ship emissions on the Rhine, although local flow obstacles and local roads are no longer considered in the model.
DU018	31.9	62.5	85.1	136%	Model overestimates significantly (136%) (right bank of the Rhine) Immission share of Rhine shipping is very high (42%), not conclusively explainable overestimation of ship emissions on the Rhine, local flow obstacles no longer represented in the model, slight underestimation to be expected.
DU019	30.5	58.1	80.7	139%	Model overestimates significantly (139%) (right bank of the Rhine) Immission share of Rhine shipping is high (38%), overestimation of ship emissions on the Rhine not conclusively explainable, Flow obstacles well represented in the model, but local roads not included in the emission register. Slight underestimation to be expected.
DU020	32.0	62.8	58.0	92%	Model fits well (92%) Flow obstacles and emissions in the immediate vicinity well represented in the model. Local side road approx. 3m horizontally away not included in emissions.

Measuring station	Masurement 2018 NO <sub>2</sub> (NO <sub>x</sub> ) [µg/m <sup>3</sup> ]	Measurement 2018 NO <sub>x</sub> (converted from NO <sub>2</sub> ) [µg/m <sup>3</sup> ]	LASAT 2018 NO <sub>x</sub> [µg/m <sup>3</sup> ]	NO <sub>x</sub> -ratio LASAT to Measurement	Rating
DU021	25.7	44.0	65.6	149%	Model overestimates significantly (149%) (left bank of the Rhine) Immission share of Rhine shipping is high (35%), not conclusively explainable overestimation of ship emissions on the Rhine, even though local flow obstacles and local roads are not covered by the model.
DU021a	29.5	55.0	85.8	156%	Model overestimates significantly (156%) (left bank of the Rhine) Immission share of Rhine shipping is very high (45%), not conclusively explainable overestimation of ship emissions on the Rhine, although local flow obstacles and local roads as well as the port of Mevissen are not covered by the model..
DU022	33.1	66.4	61.5	93%	Model fits well (93%) Flow obstacles and emissions in the immediate vicinity well represented in the model.
DU023	31.5	61.2	61.9	101%	Model fits well (101%) Flow obstacles and emissions in the immediate vicinity well represented in the model.
DU024	33.1	66.4	43.6	66%	Model underestimates significantly (66%) Flow obstacles partially not recorded due to the presence of stockpiles and shielding walls of bulk material storage sites. Local emissions partially not recorded due to very heterogeneous roadways. Underestimation to be expected.
<b>DU025</b>	30.3	57.4	81.0	141%	Model overestimates significantly (141% (right bank of the Rhine) Immission share of Rhine shipping is high (38%), overestimation of ship emissions on the Rhine not conclusively explainable, although local flow obstacles are not covered by the model (existing identical location of DU025 and DURH)
<b>DURH</b>	27.0 (49.2)	47.6	81.0	170% (165%)	Model overestimates significantly (170%, regard to NO <sub>x</sub> measurement 165%) (right bank of the Rhine) Immission share of Rhine shipping high (38%), overestimation of ship emissions on the Rhine not conclusively explainable, although local flow obstacles are not covered by the model (identical location of DU025 and DURH)

Measuring station	Masurement 2018 NO <sub>2</sub> (NO <sub>x</sub> ) [µg/m <sup>3</sup> ]	Masurement 2018 NO <sub>x</sub> (converted from NO <sub>2</sub> ) [µg/m <sup>3</sup> ]	LASAT 2018 NO <sub>x</sub> [µg/m <sup>3</sup> ]	NO <sub>x</sub> -ratio LASAT to Measurement	Rating
DUFW	41.0	94.5	72.6	77%	Model slightly underestimates (77%) Traffic station in street canyon, but buildings not included in the model, thus underestimation to be expected
DUMB	42.0	98.3	82.6	84%	Model fits well (84%) Traffic station in street canyon, but buildings not included in the model, thus underestimation to be expected
DUMP	30.5	58.1	97.3	168%	Model overestimates significantly (168%) (left bank of the Rhine) Immission share of Rhine shipping is very high (54%), not conclusively explainable overestimation of ship emissions on the Rhine, even though local flow obstacles and local roads as well as the railroad port are not covered by the model.

Tab. 9: Grading of the model results at the stations in the Neuss area with respect to source group proportions.

Measuring station	Masurement 2018 NO <sub>2</sub> (NO <sub>x</sub> ) [µg/m <sup>3</sup> ]	Measurement 2018 NO <sub>x</sub> (converted from NO <sub>2</sub> ) [µg/m <sup>3</sup> ]	LASAT 2018 NO <sub>x</sub> [µg/m <sup>3</sup> ]	NO <sub>x</sub> -ratio LASAT to Measurement	Rating
NED001	31.5	61.2	67.4	110%	Model fits well (110%) Flow obstacles and emissions in the direct vicinity well represented in the model
NED002	33.8	68.8	65.5	95%	Model fits well (95%) Flow obstacles and emissions in the direct vicinity well represented in the model
NED003	34.4	70.8	70.8	100%	Model fits well (100%) Flow obstacles and emissions in the direct vicinity well represented in the model
NED004	38.0	83.4	64.1	77%	Model slightly underestimates (77%) Characteristics similar to those expected at measuring point NED002. Emissions in the direct vicinity well represented in the model, but flow obstacles partly not included in the model (container storage yard), slight underestimation by the model to be expected.
NED005	35.7	75.2	56.1	75%	Model slightly underestimates (75%) Emissions in the direct vicinity well represented in the model, but flow obstacles partly not included in the model, slight underestimation by the model to be expected.
NED006	39.2	87.8	73.2	83%	Model fits well (83%) Emissions in the direct vicinity well represented in the model, but flow obstacles partly not included in the model, slight underestimation by the model to be expected.
NED006a	35.7	75.2	56.3	75%	Model slightly underestimates (75%) Flow obstacles in the direct vicinity well represented in the model, but local road emissions not represented in the emission register, underestimation by the model to be expected.
NED007	31.9	62.5	55.6	89%	Model fits well (89%) Flow obstacles and emissions in the direct vicinity well represented in the model

Measuring station	Measurement 2018 NO <sub>2</sub> (NO <sub>x</sub> ) [µg/m <sup>3</sup> ]	Measurement 2018 NO <sub>x</sub> (converted from NO <sub>2</sub> ) [µg/m <sup>3</sup> ]	LASAT 2018 NO <sub>x</sub> [µg/m <sup>3</sup> ]	NO <sub>x</sub> -ratio LASAT to Measurement	Rating
NED008	32.3	63.8	51.2	80%	Model fits well (80%) Emissions in the direct vicinity well represented in the model, but flow obstacles partly not included in the model, slight underestimation by the model to be expected.
NED009	30.2	57.1	46.1	81%	Model fits well (81%) Characteristics similar to those expected at measuring point NED010. Between the two stations there is a large motor vehicle transshipment point which was not included in the emission register and may cause the measured value at NED009 to be higher
NED010	28.8	52.9	51.1	97%	Model fits well (97%) Characteristics similar to those expected at measuring point NED009. Between the two stations there is a large motor vehicle transshipment center which is not included in the emission register..
NED011	32.8	65.4	49.9	76%	Model slightly underestimates (76%) Flow obstacles in the immediate vicinity well represented in the model, but local motor vehicle turnover not represented in the emission inventory, slight underestimation by the model to be expected.
NED012	29.3	54.4	61.1	112%	Model fits well (112%) Flow obstacles and emissions in the direct vicinity well represented in the model
NED013	33.4	67.4	59.6	88%	Model fits well (88%) Emissions in the direct vicinity well represented in the model, but flow obstacles partly not covered by the model, slight underestimation by the model to be expected.
NED015	35.0	72.8	67.2	92%	Model fits well (92%) Emissions in the direct vicinity well represented in the model, but flow obstacles partly not covered by the model, slight underestimation by the model to be expected.

Measuring station	Masurement 2018 NO <sub>2</sub> (NO <sub>x</sub> ) [µg/m <sup>3</sup> ]	Measurement 2018 NO <sub>x</sub> (converted from NO <sub>2</sub> ) [µg/m <sup>3</sup> ]	LASAT 2018 NO <sub>x</sub> [µg/m <sup>3</sup> ]	NO <sub>x</sub> -ratio LASAT to Measurement	Rating
NED016	31.1	59.9	57.6	96%	Model fits well (96%) Location at the edge of the tracks with open terrain, no explicit consideration of buildings in the model at this location, but no significant building influence to be expected at the measurement location, therefore also well representable by the model.
<b>NERH</b>	33.0 (63.4)	66.1	69.6	105% (110%)	Model fits well (105%, regard to NO <sub>x</sub> -Measurement 110%) Flow obstacles and emissions in the immediate vicinity well represented in the model (identical location of NED017 and NERH).
NED018	30.8	59.0	71.9	122%	Model slightly overestimates (122%) Immission share of Rhine shipping is very high, overestimation of ship emissions on the Rhine not conclusively explainable, although local ship emissions of movements in the Rhine port of Düsseldorf were not included in the emission register.
NED019	31.8	62.2	48.0	77%	Model slightly underestimates (77%) Flow obstacles in the direct vicinity well represented in the model, but local ship emissions from movements in the Rhine port of Düsseldorf and local motor vehicle transshipment not represented in the emission register, slight underestimation by the model to be expected.
DBIL	54.0	146.6	83.0	57%	Model underestimates significantly (57%) Measuring point with street canyon character and multi-lane road, but flow obstacles not covered by the model, significant underestimation by the model to be expected.
DDBG	43.0	102.1	66.9	66%	Model underestimates significantly (66%) Measuring point with street canyon character and structural separation of the driving directions, but flow obstacles not covered by the model, significant underestimation by the model to be expected.

Measuring station	Masurement 2018 NO <sub>2</sub> (NO <sub>x</sub> ) [µg/m <sup>3</sup> ]	Masurement 2018 NO <sub>x</sub> (converted from NO <sub>2</sub> ) [µg/m <sup>3</sup> ]	LASAT 2018 NO <sub>x</sub> [µg/m <sup>3</sup> ]	NO <sub>x</sub> -ratio LASAT to Measurement	Rating
NEKS	44.0	106.0	57.0	54%	Model underestimates significantly (54%) Measuring point with narrow street canyon character, but flow obstacles not covered by the model, significant underestimation by model to be expected.
VDSR	39.0	87.0	84.1	97%	Modell fits well (97%) although measuring point close to the street and no explicit consideration of buildings in the model at this point, but no street canyon character, therefore also well representable by the model.
VNEB	45.0	109.9	86.0	78%	Model slightly underestimates (78%) Emissions in the direct vicinity well represented in the model, but flow obstacles partly not covered by the model, slight underestimation by the model to be expected.
VNEM2	40.0	90.7	69.0	76%	Model slightly underestimates (76%) Emissions in the direct vicinity well represented in the model, but flow obstacles partly not covered by the model, slight underestimation by the model to be expected.

## 6. Conclusion and Outlook

### 6.1 Conclusion

The aim of this part of the CLINSH project was to obtain as accurate as possible a picture of the pollution situation with nitrogen oxides in the large inland ports of Duisburg and Neuss and to identify the polluters of the air pollution. To achieve this, a very dense measurement network with passive samplers (NO<sub>2</sub> measurement) was set up in both ports. The measurement networks were designed to be considerably denser than is otherwise typical within the official air monitoring measurement network. A total of 47 monitoring sites (19 Neuss; 28 Duisburg) were investigated for CLINSH and, in addition, the results of 8 traffic monitoring sites of the NRW state monitoring network were included in the evaluations (**LANUV Fachbericht 115/CLINSH Report: Harbour Monitoring Part A**).

The additional use of two automatic measuring stations made it possible to record the dynamics of the changes in air pollution with nitrogen oxides with a high temporal resolution. Together with the meteorology also recorded here, it was possible to create a reliable, site-typical data basis for the modeling of the causes of pollution at the CLINSH measuring points presented in this report.

For the modeling it has to be kept in mind that the ratio of NO and NO<sub>2</sub> in the emitted exhaust gas in the ambient air does not remain static but can change continuously, influenced by various factors (temperature, ozone content, etc.). For this reason, the NO<sub>2</sub> measurement results are converted into NO<sub>x</sub> concentrations (calculated total nitrogen oxides) for the validation of the modeling results.

The modeling carried out for CLINSH has succeeded in describing the pollution situation in the port areas of Duisburg and Neuss over a large area based on the shares of emissions from the individual polluter groups. The validation of the modeling results using the NO<sub>x</sub> concentrations calculated from the measurement results in the study area shows that a very good agreement was achieved across the area at most of the measurement sites.

At a few measuring sites, the NO<sub>x</sub> pollution situation determined from the NO<sub>2</sub> measurements could not be completely reproduced by the modeling. This is not unusual due to the size of the area observed and the resulting large number of sources to be considered and potential factors influencing the dispersion modeling (flow obstacles, model resolution, etc.) and can usually be justified, as shown in **chapter 5.1.2**.

Especially in Duisburg, it was shown that at the measuring stations located directly on the Rhine, the modeled emission levels of the moving ships on the Rhine overestimate the actual situation. The modeled NO<sub>x</sub> concentrations for the stations along the Rhine are systematically

significantly higher than the NO<sub>x</sub> values converted from the measured NO<sub>2</sub> concentrations. An open question is, whether the Schlamberger calculation ansatz can be optimized for the composition of ship exhaust near the source. The measuring sites in the port and settlement areas could generally be described very well with the model results.

As expected, the polluter analysis show a high share of ship emissions at the measuring sites on the Rhine and in the navigable waters of the ports. The same applies at the measuring sites located directly in the ports for the emissions from shipping-related port operations. In the navigation channels themselves, high NO<sub>x</sub> concentrations are found, where the load shares of ship emissions strongly dominate, since other ground-level emissions do not have a serious effect there. Already at a distance of 100-150 m from the Rhine, however, significant pollution shares of other emitter groups can be observed.

The measuring stations located in the study area at the traffic hotspots of the state measuring network show a clearly different pollution profile. Here, the effects of NO<sub>x</sub> emissions from motorized road traffic dominate with shares of mostly more than 50 %. The load shares of ships are usually below 10 %. This even applies to the traffic measuring sites in Neuss, which are located directly next to the port area. The thesis previously put forward in public discussions, that ship emissions have a dominant share in the pollution situation in the large cities near the Rhine could not be confirmed.

## 6.2 Outlook

It becomes clear that the investigations carried out by the LANUV as part of the CLINSH project were a very ambitious task.

The port monitoring made it possible to describe the pollution situation and the causes of pollution in the port areas of Duisburg and Neuss. Furthermore, with the data of the automatic measuring stations (dense measuring sequence of five seconds) it was also possible to measure the emission peaks (NO<sub>2</sub>, NO) of passing ships directly with a suitable wind direction and to assign them to the respective ship causing the emission.

With these results, it was possible to develop, in close cooperation with the University of Bremen, the method described in the LANUV Technical Report 126/CLINSH Report: Harbour Monitoring Part E for determining the emission factors of passing ships based on onshore measurements. This allows a more realistic estimation of emissions from passing ships on the Rhine (see **LANUV Technical Report 119/CLINSH Report Harbour Monitoring Part B**) and in ports (see **LANUV Technical Report 126/CLINSH Report Harbour Monitoring Part E**). The new method allows including the composition (classification) of the real passing fleet as well as its speed profile in the emission estimates.

In addition, the LANUV has developed a method within CLINSH that can also be used to more realistically estimate emissions from ships docked in the port, and which has already been used by other project partners within CLINSH.

The comprehensive (onshore measured) data base as well as the two newly developed methods represent a great gain in knowledge, because the determination of inland waterway emissions in the ports in particular has been difficult so far and required a high degree of simplifications and generalizing assumptions. Moreover, a reliable database on road traffic in the ports and on emissions from port operations did not exist before the CLINSH project.

The newly developed method still shows potential for optimization in the description of inland waterway vessel emissions from ships sailing on the Rhine. Here, the method described in (LANUV Technical Report 126/CLINSH Report: Harbour Monitoring Part E) is to be further developed and improved by further investigations in order to be able to record the inland vessel emissions even more realistically.

The data basis created as part of the CLINSH project and the method developments as a result of the CLINSH project provide the basis for the currently pending update of the emission register "Schiff" of the state of NRW.

## 7. Literature

### CLINSH Reports by LANUV NRW

- *“Harbour Monitoring Part A: Air quality on the Rhine and in the inland ports of Duisburg and Neuss/Düsseldorf. Immission-side effect of emissions from shipping and port operations on nitrogen oxide pollution” (already published)*
- *“Harbour Monitoring Part B: Determination of NO<sub>x</sub> and particulate matter emissions from inland vessels at berth” (already published)*
- *“Harbour Monitoring Part C: Emission inventories for the ports of Duisburg and Neuss/Düsseldorf”*
- *“Harbour Monitoring Part D: Analysis of shipping traffic on the Rhine for the years 2018-2020”*
- *“Harbour monitoring Part E: Determination of NO<sub>x</sub> emission rates of passing vessels from onshore measurements, comparison to onboard observations and application for emission calculations”*

### LANUV Fachberichte

- *LANUV Fachbericht 108: „Messen von Stickstoffdioxid in der Außenluft: Nachweis der Gleichwertigkeit von Passivsammlern“*
- *LANUV Fachbericht 115: „Hafenmonitoring: Luftqualität auf dem Rhein und in den Binnenhäfen von Duisburg und Neuss/Düsseldorf – Teil A: Immissionsseitige Effekte der Emissionen aus Schiffs- und Hafenbetrieb auf die Luftbelastung mit Stickoxiden“*
- *LANUV Fachbericht 119: „Bestimmung der NO<sub>x</sub>- und Feinstaubemissionen (PM<sub>10</sub>) von Binnenschiffen am Liegeplatz“*
- *LANUV Fachbericht 122: „Analyse des Schiffsverkehrs auf dem nordrhein-westfälischen Niederrhein in den Jahren 2018-2020 für das EU-Life-Projekt CLINSH“*
- *LANUV Fachbericht 123: „Hafenmonitoring – Teil B: Emissionsinventare der Hafengebiete Neuss und Duisburg.“*
- *LANUV Fachbericht 126: „Hafenmonitoring – Teil E: Bestimmung von NO<sub>x</sub>-Emissionen fahrender Schiffe aus landseitigen Onshore-Messungen und Anwendung zur Emissionsberechnung“*

### Other literature sources

- *Schlamberger 2020: Methodenverbesserung zur modelltechnischen NO<sub>2</sub>-Bestimmung, Professur für Umweltmeteorologie Christen, Dr. A.; Matzarakis, Prof. Dr. A., Bachelorarbeit von Carina Schlamberger, Freiburg, 2020*

## 8. Appendix

### 8.1 Source group shares at the Duisburg measuring stations (pie charts)

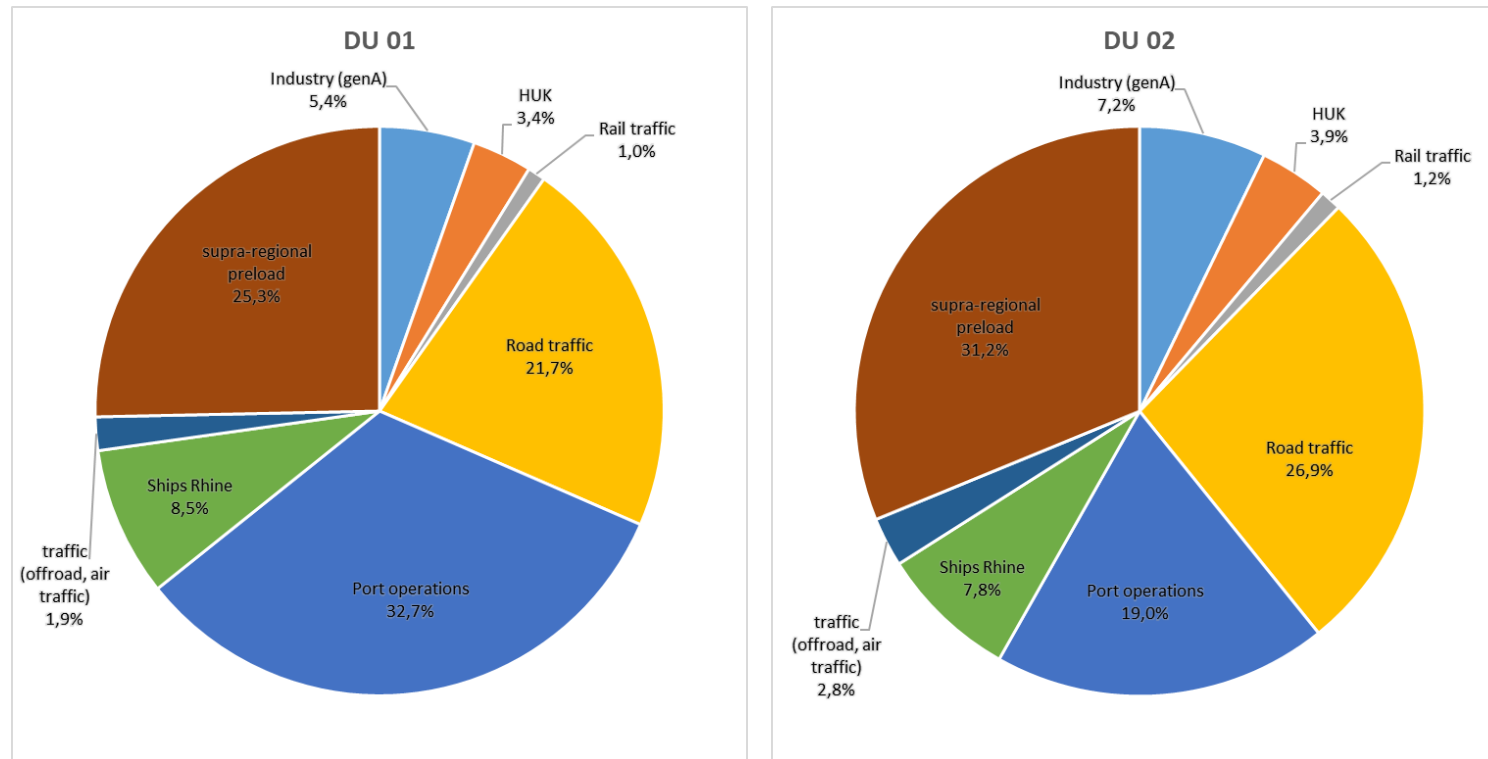


Fig. 32: Source group shares at monitoring stations DU001 (left) and DU002 (right).

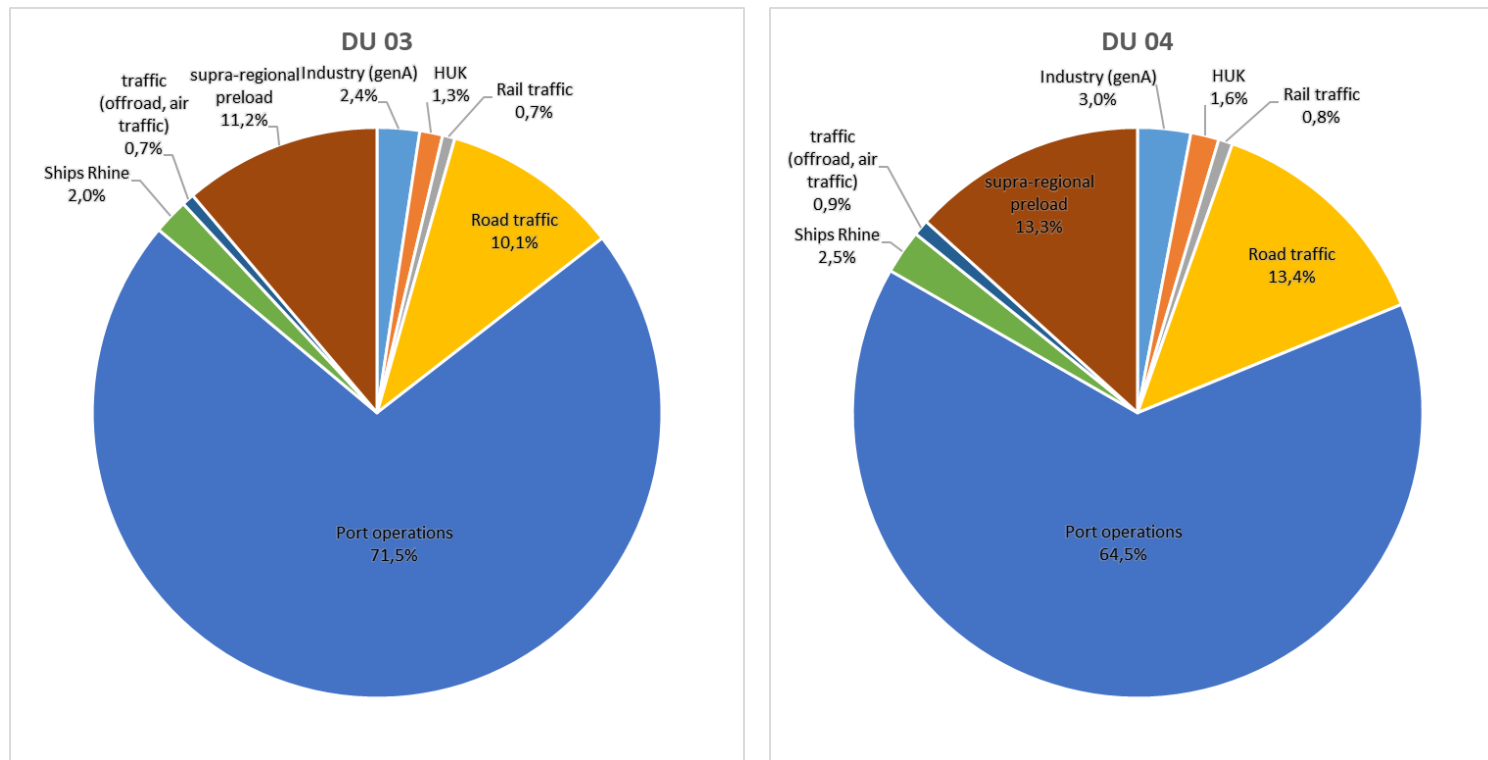


Fig. 33: Source group shares at monitoring stations DU003 (left) and DU004 (right).

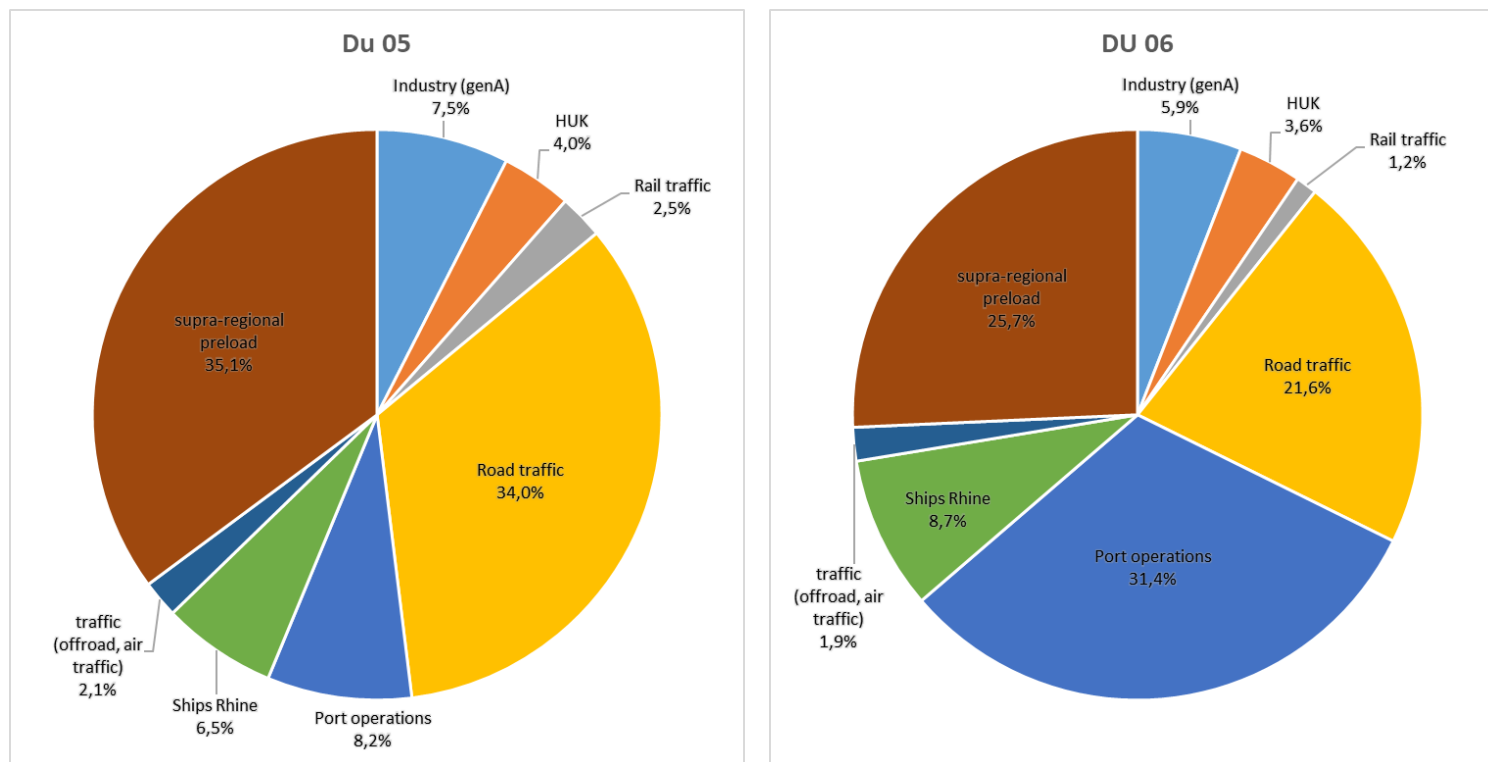


Fig. 34: Source group shares at monitoring stations DU005 (left) and DU006 (right).

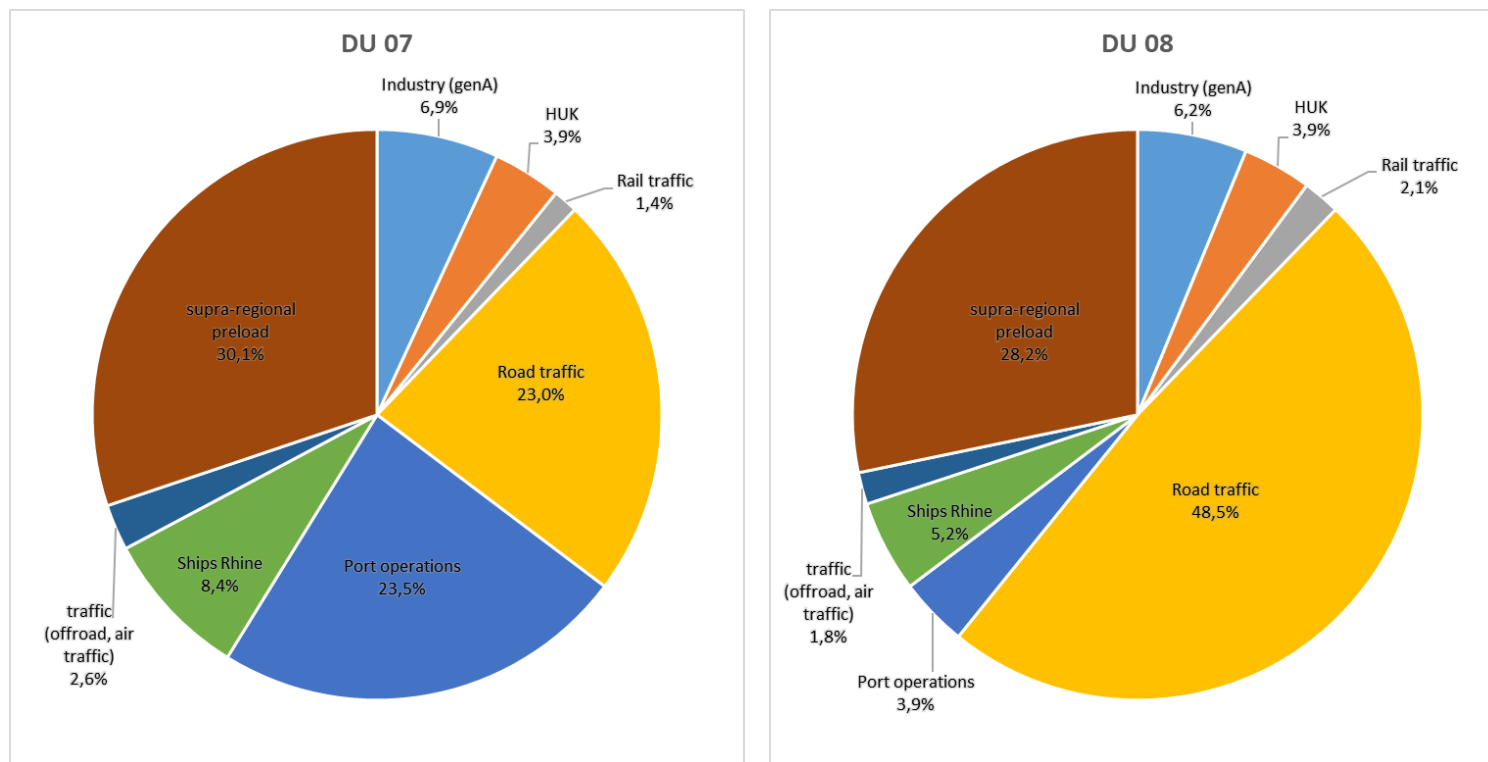


Fig. 35: Source group shares at monitoring stations DU007 (left) and DU008 (right).

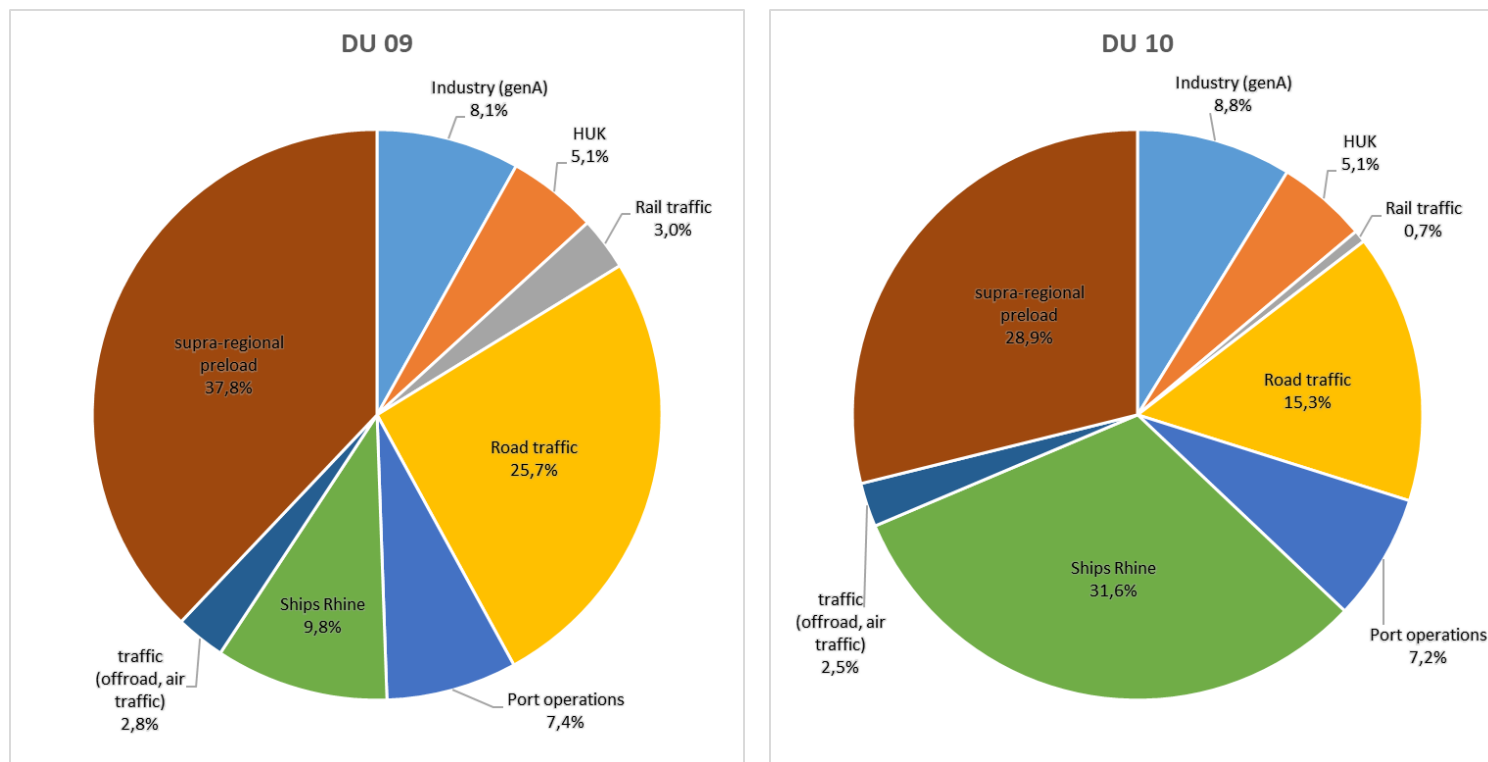


Fig. 36: Source group shares at monitoring stations DU009 (left) and DU010 (right).

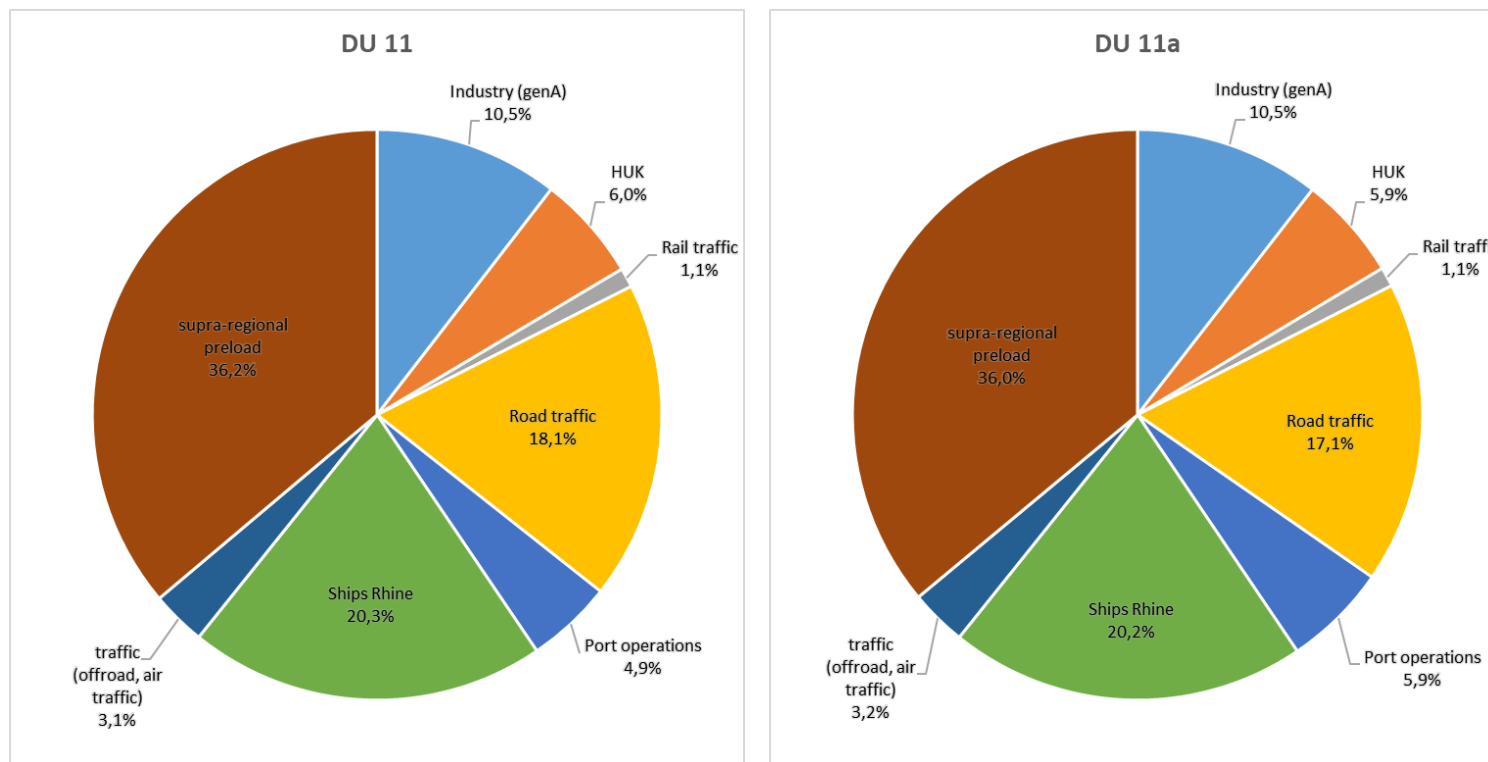


Fig. 37: Source group shares at monitoring stations DU011 (left) and DU011a (right).

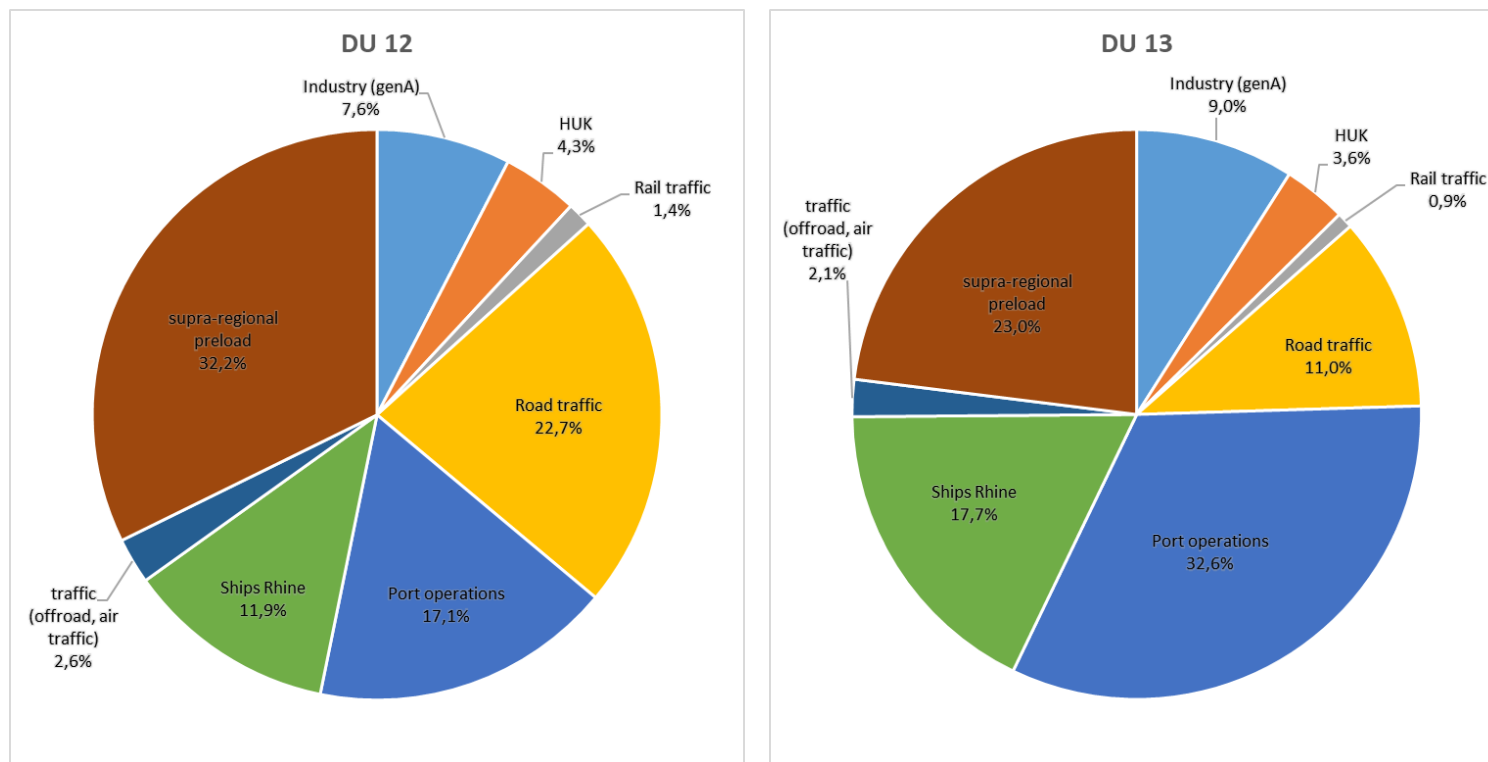


Fig. 38: Source group shares at monitoring stations DU012 (left) and DU013 (right).

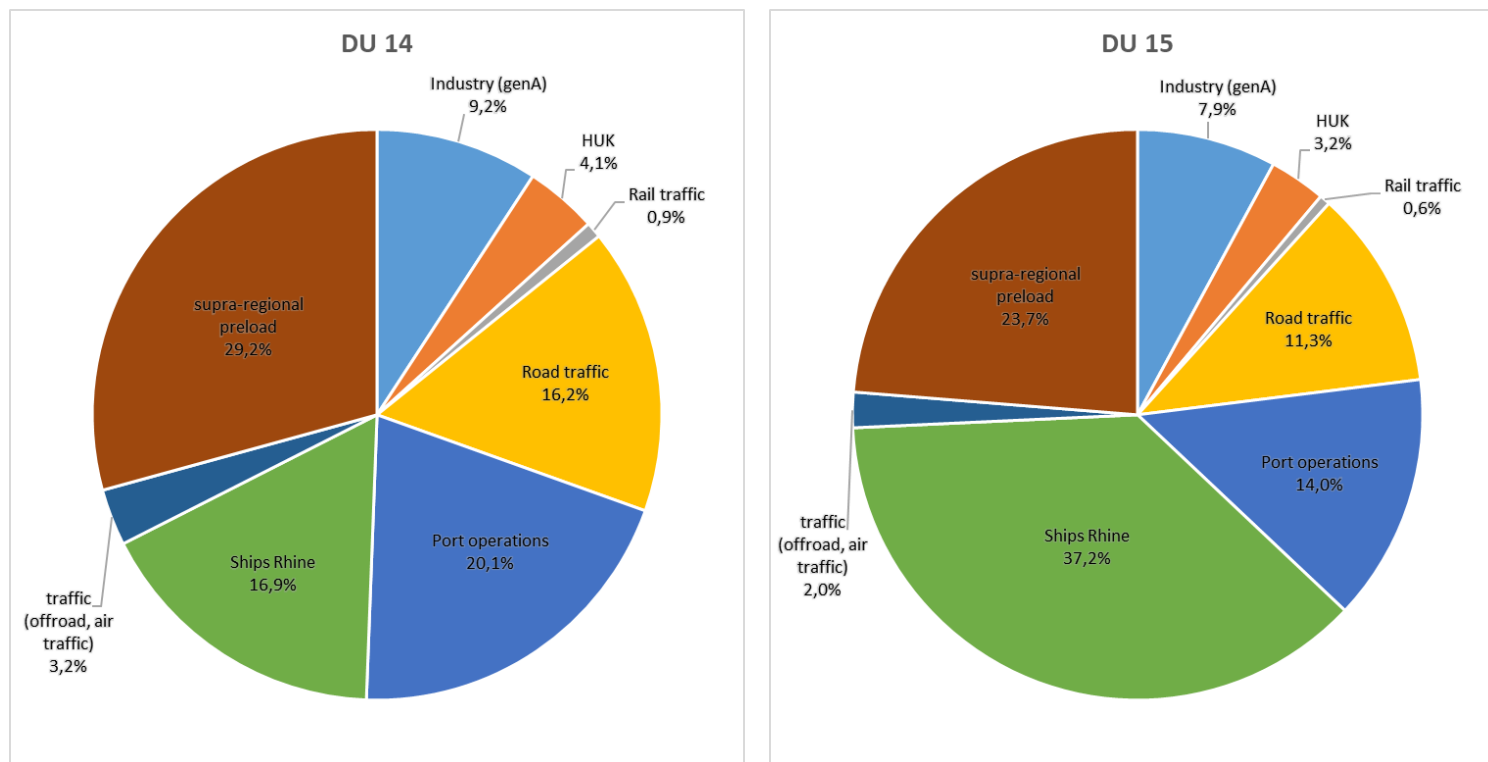


Fig. 39: Source group shares at monitoring stations DU014 (left) and DU015 (right).

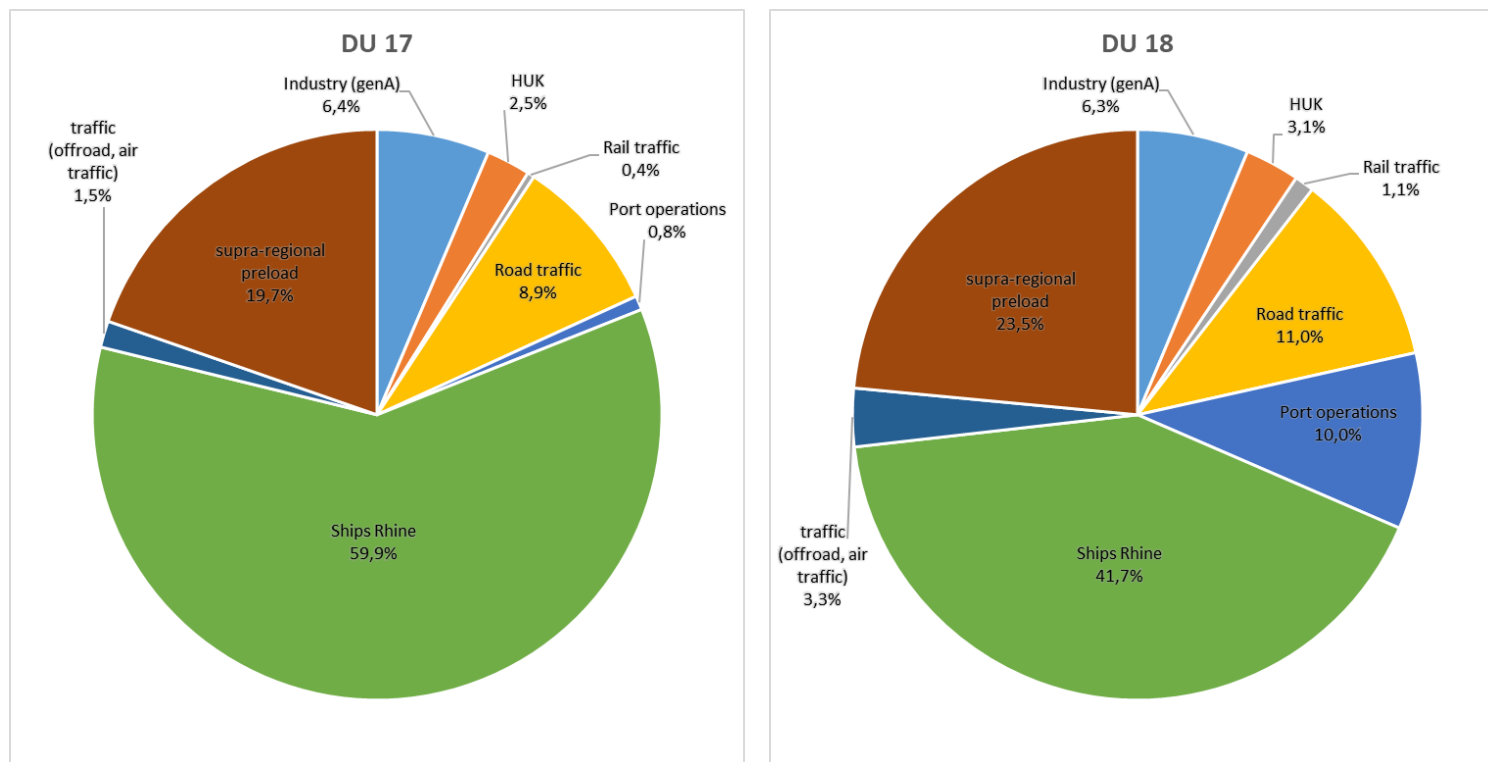


Fig. 40: Source group shares at monitoring stations DU017 (left) and DU018 (right).

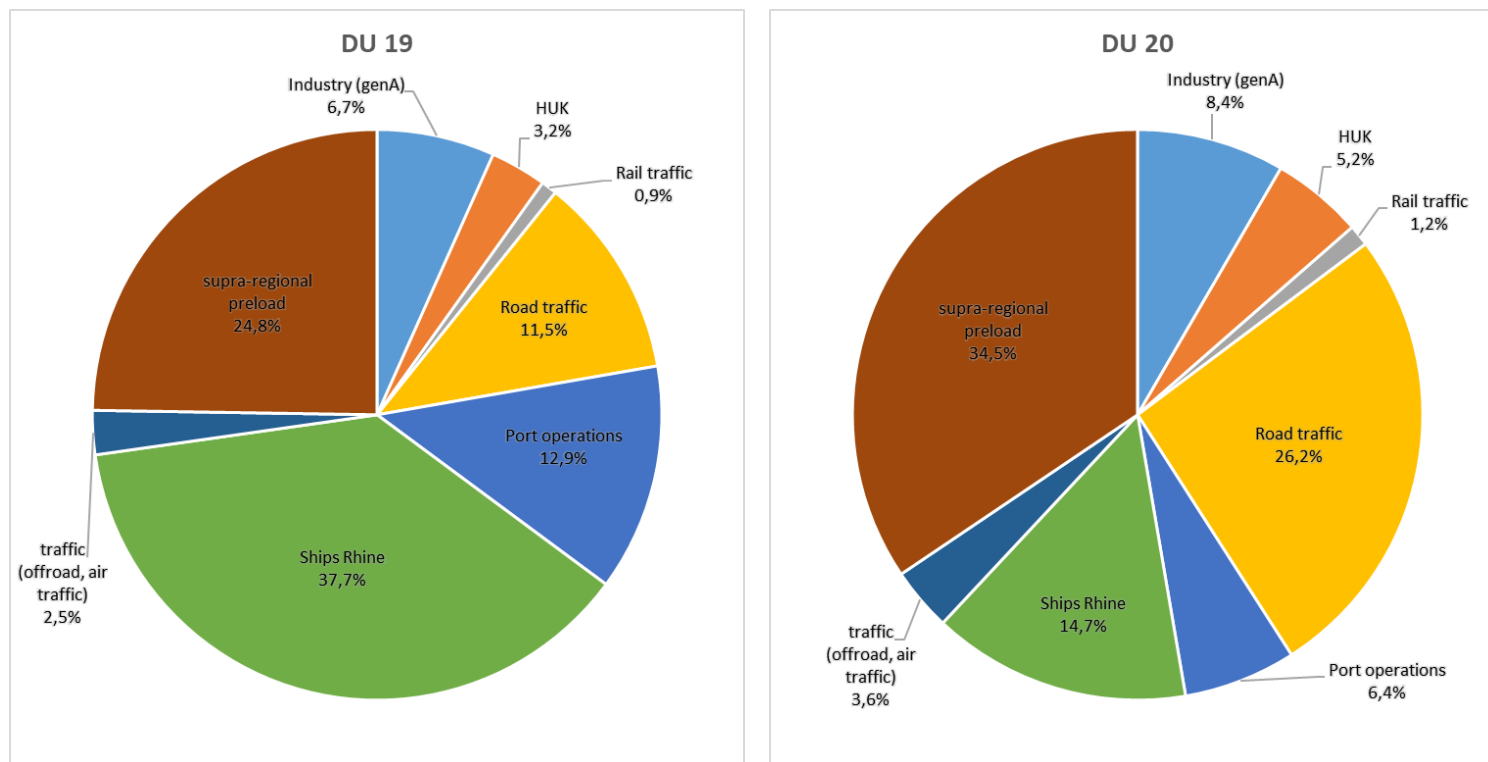


Fig. 41: Source group shares at monitoring stations DU019 (left) and DU020 (right).

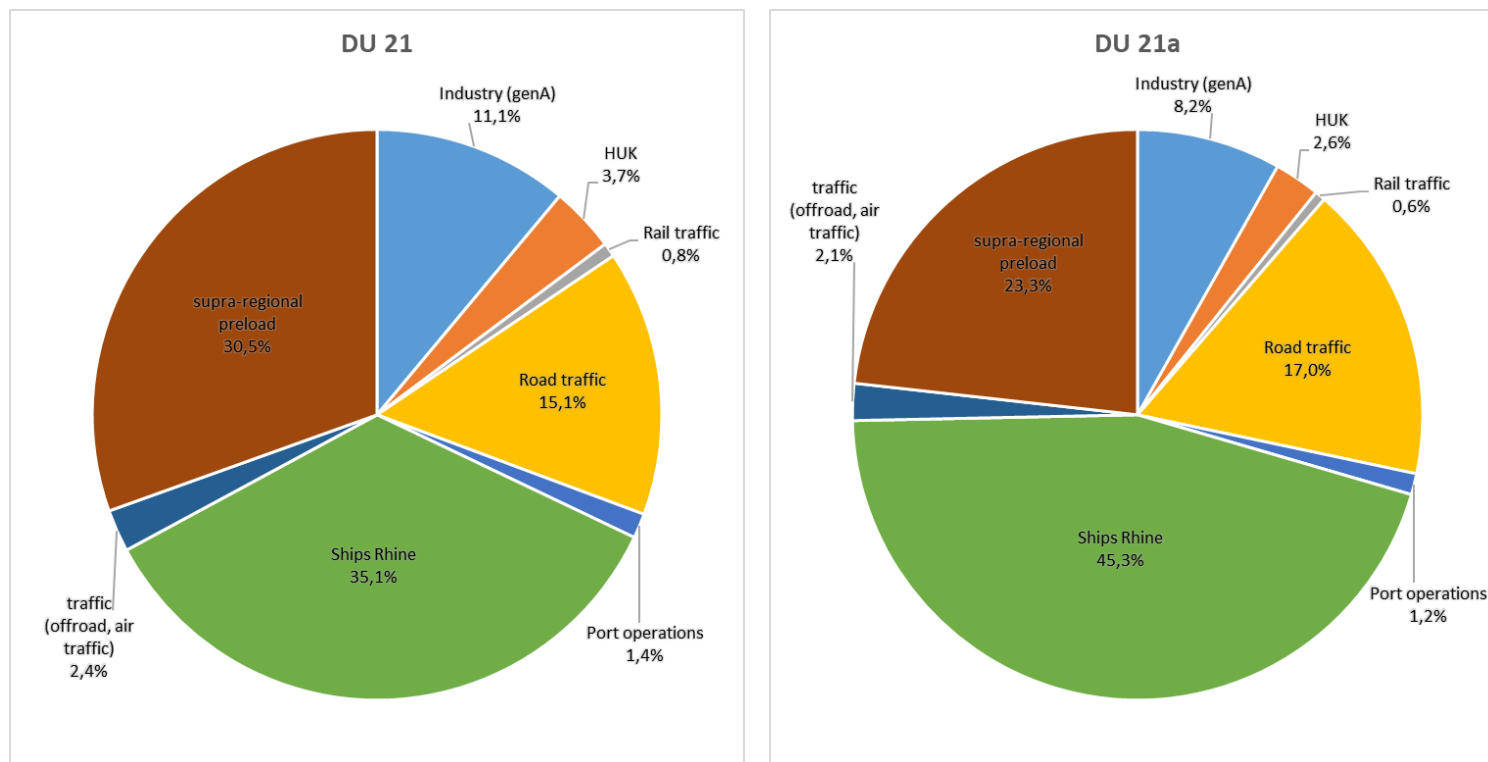


Fig. 42: Source group shares at monitoring stations DU021 (left) and DU021a (right).

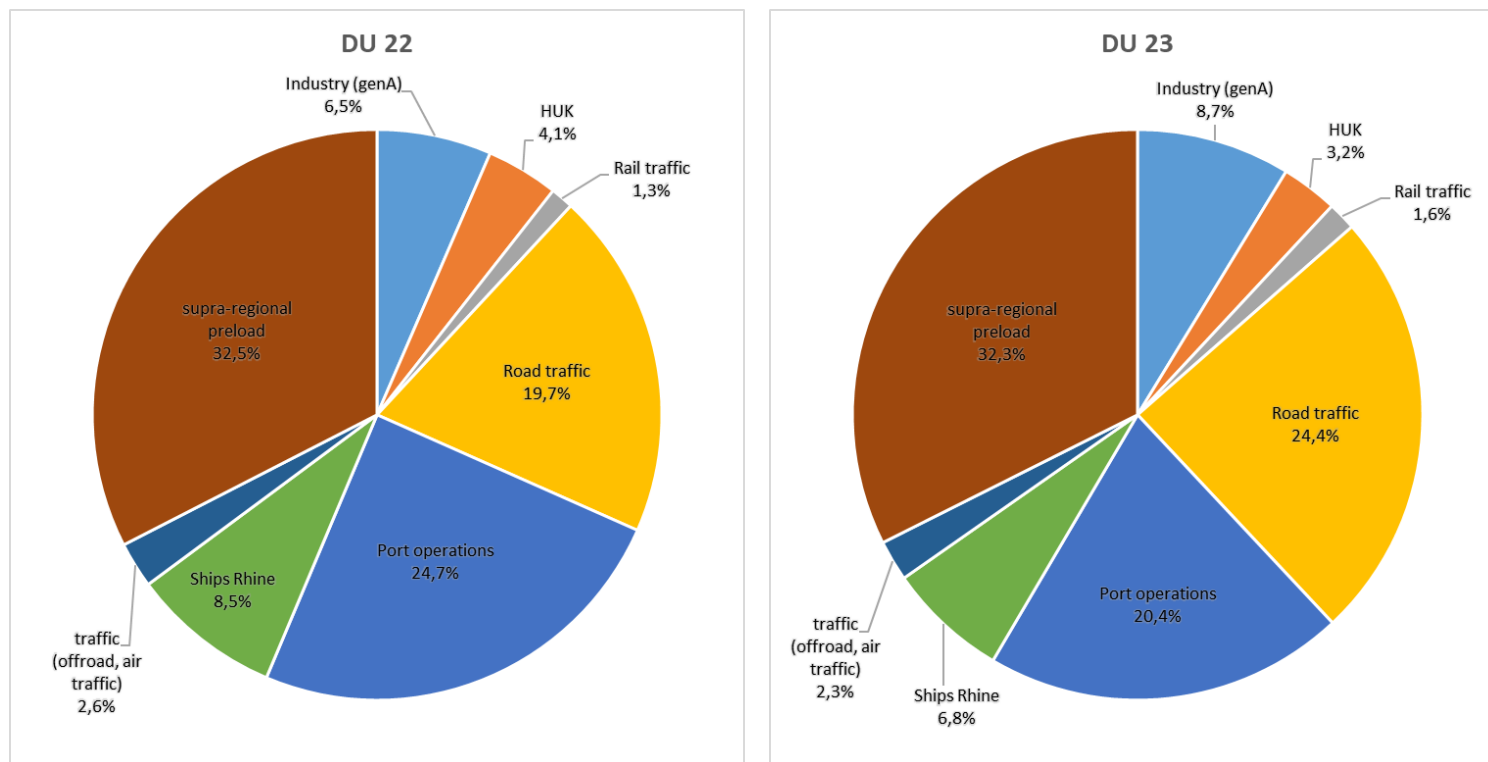


Fig. 43: Source group shares at monitoring stations DU022 (left) and DU023 (right).

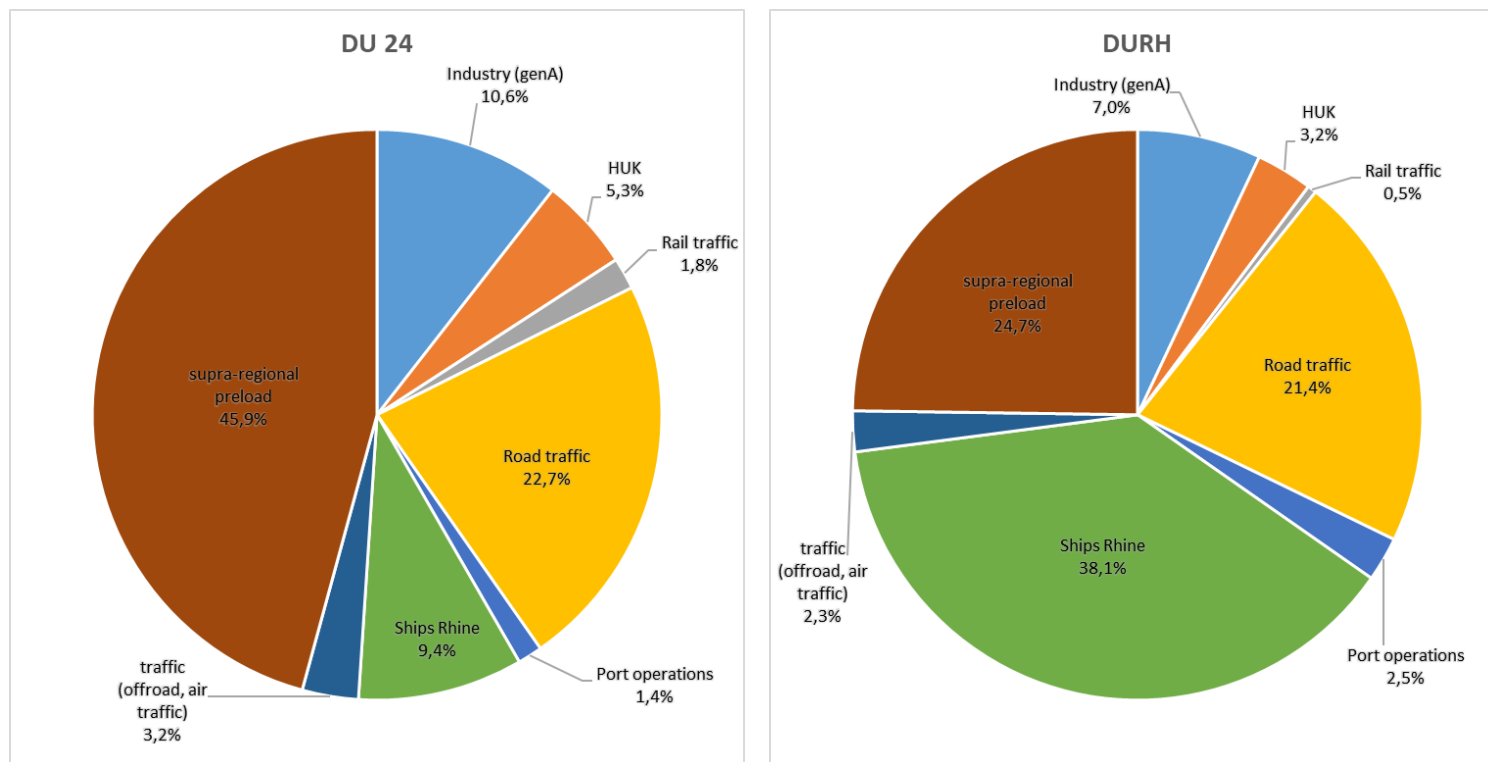


Fig. 44: Source group shares at monitoring stations DU024 (left) and DURH (right).

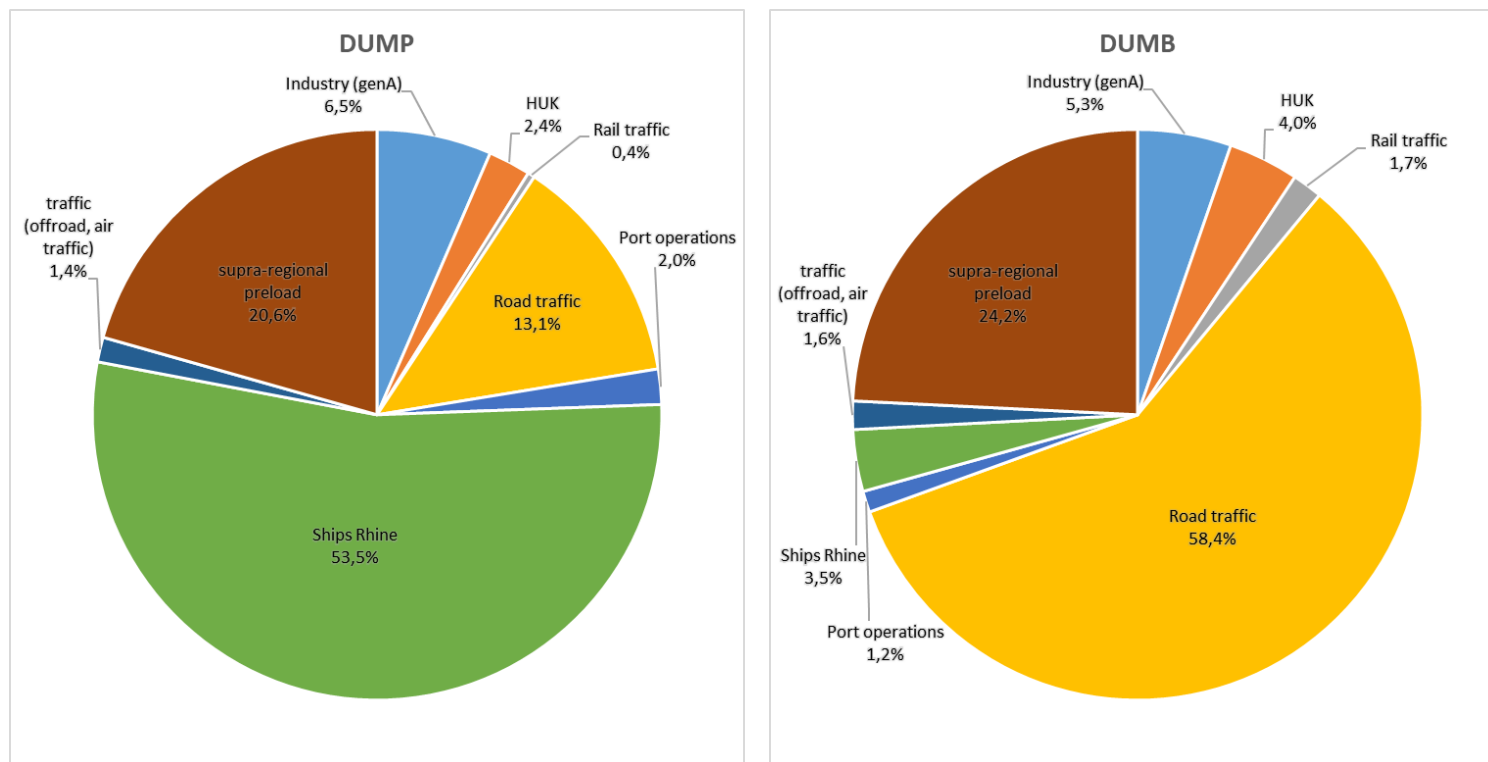


Fig. 45: Source group shares at monitoring stations DUMP (left) and DUMB (right).

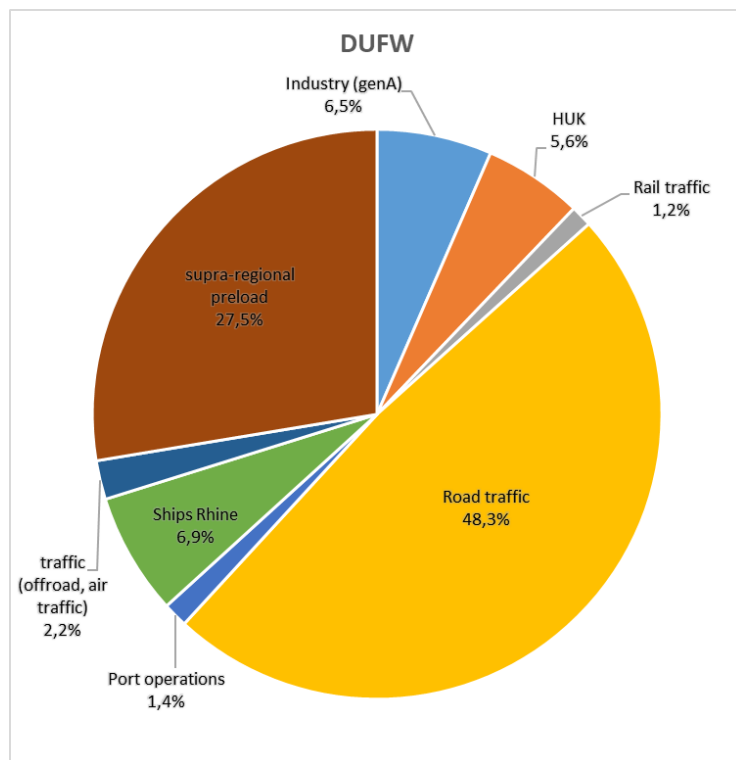


Fig. 46: Source group shares at monitoring station DUFW.

## 8.2 Source group shares at the Neuss measuring stations (pie charts)

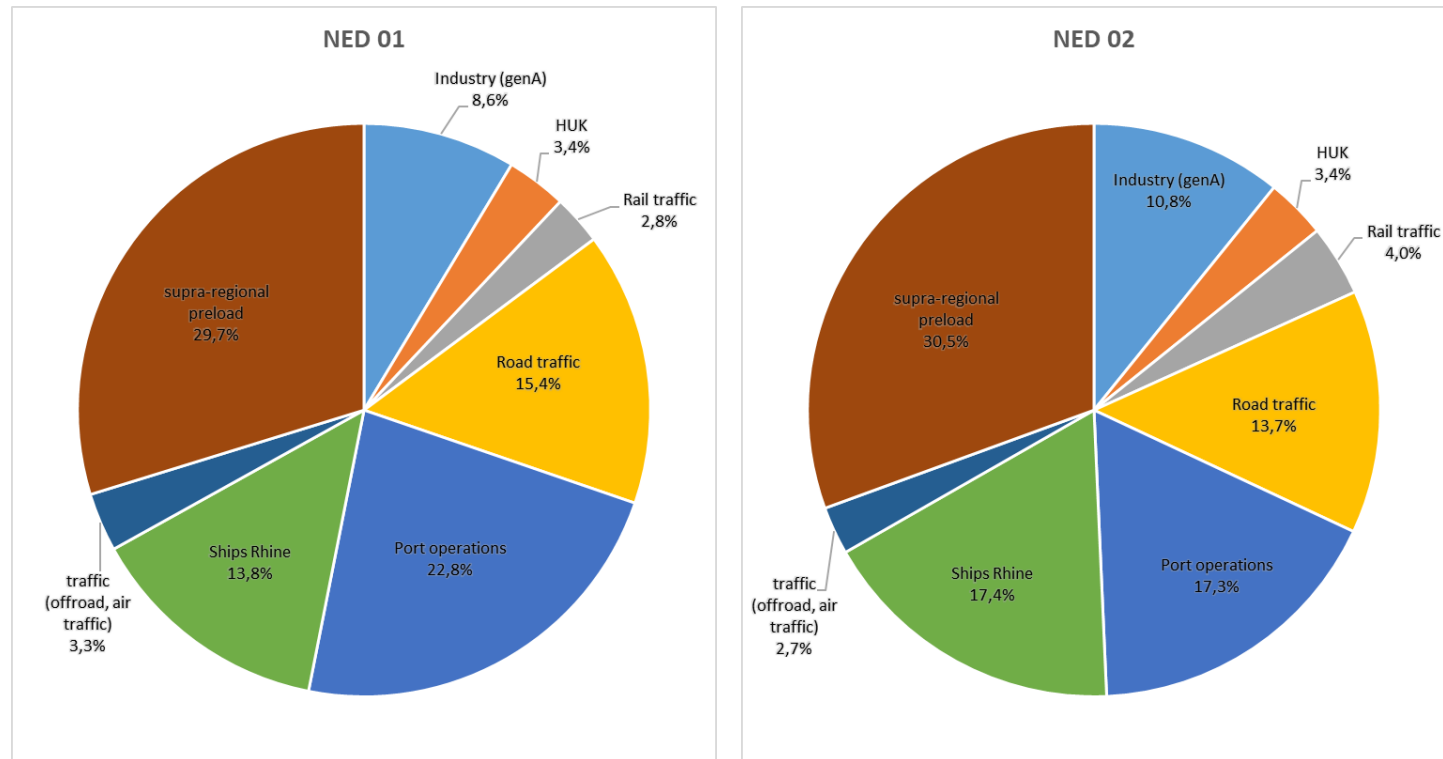


Fig. 47: Source group shares at monitoring stations NED001 (left) and NED002 (right).

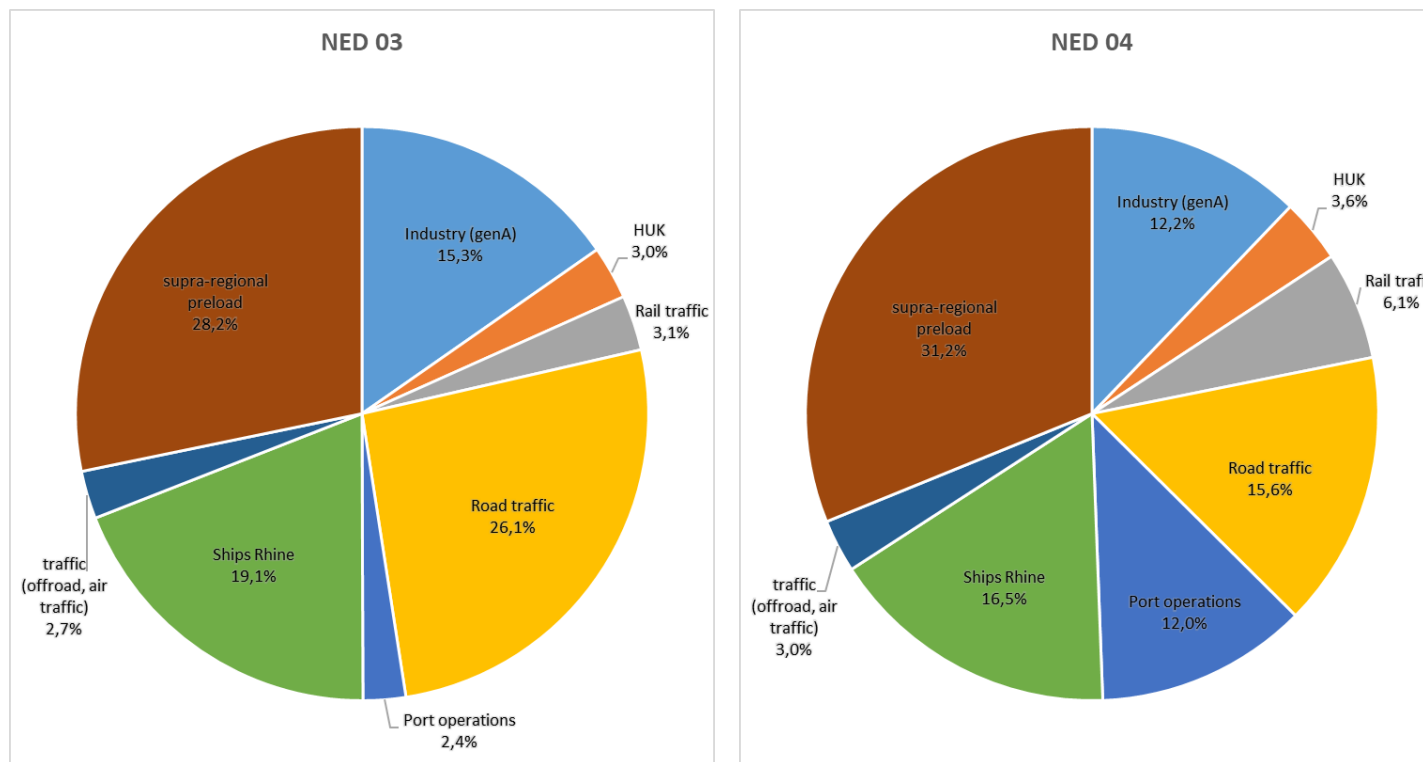


Fig. 48: Source group shares at monitoring stations NED003 (left) and NED004 (right).

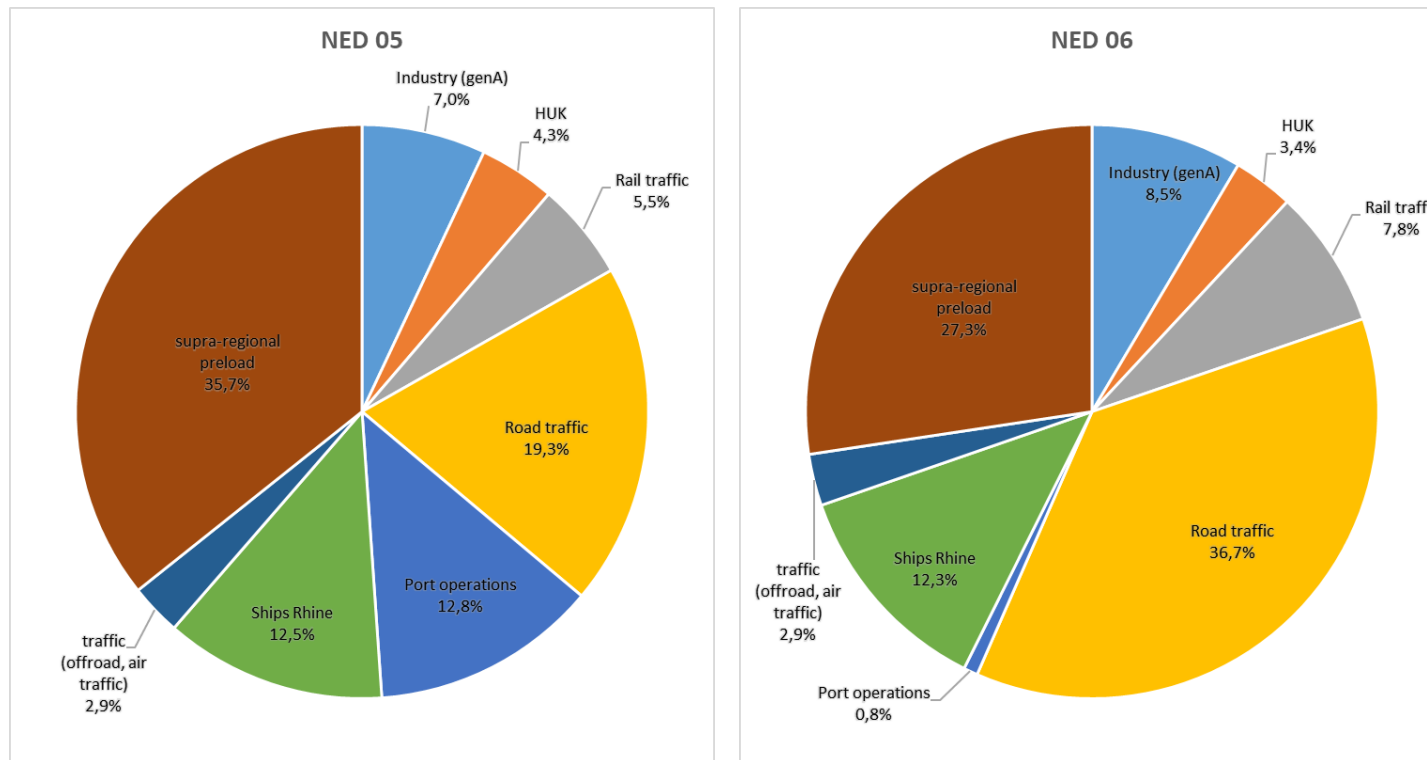


Fig. 49: Source group shares at monitoring stations NED005 (left) and NED006 (right).

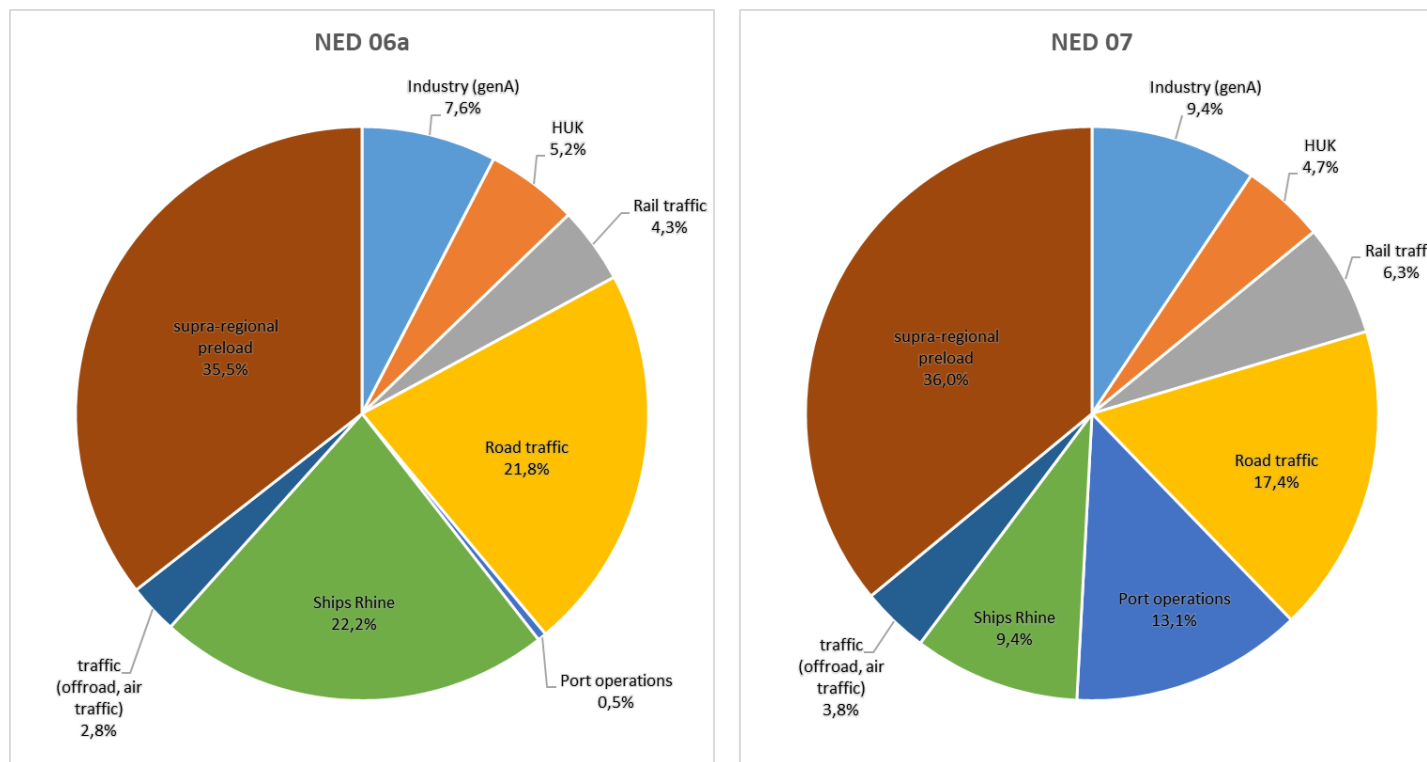


Fig. 50: Source group shares at monitoring stations NED006a (left) and NED007 (right).

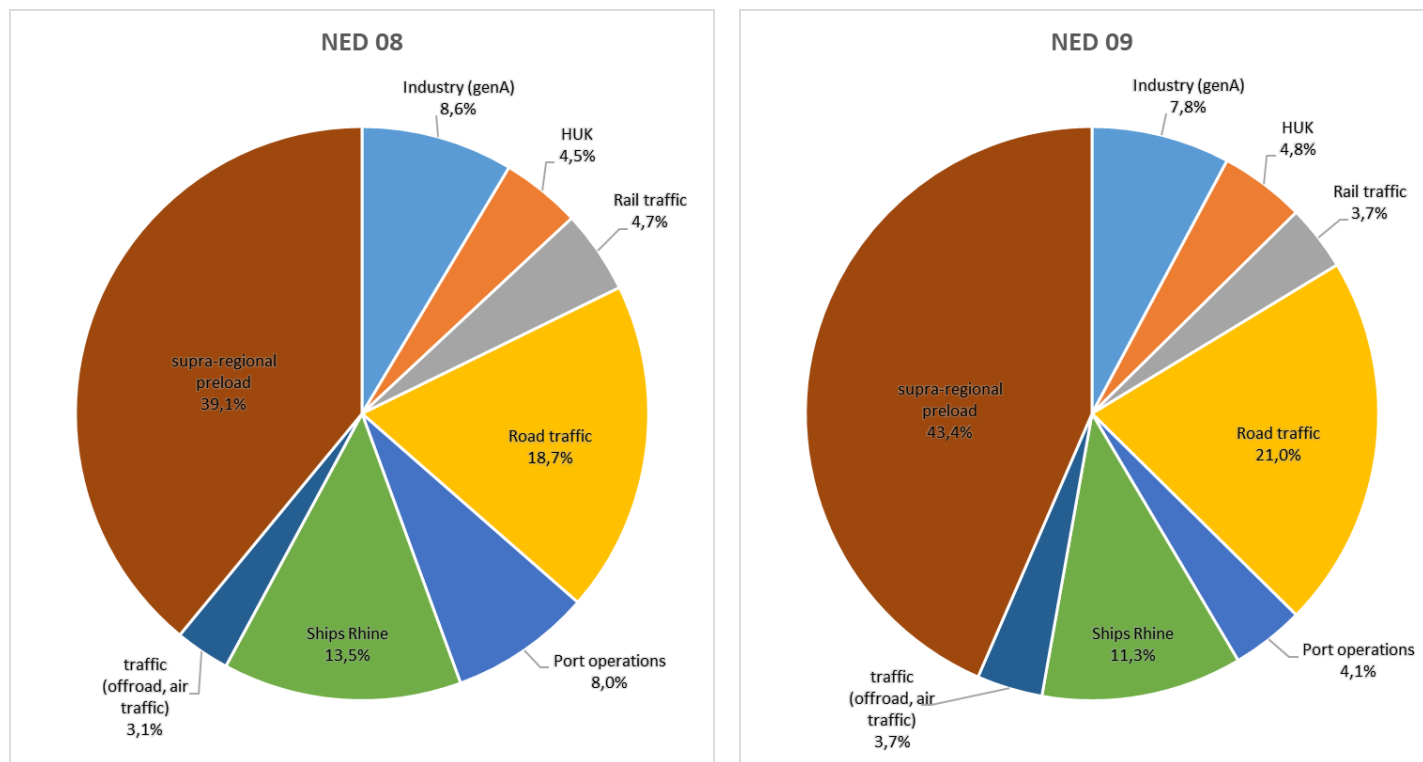


Fig. 51: Source group shares at monitoring stations NED008 (left) and NED009 (right).

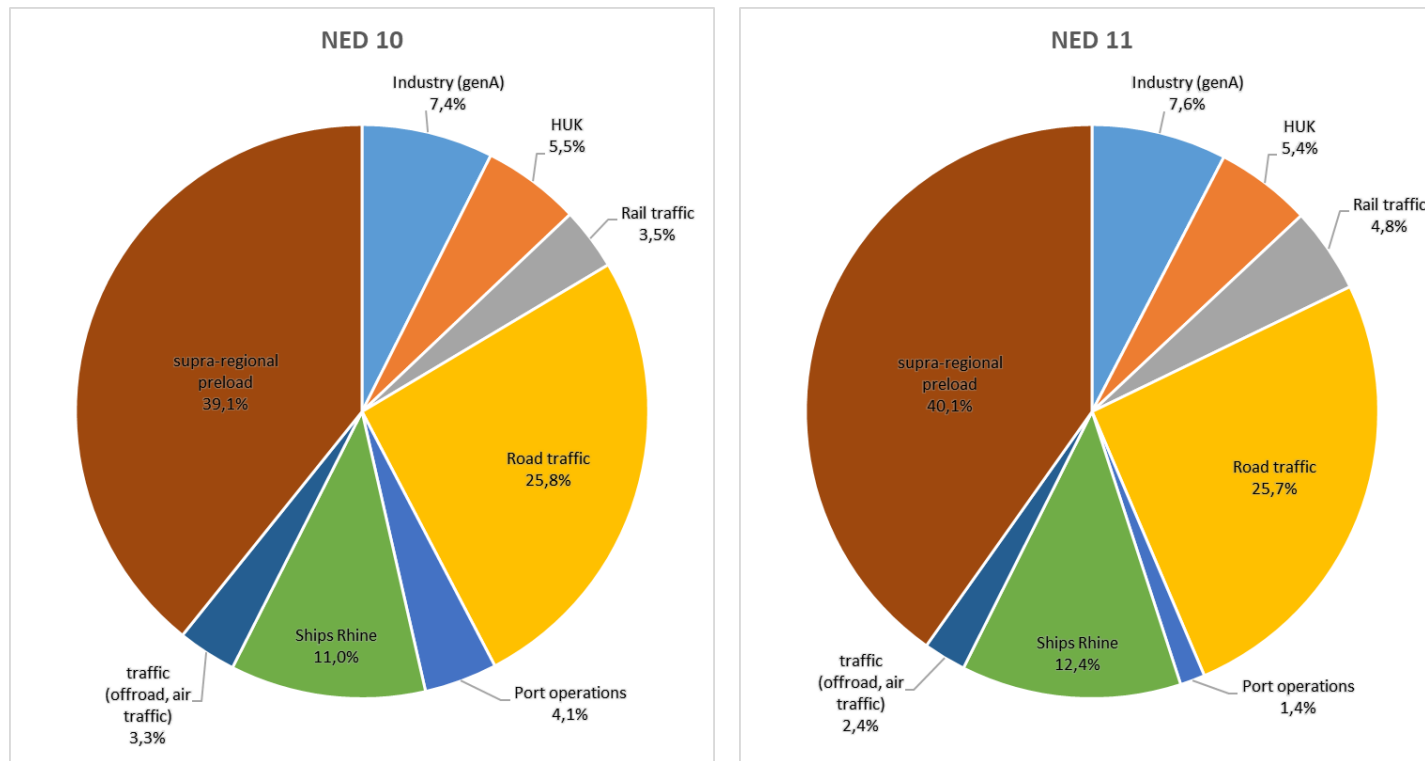


Fig. 52: Source group shares at monitoring stations NED010 (left) and NED011 (right).

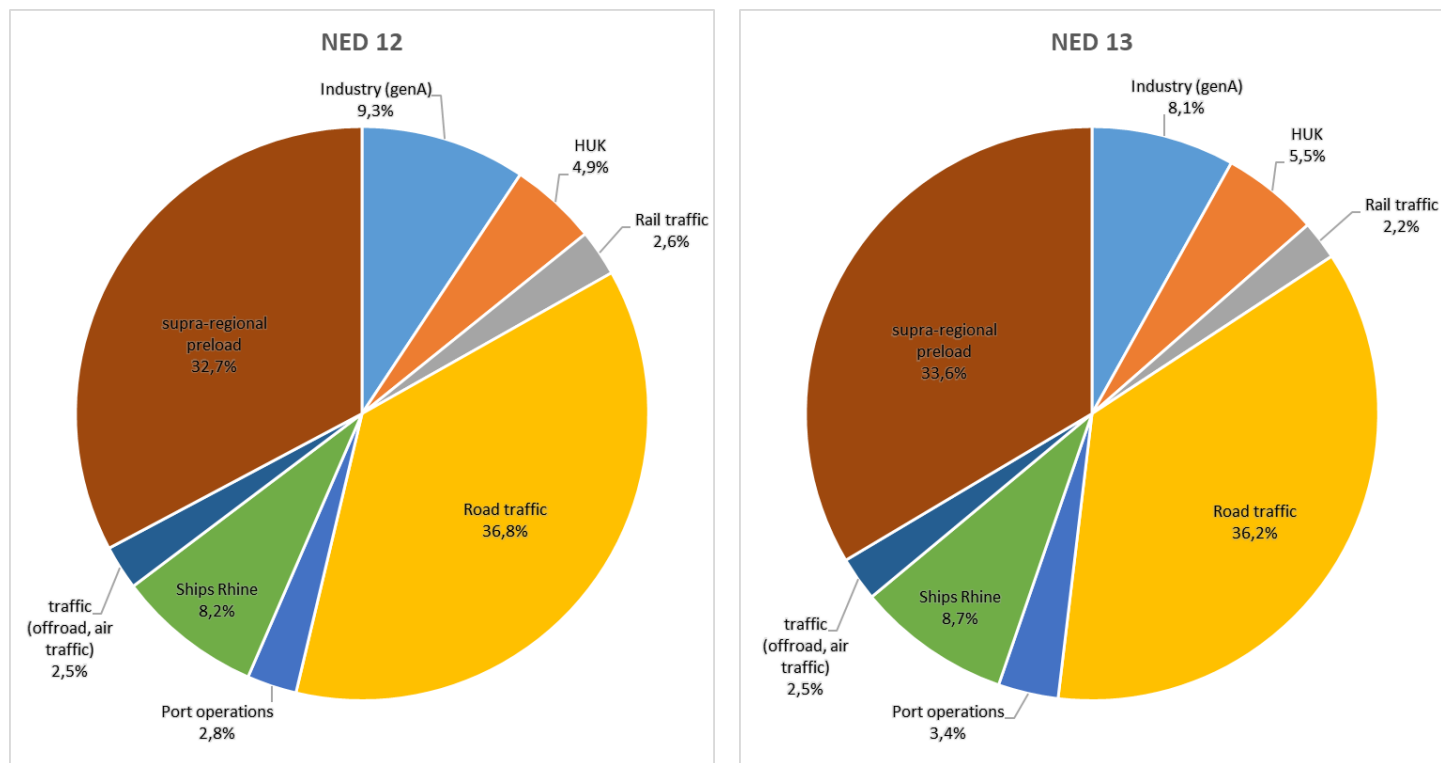


Fig. 53: Source group shares at monitoring stations NED012 (left) and NED013 (right).

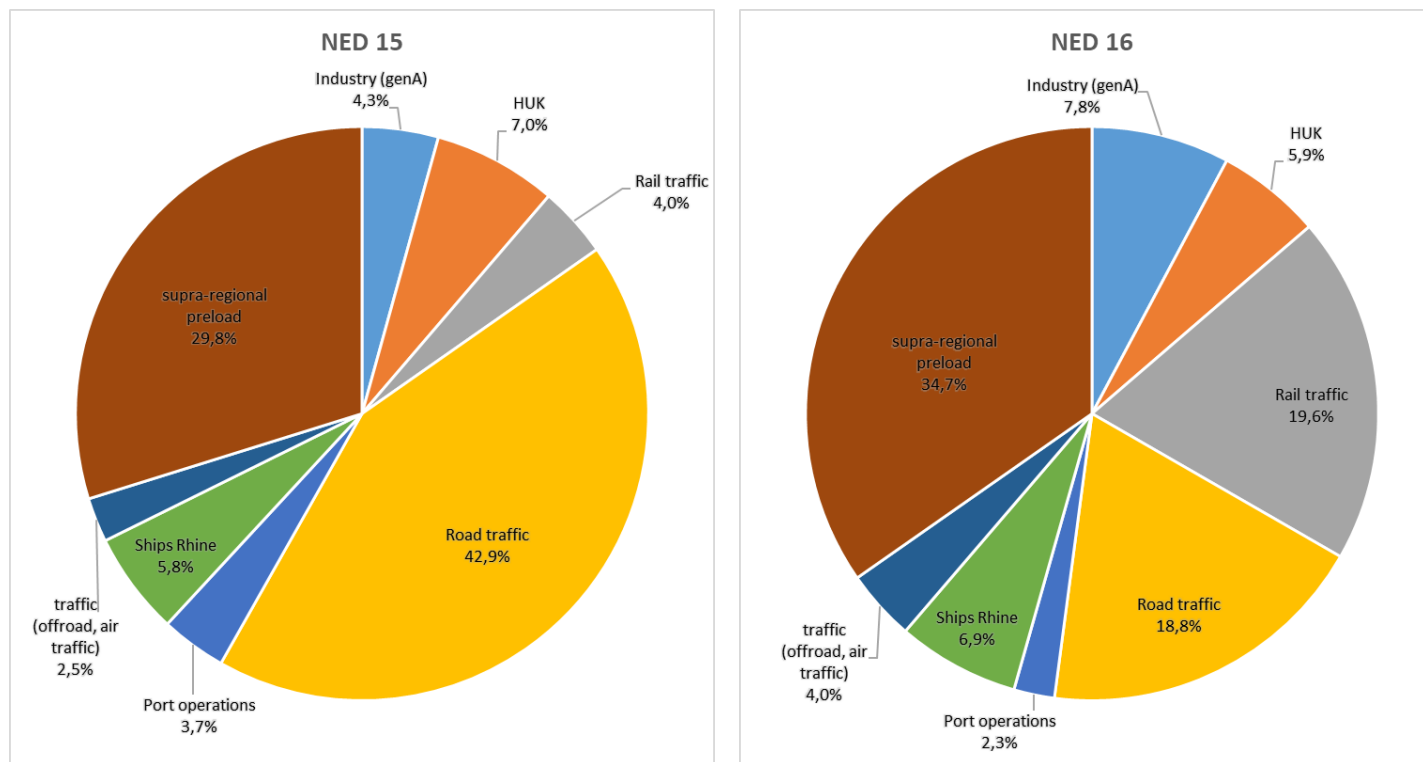


Fig. 54: Source group shares at monitoring stations NED015 (left) and NED016 (right).

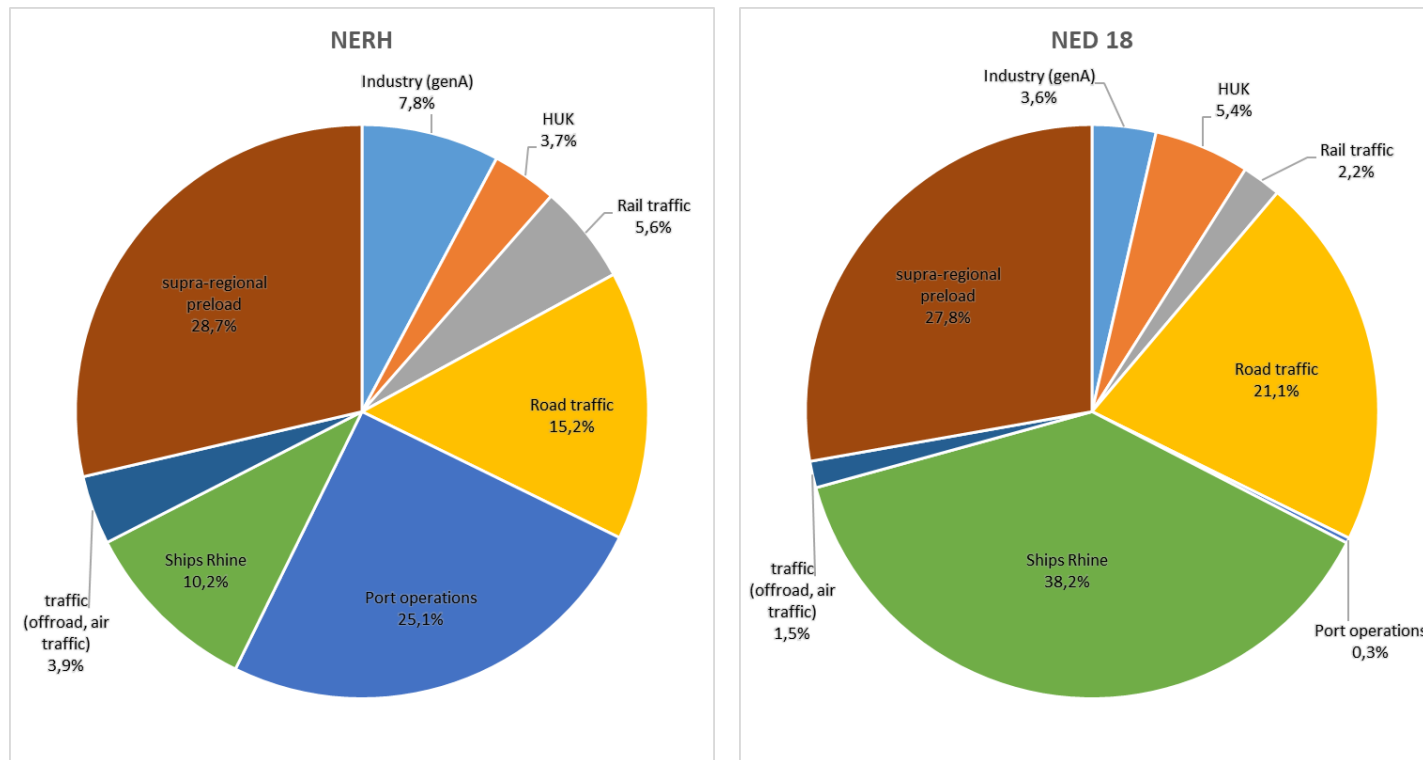


Fig. 55: Source group shares at monitoring stations NERH (left) and NED018 (right).

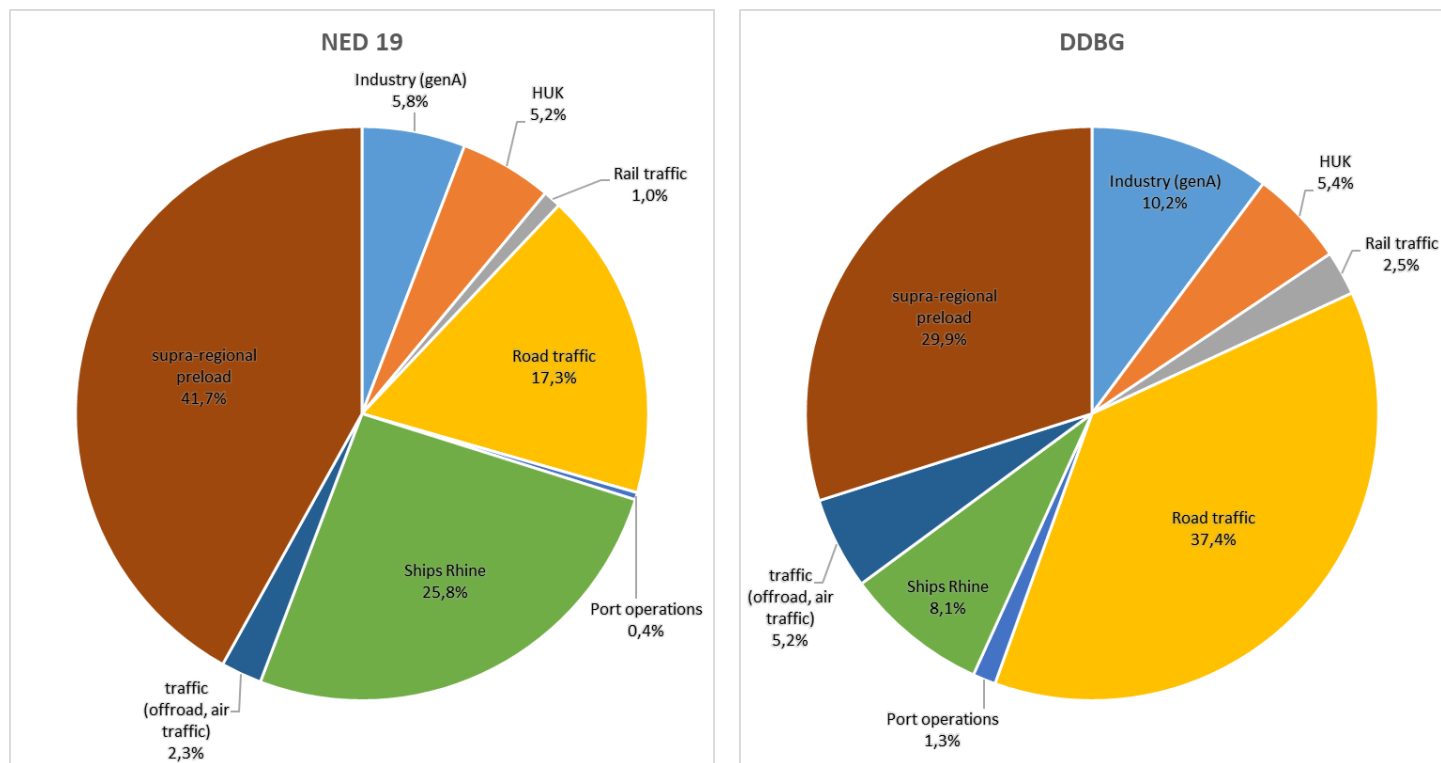


Fig. 56: Source group shares at monitoring stations NED019 (left) and DDBG (right).

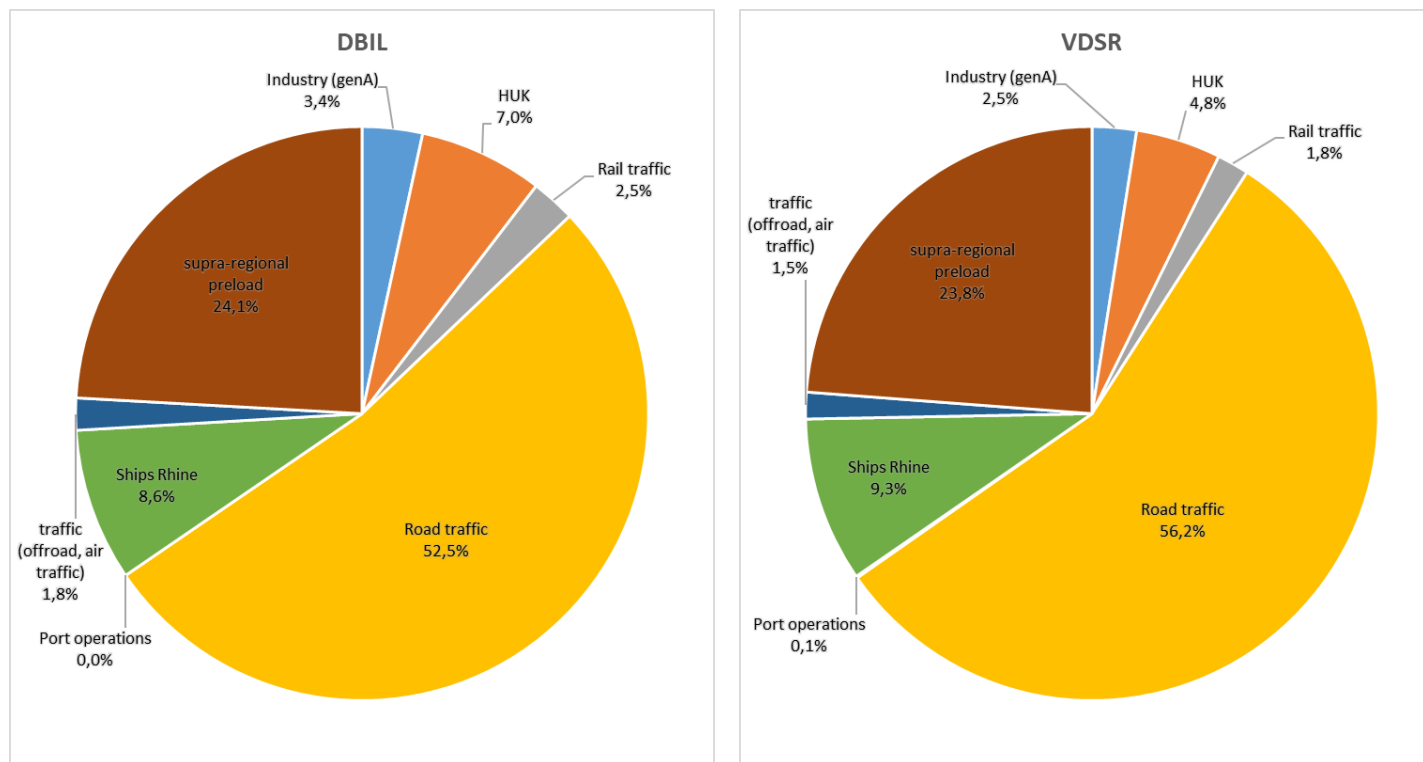


Fig. 57: Source group shares at monitoring stations DBIL (left) and VDSR (right).

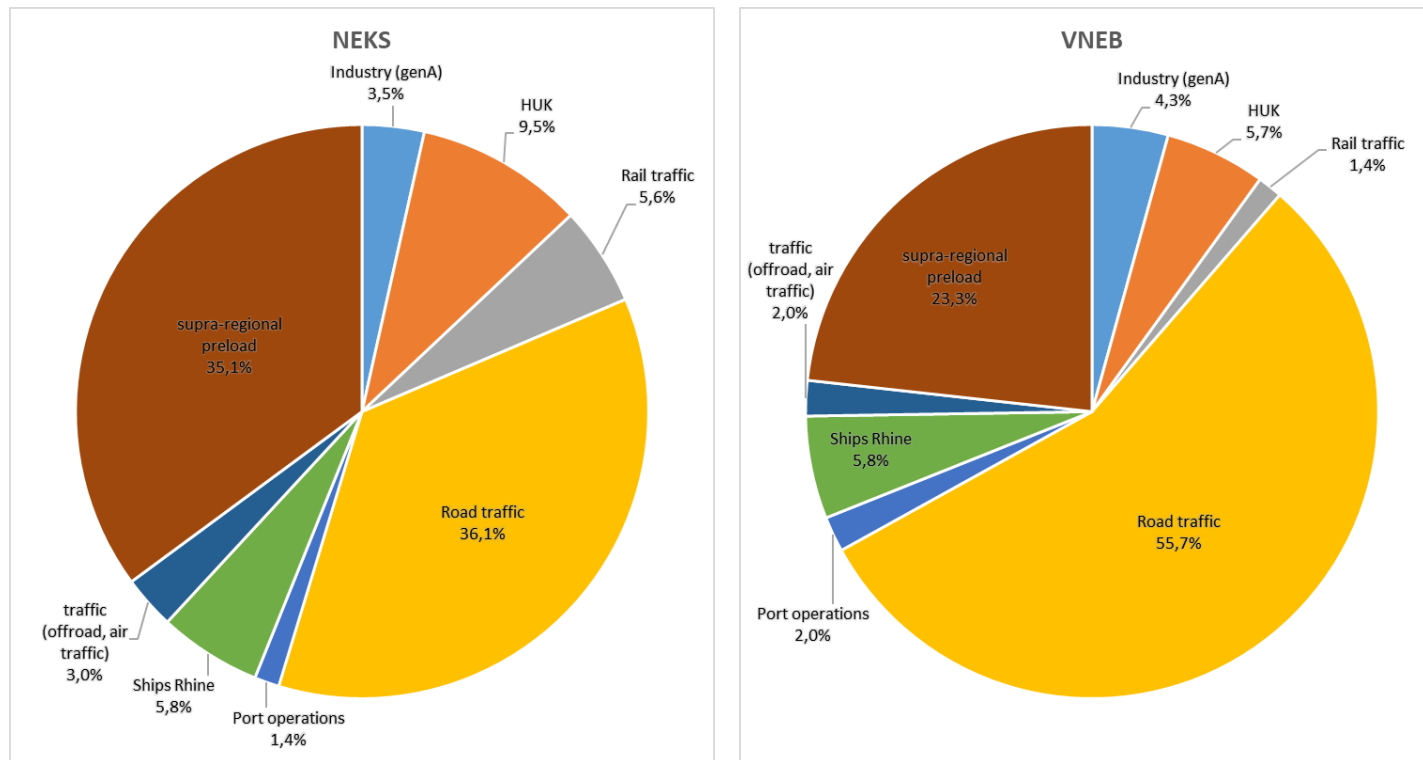


Fig. 58: Source group shares at monitoring stations NEKS (left) and VNEB (right).

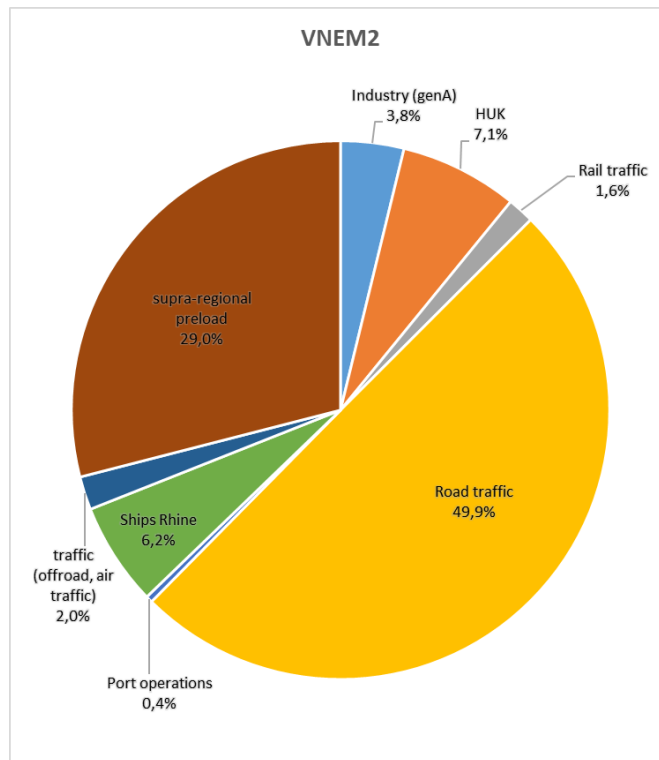


Fig. 59: Source group shares at monitoring station VNEM2.

### 8.3 Additional source group shares (Port of Duisburg, spatial presentation)

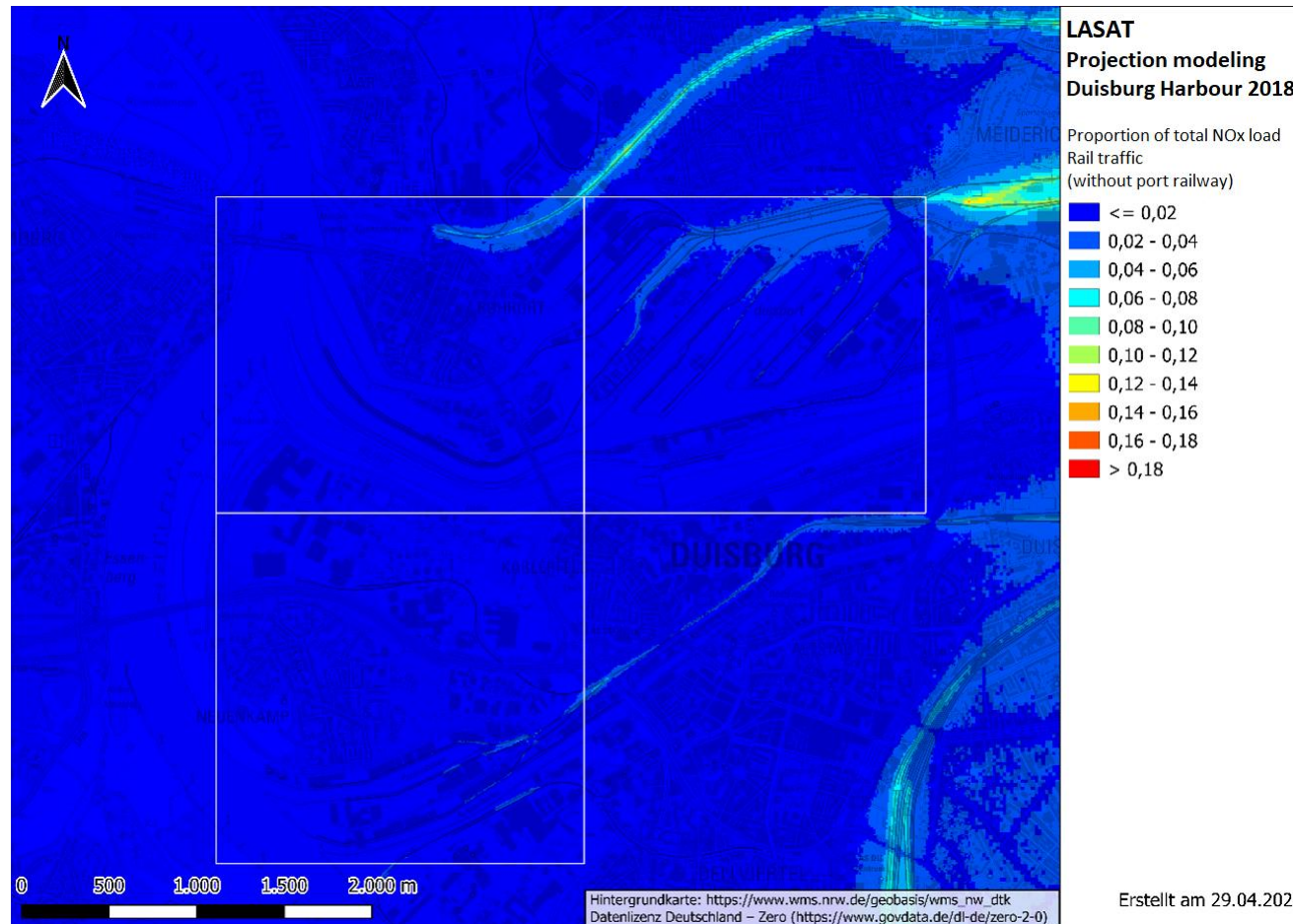


Fig. 60: Proportion of total NO<sub>x</sub> load from rail traffic emissions in the Duisburg port area - modeled with LASAT (a value of 0.1 corresponds to a proportion of 10 %).

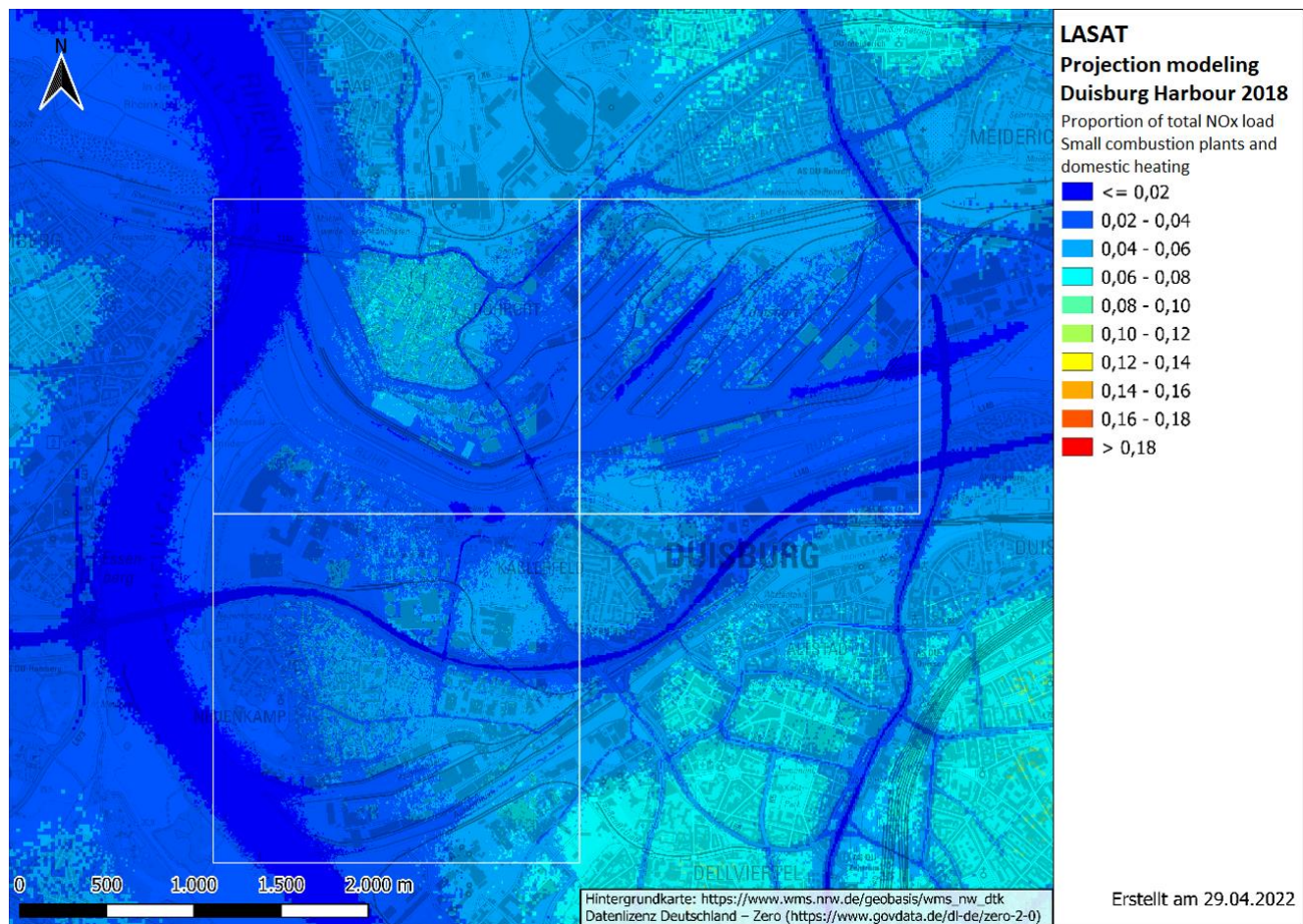


Fig. 61: Proportion of total NO<sub>x</sub> load from emissions from domestic heating and small combustion plants in the Duisburg port area - modeled with LASAT (a value of 0.1 corresponds to a proportion of 10 %).

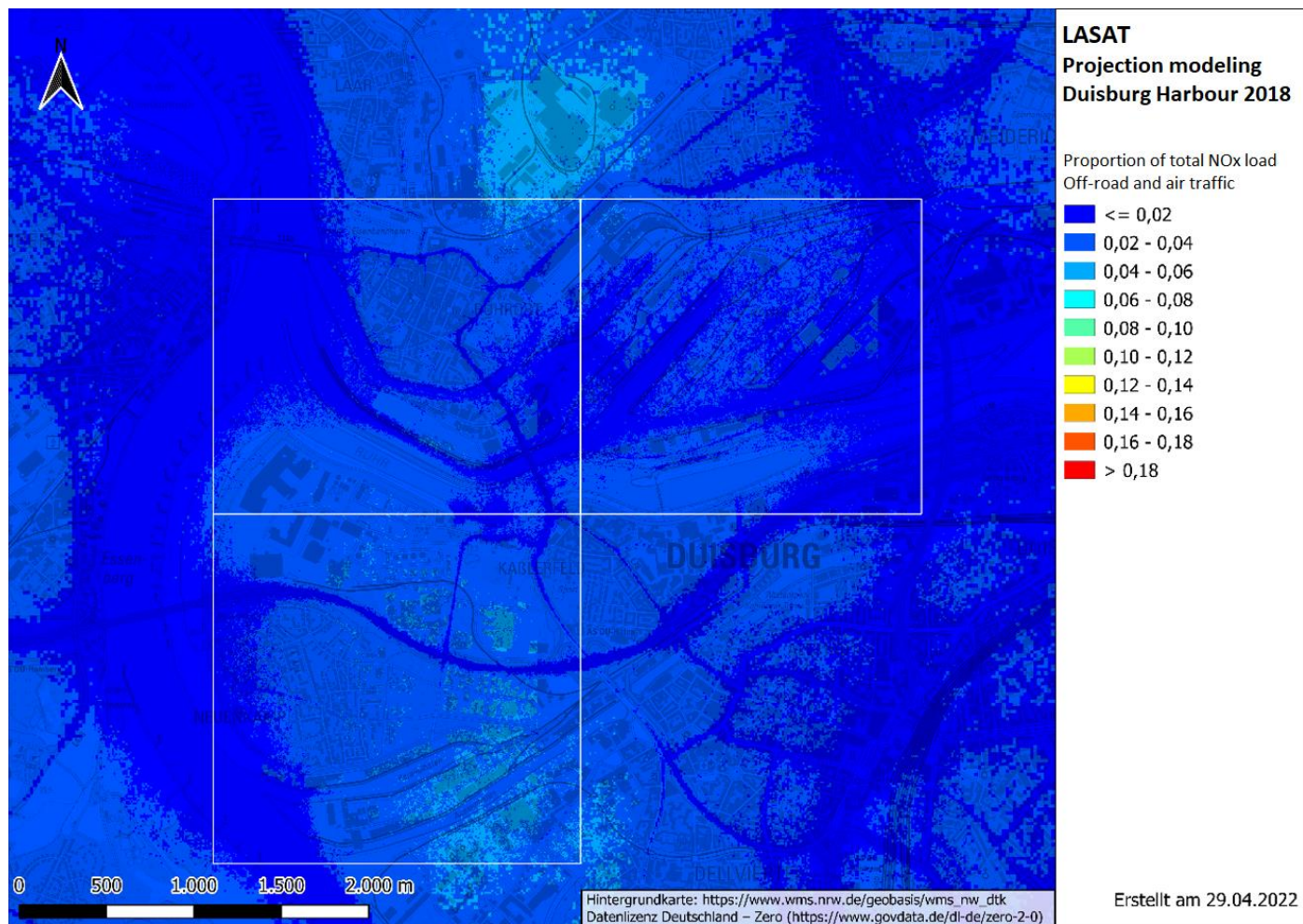


Fig. 62: Proportion of total NO<sub>x</sub> load from emissions from aviation and off-road traffic in the Duisburg port area - modeled with LASAT (a value of 0.1 corresponds to a proportion of 10 %).

#### 8.4 Additional source group shares (Port of Neuss, spatial presentation)

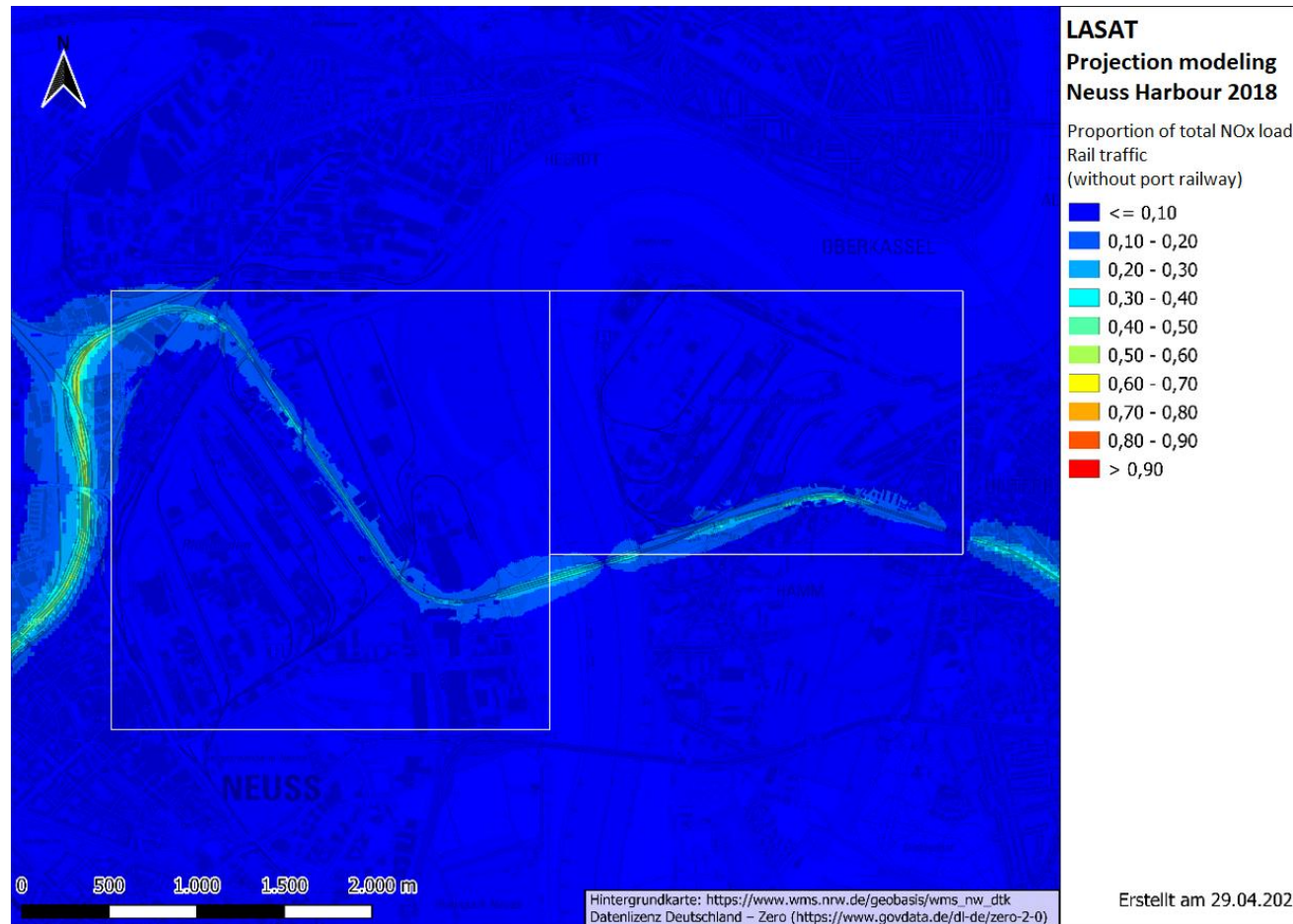


Fig. 63: Proportion of total NO<sub>x</sub> load from rail traffic emissions in the Neuss port area - modeled with LASAT (a value of 0.1 corresponds to a proportion of 10 %).

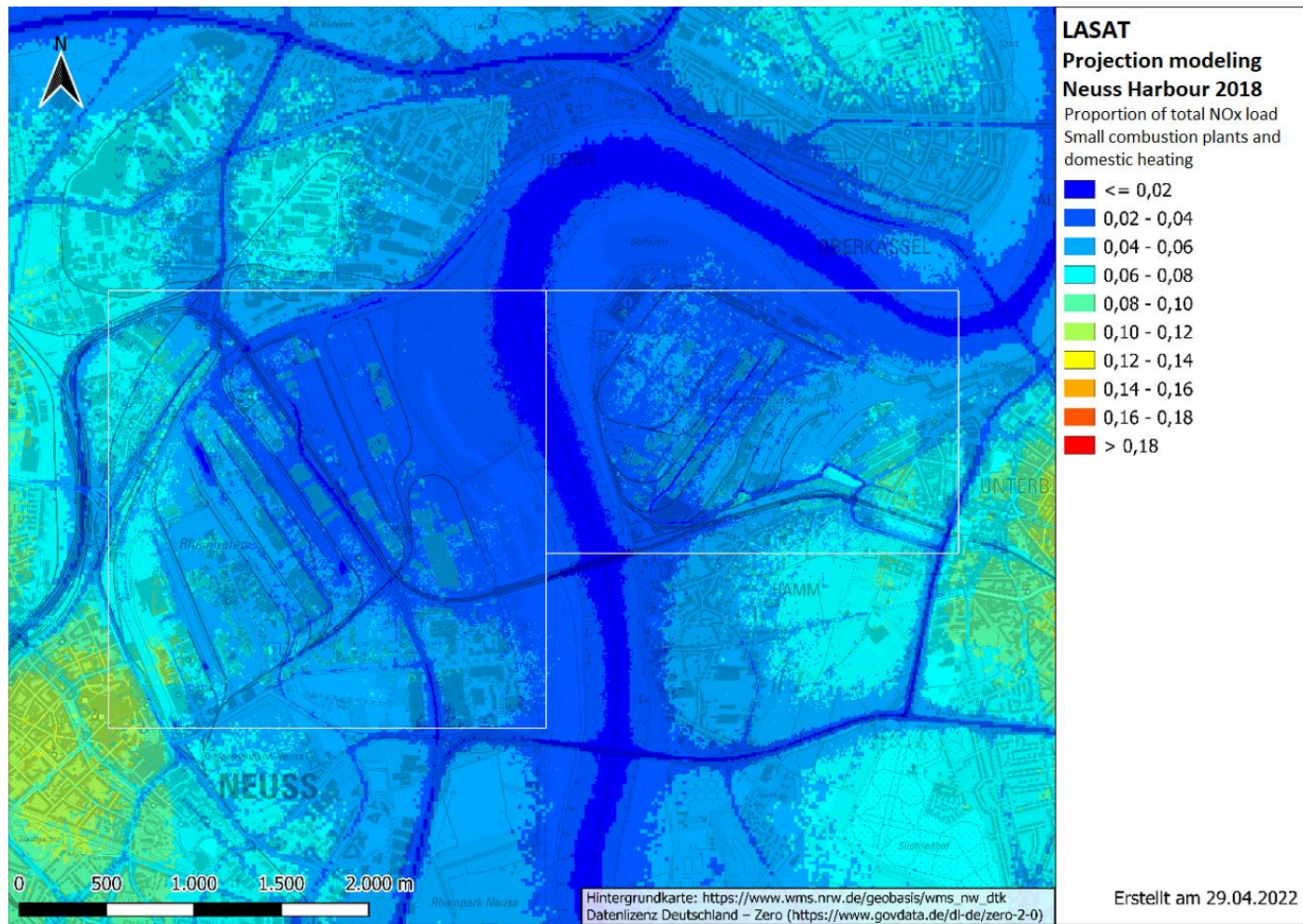


Fig. 64: Proportion of total NO<sub>x</sub> load from emissions from domestic heating and small combustion plants in the Neuss port area - modeled with LASAT (a value of 0.1 corresponds to a proportion of 10 %).

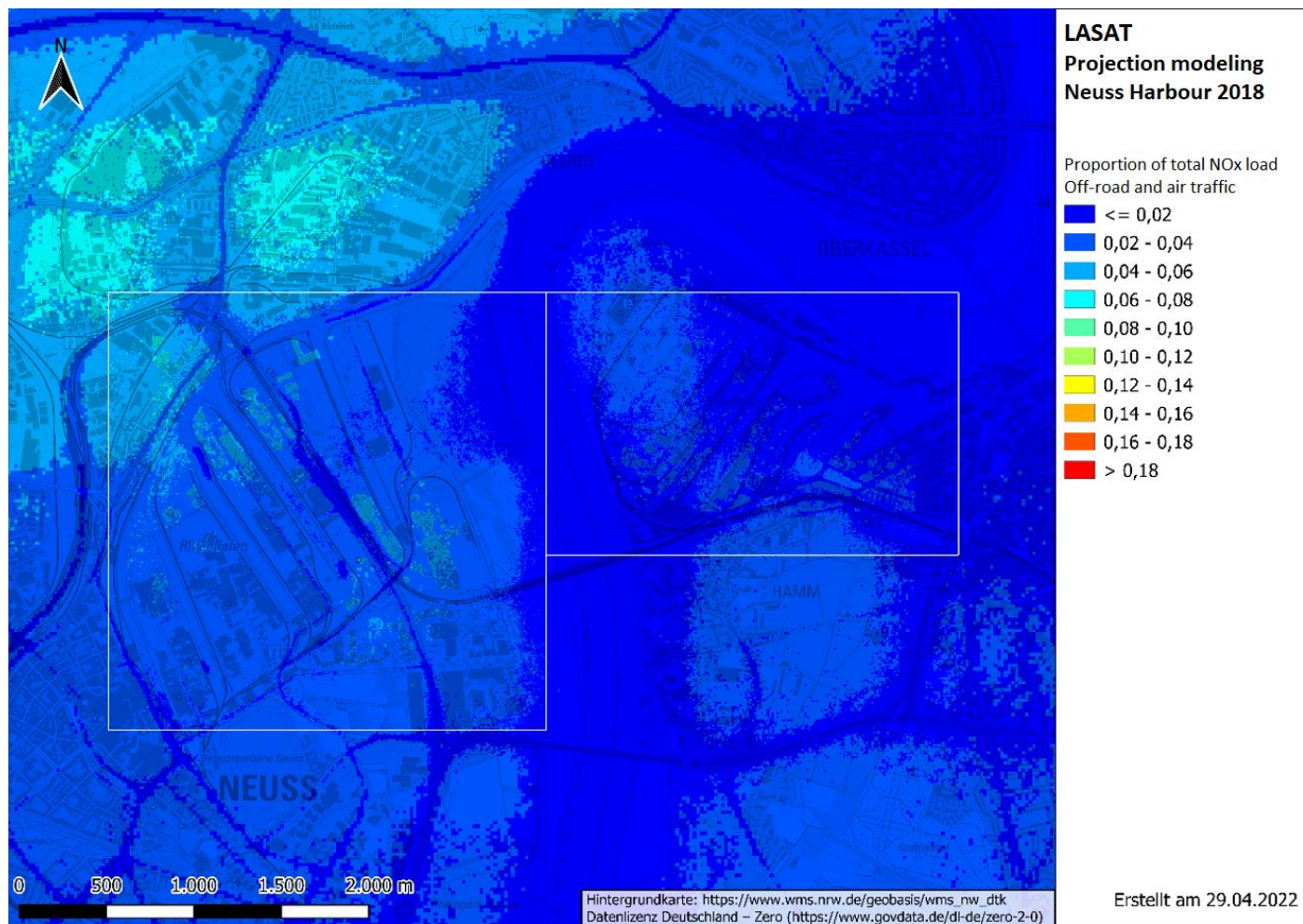


Fig. 65: Proportion of total NO<sub>x</sub> load from emissions from aviation and off-road traffic in Neuss port area - modeled with LASAT (a value of 0.1 corresponds to a proportion of 10 %).

## 9. CLINSH Partners



### Visiting address

Provinciehuis Zuid-Holland  
Zuid-Hollandplein 1  
2596 AW The Hague  
The Netherlands

### Mailing address

Provincie Zuid-Holland  
Postbus 90602  
2509 LP The Hague  
The Netherlands

### Visiting address

Provinciehuis Zuid-Holland  
Zuid-Hollandplein 1  
2596 AW The Hague  
The Netherlands

### Mailing address

Provincie Zuid-Holland  
Postbus 90602  
2509 LP The Hague  
The Netherlands

